Cap-dependence of the Poly(A)-specific Ribonuclease PARN

Dissertationsschrift

zur Erlangung des adakemischen Grades
Doktor der Naturwissenschaften
-Dr. rer. Nat.-

vorgelegt der

Mathematisch-Naturwissenschaftlich-Technischen Fakultät
der Martin-Luther-Universität Halle-Wittenberg

von

Eva Dehlin

Datum der Verteidigung: 20. Februar 2004

Gutachter: Prof. E. Wahle
Prof. M. Worminton
Dr. Simon Morley

urn:nbn:de:gbv:3-000007155
[http://nbn-resolving.de/urn/resolver.pl?urn=nbn%3Ade%3Agbv%3A3-000007155]

TABLE OF CONTENTS

1.	**INTRODUCTION**	**1**
1.1	The major mRNA degradation pathways.	1
1.2	Nonsense-mediated decay (NMD).	5
1.3	Nonstop-mediated decay (NSD).	6
1.4	*cis*-elements and *trans*-acting factors controlling mRNA in somatic cells.	6
1.5	Translation.	9
1.6	Deadenylation and translation.	12
1.7	Deadenylating nucleases.	14
1.8	Aim of the thesis.	18
2.	**MATERIALS AND METHODS**	**20**
2.1	**Materials**	**20**
2.1.1	Bacterial strains and cell lines.	20
2.1.2	Culture media	20
2.1.3	Proteins and enzymes.	21
2.1.4	Antibodies.	22
2.1.5	Nucleotides and Nucleic Acids.	22
2.1.6	Plasmids and vectors.	22
2.1.7	Oligonucleotides.	23
2.1.8	Kits.	23
2.1.9	Column materials.	24
2.1.10	Chemicals	24
2.1.11	Miscellaneous.	25
2.2	**Methods**	**25**
2.2.1	Standard methods.	25
2.2.2	DNA methods.	27
2.2.3	Transfection of eukaryotic cells.	28

2.2.4	Protein methods.	30
2.2.4.1	Purification of recombinant proteins.	30
2.2.4.2	m^7GTP-Sepharose affinity chromatography.	34
2.2.4.3	GST pull-down assay.	34
2.2.4.4	m^7GTP pull-down assay.	35
2.2.4.5	UV-cross-linking.	35
2.2.5	Preparation of substrate RNA.	35
2.2.5.1	Cap analysis.	37
2.2.6	PARN activity assays.	37
2.2.7	Sedimentation-equilibrium.	38
3.	**RESULTS**	**40**
3.1	Cap-dependent deadenylation by purified bovine PARN.	40
3.1.1	The 7-methyl guanosine cap stimulates deadenylation in HeLa cell extracts.	40
3.1.2	A m^7GpppG-capped RNA is the preferred substrate for bPARN.	41
3.1.3	Bovine PARN is a cap-binding protein.	45
3.2.	Cap-dependent deadenylation by recombinant human PARN.	46
3.2.2	Over-expression of hPARN in Schneider 2 cells.	48
3.2.3	Purification of hPARN from Schneider 2 cells.	49
3.2.4	Purification of recombinant 6xHis-tagged hPARN.	51
3.2.5	The N-terminal His6-tag does not influence the m^7cap-preference of hPARN.	52
3.3	The effect of the 7-methyl group in the 5´ cap structure on hPARN reaction mechanism.	54
3.3.1	Transient transfection and expression of hPARN in HEK293-EBNA cells.	54
3.3.2	Purification of recombinant hPARN expressed in HEK293-EBNA cells.	56
3.4	The m^7GpppG-cap induces a processive reaction mechanism.	58
3.5	HEK PARN has a higher affinity to the m^7G-cap than *E.coli* expressed PARN.	62
3.6	Deadenylation and translation	65
3.6.1	PARN-mediated deadenylation is inhibited by translation initiation factors.	65
3.6.2	Inhibition of deadenylation by translation initiation factors is independent of the cap.	66
3.6.3	The inhibitory effect on deadenylation does not depend on the RNA binding property of eIF4G.	71
3.6.4	eIF4G interacts with PARN	72

3.7 PARN is a homodimer 75

3.8 Identification of a mouse PARN homologue and investigation of its genomic organization. 77

4. DISCUSSION **80**

3.9 Cap-dependent deadenylation in cell extracts. 80

4.2 Cap-dependent deadenylation by purified PARN. 82

4.3 Cap-dependent deadenylation by recombinant hPARN. 83

4.3.1 Purification of recombinant hPARN expressed in mammalian cells. 83
4.3.2 Purification of recombinant hPARN from S2 cells 84
4.3.3 Post-translational modification of recombinant PARN restores a stringent cap-dependency. 85
4.3.4 HEK PARN has a higher affinity for the m^7G-cap than *E.coli* expressed PARN. 86
4.3.5 Binding of hPARN to the 5´cap induces a processive reaction mechanism . 87

4.4 PARN is a homodimer. 88

4.5 PARN acts via both processive and distributive reaction modes. 89

4.6 Trimming or rapid deadenylation? 91

4.7 Inhibition of PARN by translation initiation factors is independent of the 5´ cap. 92

4.8 A physical interaction between PARN and eIF4G. 93

5. SUMMARY **96**

6. REFERENCES **98**

7. APPENDIX

Plasmid maps of expression vectors A1
Abbreviations A2
Curriculum vitae A4
Acknowledgements A6

1. INTRODUCTION

Gene expression depends to a large extent on the concentration of mRNA in the cell which in turn is determined by the ratio between transcription and degradation. Transient expression of regulatory proteins, such as transcription factors or cytokines, is not only a consequence of transitory transcription but also the short lifetime of their mRNAs. In contrast, mRNAs that encode stable proteins such as α-globin have been shown to have extraordinarily long half-lives (*Holcik and Liebhaber, 1997*). The stability of a given transcript is determined by the presence of sequences within an mRNA known as *cis*-elements, which can be bound by trans-acting RNA-binding proteins forming mRNPs that inhibit or enhance mRNA decay. The half-life of individual mRNAs can be affected by a variety of stimuli and cellular signals including hormones, cell cycle progression and cell differentiation or stress treatment (*Shim and Karin, 2002*). A study using cDNA microarrays to estimate and compare the change in total transcript levels and the change in abundance of nascent transcripts following stress treatment of lung carcinoma cells revealed that mRNA stabilisation and destabilisation influenced the expression of approximately 53% of the stress-regulated genes (*Fan et al., 2002*). The regulatory potential of mRNA turnover therefore plays a more important role in gene expression than has been anticipated so far.

1.1. The major mRNA degradation pathways

Degradation of mRNAs in eukaryotes is usually initiated by a gradual shortening of the poly(A) tail (Figure 1.1). Evidence that the poly(A) tail removal is required for mRNA degradation comes from assessing the kinetics of deadenylation relative to the decay of several yeast and mammalian mRNAs (*Brewer and Ross,1988; Shyu et al., 1991, Decker and Parker, 1993*). Transcriptional puls-chase experiments showed that these mRNAs do not decay until their poly(A) tails have been shortened. Furthermore, transcripts that are known to be unstable are also deadenylated more rapidly than a stable transcript. The unstable yeast MFA2 transcript, for example, was deadenylated with a 3-fold higher rate (~13 As/min) than the stable PGK1 transcript (~4 As/min) (*Decker and Parker, 1993*). Sequences that cause rapid mRNA decay often do so by increasing the deadenylation rate (*Caponigro and Parker, 1996*). Thus, deadenylation is probably a rate limiting process in mRNA turnover.

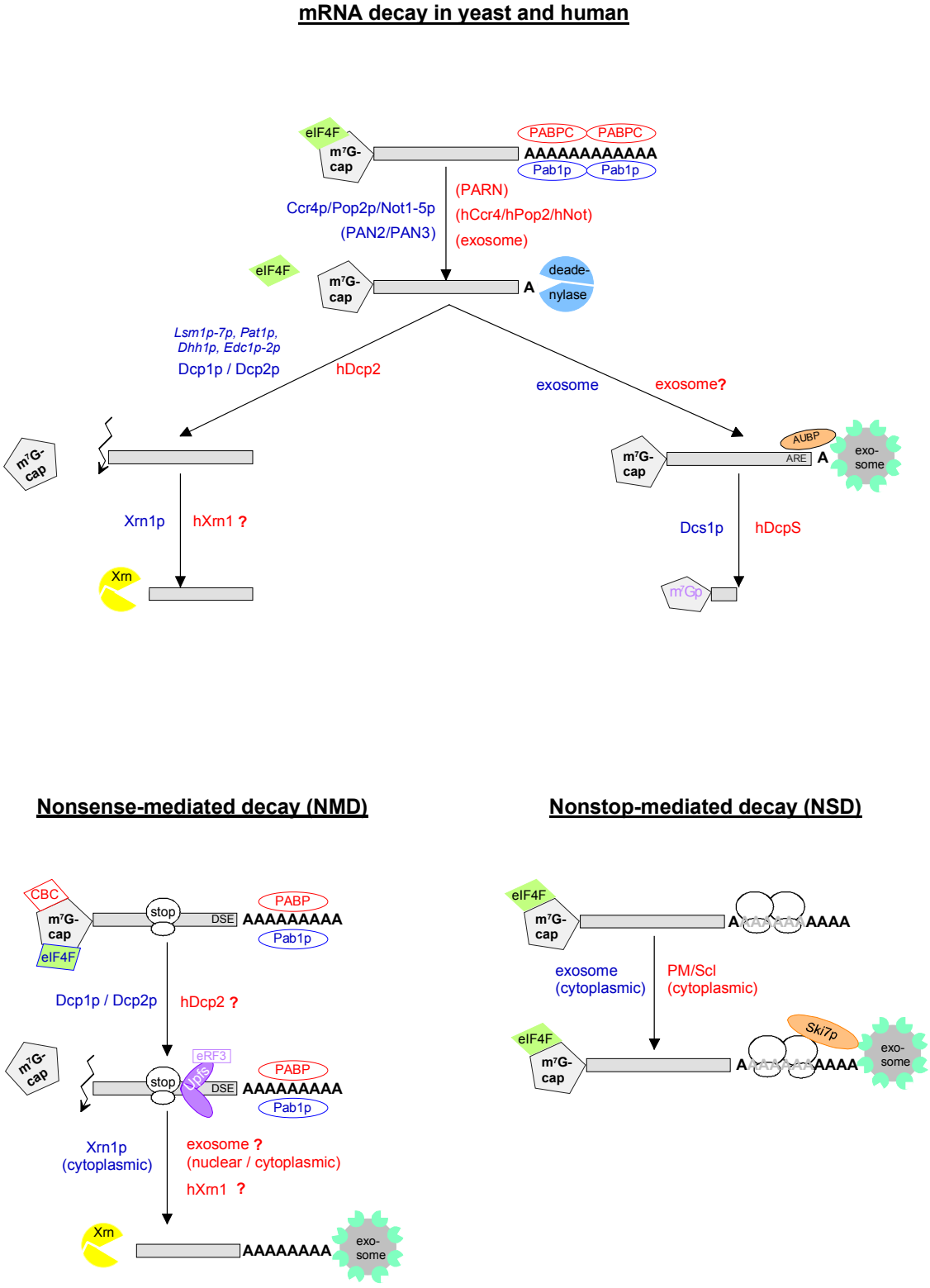

Figure 1.1. The major mRNA decay pathways in yeast and human. Yeast enzymes that are involved in the different steps are shown in blue and the human enzymes are indicated in red. The enzymes and pathways are described in the text.

The understanding of the mechanisms of mRNA degradation is mainly based on studies in *Saccharomyces cerevisiae*. Deadenylation of the 3´ poly(A) tail to a length that is too short to bind the major poly(A)-binding protein, Pab1p, leads to one of two different degradation pathways in yeast (Figure 1). First, the loss of Pabp1 leads to disruption of the eIF4F translation initiation complex (consisting of eIF4E, eIF4G and PABPC) which is bound to the 5´ cap structure via the cap binding protein eIF4E (see section 1.5.). This disposes the 5´ cap to be rapidly cleaved (*Muhlrad et al., 1994, 1995*). Decapping is followed by degradation of the mRNA body executed by a 5´-3´ exonuclease, Xrn1p (*Hsu and Stevens, 1993*).
Decapping in yeast requires at least two proteins, Dcp1p and Dcp2p, that physically associate with each other (*Beelman, et al., 1996*). Yeast Dcp1p is required for decapping *in vivo* but the recombinant protein is inactive. Thus, Dcp1p has been suggested to undergo a Dcp2p-dependent activation to become decapping competent (*Dunckley et al., 2001*). However, Dcp2p contains a MutT/Nudix motif in its N-terminus. This motif is found in a class of pyrophosphatases that hydrolyse a nucleoside diphosphate linked to another moiety and is required for catalytic activity of these enzymes. More recent data show that a recombinant C-terminal truncation of yeast Dcp2p functions as a decapping enzyme generating m^7GDP products (*van Dijk et al., 2002; Steiger et al., 2003*). It is therefore possible that the Dcp1p/Dcp2p complex consists of two different decapping enzymes. Furthermore, the human Dcp2 homologue has been shown to be the catalytically active decapping enzyme (*van Dijk et al., 2002; Wang et al., 2002*). The efficiency of the decapping reaction is stimulated by a complex of seven Lsm proteins and the Pat1p protein as well as Dhh1p, a member of the DEAD box family of RNA helicases (*Bonnenrot et al., 2000; Bouveret et al., 2000; Tharun et al., 2000*). Co-immunoprecipitation experiments revealed that the Lsm1p-7p complex preferentially interacts with deadenylated mRNAs, suggesting that transcripts bound to the Lsm complex are targeted for decay (*Tharun et al., 2000; Bouveret et al.,2000*). In addition, two related RNA-binding proteins, Edc1p and Edc2p, are enhancing the activity of the decapping enzyme possibly by binding to both the Dcp1p/Dcp2p complex and the mRNA substrate (*Dunckley et al, 2001; Schwartz et al., 2003*).

In the other pathway (Figure 1.1), poly(A) shortening leaves the 3´ end susceptible to a complex of 3´-5´ exonucleases called the exosome (*Muhlrad et al., 1995; Jacobs Anderson and Parker, 1998*). The exosome is a protein complex consisting of at least ten proteins and is highly conserved over evolution (*Allmang et al., 1999a; Brouwer et al., 2001*). Each of the core subunits is an essential protein presumably because defects in one exosome subunit cause

a failure to assemble the complex properly (*van Hoof and Parker, 1999*). The human counterpart to the yeast exosome, the PM/Scl complex, is recognized by autoimmune antibodies that are present in patients with polymyositis-scleroderma *(Reichlin et al., 1984*). Up to date, 10 human homologues to the yeast proteins have been identified although the PM/Scl complex is thought to consist of 11-16 proteins. Like in yeast, the human exosome has been detected in both the nucleus and the cytoplasm (*Brouwer et al., 2001*). The two forms differ by the presence of the nonessential Rrp6p (PM/Scl100 in humans) which is found specifically in the nuclear complex (*Allmang et al., 1999; Briggs et al., 1998*). Interestingly, cytoplasmic 3′ to 5′ mRNA degradation is inhibited by mutation of any of the exosome components except for the Rrp6p (*Mitchell and Tollervey, 2000*). The exosome was originally implicated in the processing and degradation of small nuclear RNAs (snRNAs), ribosomal RNAs (rRNAs), small nucleolar RNAs (snoRNAs) and pre-rRNA spacer fragments (*Mitchell et al., 1997; Allmang et al., 1999b: Allmang et al., 2000; van Hoof et al., 2000*). Individual, recombinant proteins of the exosome are active *in vitro* but the complex purified from yeast shows little activity (*Mitchell et al., 1997*). This implies that assembly of the proteins into the exosome complex might repress their activity and/or that certain cofactors were missing in the purification procedure. Such potential cofactors are ATP-dependent RNA helicases and GTPases (*Mitchell and Tollervey, 2000*). Considering the wide range of RNA substrates and the different modes of action, specific cofactors could act as exosome "adaptors" (*Jacobs Anderson and Parker, 1998*) or the exosome may interact directly with a RNP structure on the substrate (*Mitchell and Tollervey, 2000*). It should also be noticed that the exosome is different from the exonuclease that removes the poly(A) tail. Associated with the exosome is a scavenger decapping activity, DcpS in mammals (*Wang and Kiledjian., 2001*) and Dcs1p in yeast (*Liu et al., 2002*) that hydrolyses the residual cap after the body of the mRNA has been degraded.

Decapped mRNA decay intermediates have been isolated from mouse liver cells, and homologues of the yeast Dcp1,Dcp2, Lsm and Xrn1 proteins as well as the exosome complex have been identified in mammals. Thus, the two major pathways of decay are conserved in mammalian cells, but it is nevertheless unclear whether the body of the mammalian mRNAs is degraded primarily by 5′or 3′ exonucleases. Recent papers have suggested, that the 3′-5′ degradation by the exosome may be the major pathway of decay for at least some mammalian mRNAs *(Chen et al., 2001; Wang and Kiledjian, 2001; Mukherjee et al., 2002*). Although the exosome-mediated pathway in yeast is slower than the Xrn1p-mediated 5′-3′ pathway, the

mammalian and yeast cells could degrade mRNAs by the same mechanisms but the relative rates of the two pathways may vary (*van Hoof and Parker, 2002*).

1.2. Nonsense-mediated decay (NMD)

Cells have evolved complex mechanisms to remove aberrant transcripts which, if translated code for non-functional peptides. Such pathways function as sensors for inappropriate polypeptide synthesis. mRNA surveillance increases the fidelity of translation by degrading aberrant mRNAs that, if translated, would produce truncated proteins. Nonsense-mediated mRNA decay (NMD) eliminates transcripts with a premature stop codon.

NMD in yeast

NMD in yeast (Figure 1.1) involves the normal translation apparatus which, upon recognition of a premature termination codon, triggers decapping without prior deadenylation thereby allowing the 5′ to 3′ exonuclease, Xrn1p to degrade the mRNA body (*Muhlrad and Parker, 1994; Hagan et al., 1995; Beelman et al., 1996; Hatfield et al., 1996*). Additional proteins that are required in this process are the Upf1p, Upf2p and Upf3p proteins. Upf1p has been purified from yeast and shown to possess RNA binding as well as RNA-dependent ATPase and RNA helicase activities (*Czaplinski et al., 1995; Weng et al., 1996a*). Upf2p is an acidic protein without significant homology to other proteins and Upf3p is a protein that is able to shuttle between the nucleus and cytoplasm (*Cui et al., 1995; He and Jacobson, 1995; Shirley et al., 1998*). These proteins link the recognition of an improper translation termination event to rapid decapping by interacting with the translation-release factor eRF3 (*Weng et al., 1996b; Weng et al., 1998*). This complex is thought to inspect the mRNA in a 5′ to 3′ direction for a specific downstream element (DSE) or an intron mark. Upon recognition of the DSE the surveillance complex communicates a signal that the termination is premature (*Hilleren and Parker, 1999*).

NMD in mammalian cells

Most mammalian mRNAs, on the other hand, are subjected to NMD before they are released from an association with nuclei into the cytoplasm. However, NMD depends on reading frame recognition by ribosomes. If translation termination occurs more than 50-55 nucleotides upstream of the last 3′ exon-exon junction of an mRNA it will be recognized as premature termination and trigger NMD (*Zhang et al., 1998*). An exon-junction protein complex left

behind after RNA splicing was found to travel with the mature mRNA to the cytoplasm and might be recognised by the surveillance complex as a downstream signal. One or more proteins in this complex could recruit Upf3, a nucleocytoplasmic shuttling protein, which then interacts with the cytoplasmic Upf2 and Upf1 proteins (*Le Hir et al., 2000; Lykke-Andersen et al., 2000*). Therefore, one possibility is that NMD takes place when the mRNA still is associated with the nucleus but translated by cytoplasmic ribosomes. Evidence for a pioneering round of translation that leads to NMD while mammalian mRNAs are still bound to the nuclear cap binding complex and the nuclear poly(A) binding protein, was provided by the Maquat lab. (*Ishigaki et al., 2001*). Also, significant amounts of the translation initiation factor eIF4G have been found in the nucleus (*Fortes et al., 2000; McKendrick et al., 2001*).

1.3. Nonstop-mediated decay (NSD)

Transcripts lacking termination codons are also subjected to rapid degradation, however the mechanism is quite different from NMD. Unlike NMD, nonstop decay (NSD) is localised to the cytoplasmic compartment in both mammalian and yeast cells. Furthermore, degradation of "nonstop" mRNAs is performed by the cytoplasmic form of the exosome, a process that begins at the 3´-poly(A) tail and requires the exosome-associated protein Ski7p. The cytoplasmic Ski7p protein is related to the translation elongation factor EF1A and the translation termination factor eRF3. Therefore, the function of Ski7p may be to distinguish nonstop from normal mRNAs by binding to the empty A site of stalled ribosomes that have reached the 3´ end of a mRNA. This interaction could bring the exosome to the mRNA as Ski7p interacts with both the ribosome and the exosome (*van Hoof et al., 2002; Frischmeyer et al., 2002*) see Figure 1.1.

1.4. *cis*-elements and *trans*-acting factors controlling mRNA decay in somatic cells

Searches for sequences that modulate mRNA stability, have revealed several types of *cis*-acting sequence elements that are found throughout the message. Many of these elements promote rapid degradation of the mRNA by stimulating deadenylation. The mRNAs for transiently expressed proteins such as transcription factors, growth factors, cytokines and proto-oncogenes usually contain AU-rich elements (AREs). Three different subclasses of AREs: class I AREs contain one to three copies of AUUUA repeats embedded in U-rich sequences and are present in early response genes (*c-fos*, *c-myc*) and cytokine encoding genes;

class II AREs contain five to eight AUUUA copies and are only found in cytokine mRNAs (GM-CSF, TNF-β and IL-3); class III AREs are lacking the AUUUA repeats but contain a long U-rich region; these elements are found in the *c-jun* proto-oncogene and β-adrenergic receptor mRNAs. Apparently, class I and class III AREs mediate a distributive poly(A)-tail shortening whereas class II ARE-containing mRNAs are deadenylated in a processive manner (*Xu et al., 1997*).

The effect on mRNA stability is mediated by different mechanisms. ARE-binding proteins, either stabilize the transcript by preventing recognition or destruction by RNases or facilitate mRNA degradation by altering the RNA secondary structure or physically recruit RNases. Examples of stabilizing proteins include a class of mammalian proteins that are closely related to the *Drosophila* neuron-specific RNA-binding protein ELAV (*Campos et al, 1985; Jain et al., 1997; Fan and Steitz, 1998a*). In humans, there are four members; HuR is expressed in all proliferating cells, whereas Hel-N1, HuC and HuD are expressed in terminally differentiated neurons *(Peng et al., 1998*). All members of the ELAV Hu family contain three RNA-interacting domains of the RRM (RNA recognition motif) type (*Szabo et al.,1991*) The first two domains recognize and specifically associate with the ARE sequences whereas the third domain seems to bind the poly(A) tail (*Ma et al., 1997*). HuD/HuR travel between the nucleus and cytoplasm due to the presence of a nuclear-cytoplasmic shuttling signal (*Fan and Steitz, 1998a; 1998b; Atasoy et al., 1998*). A yeast ARE-binding protein, Pub1p, has been identified and shown to belong to the ELAV protein-family (*Vasudevan and Peltz, 2001*).

Another ARE-binding protein (AUF1) was originally identified from an enriched protein fraction that accelerated ARE-dependent *in vitro* mRNA decay of *c-myc* mRNA (*Brewer, 1991*). Similar *in vitro* stimulating activity was later demonstrated for the degradation of *c-fos*, GM-CSF and the β-adrenergic receptor mRNAs (*Xu et al., 2001; Buzby et al., 1999, Pende et al., 1996*). Nevertheless, ubiquitination and degradation of AUF1 by proteasomes have been associated with rapid decay of GM-CSF in HeLa cells, an observation that suggests a stabilising role for AUF1 (*Laroia et al., 1999*). cDNA cloning and sequencing revealed that AUF1 belongs to the hnRNP-D protein family (*Zhang et al., 1993*; *Kajita et al., 1995*), which are proteins that may be able to shuttle between the nucleus and the cytoplasm (*Dreyfuss et al., 2002*).

Tristetraprolin (TTP) is an ARE-binding protein that promotes deadenylation and decay of TNF and other cytokine mRNAs. TTP-deficient mice showed many inflammatory symptoms due to increased stability of TNFβ and GM-CSF mRNAs (*Lai et al., 1999;*

Carballo et al., 1998; 2000). Another ARE-binding protein distantly related to TPP, butyrate response factor-1 (BRF1), was identified in a retroviral cDNA library screen to rescue a mutagenized cell line that fails to degrade cytokine mRNA. BRF1 was found in all revertants with reconstituted rapid mRNA decay. Both BRF1 and TTP are localized in the cytoplasm as well as in the nucleus and belong to a protein family containing two characteristic zinc finger domains (*Stoecklin et al., 2002*). In fact, TTP binds to the ARE in TNF-β mRNA via its zinc finger domains (*Carballo et al., 1998; Lai et al., 1999*).
RNAs which are destabilized by AREs are stabilized in lysates that have been immuno-depleted with anti-exosome antibodies, suggesting that the AREs are recruiting the exosome. This can be accomplished either by the binding of one of the exosomal subunits directly to transcripts that contain an ARE (*Mukherjee et al., 2002*) or via ARE-binding proteins that physically interact with the exosome. ARE-crosslinked proteins that were precipitated with anti-PM-Scl antibodies identified AUF1, TTP and KSRP, a K-type RNA-binding protein that is capable of promoting ARE-mediated decay. HuR, although readily crosslinked, was neither immunoprecipitated nor could it be detected in purified exosome preparations. Hence, the inability of HuR to interact with the exosome might be a part of its stabilizing feature (*Chen et al., 2001*).

The Pumilo-homology domain-protein family (Puf) of RNA-binding proteins that are known to bind to specific 3´-UTRs and regulate key steps in early development. Members of the Puf-protein family have been found in the genomes of flies, humans, worms, plants and yeast (*Zamore et al., 1997*). Puf3p is the first yeast protein that has been shown to promote deadenylation by binding to the *COX17* mRNA 3´-UTR in a transcript-specific manner. Puf3p does not affect translation but interacts directly with the mRNA degradation machinery. Hence, Puf-proteins, as specific regulators of mRNA deadenylation, have been conserved throughout eukaryotes (*Olivas and Parker, 2000*).

The AREs are generally found in the 3´UTR of a transcript but destabilizing elements have also been found in the coding region. Interestingly, the distance between these fairly large elements and the poly(A) tail determines their destabilising function (*Grosset et al., 2000*). Such coding region instability determinants (CRD) have been found in *c-fos* (*Wellington et al., 1993; Schiavi et al., 1994*), *c-myc* (*Wisdom and Lee, 1991*) *Drosophila fushi tarazu* (*Ito and Jacobs-Lorena, 2001*) and MAT1α (*Parker and Jacobson, 1990*) mRNAs. The function of the CRDs requires movement of the ribosome across the RNA that contains them. Five

CRD-associated proteins have been identified so far: Unr, a purine-rich RNA binding protein; the cytoplasmic poly(A) binding protein, PABPC; PAIP-1, a PABPC interacting protein; hnRNP D; and NSAP1, an hnRNP R-like protein. These proteins form a multiprotein complex that might bridge the poly(A) tail to the major CRD (mCRD) in the *c-fos* mRNA. As the ribosome transits the mCRD the complex may be disrupted leading to deadenylation and decay of the transcript (*Grosset et al., 2000*).

1.5. Translation

Changing the translational status of a mammalian or yeast mRNA by mutations or by addition of translation inhibitors can alter the degradation rate of a mRNA (*Jacobson and Peltz, 1996*) indicating that translation and mRNA turnover are connected (see also NMD, section 1.2 and NSD, section 1.3 above). Some proteins are also involved in both processes (e.g.Upfs).
Protein synthesis can be divided into three steps: initiation, elongation and termination. This process is regulated by soluble proteins called initiation factors (IFs), elongation factors (EFs) and termination factors (RFs) respectively (*Hershey, 1991*)

Initiation

Formation of the initiation complex is rate limiting in translation and the most frequently targeted step for control. The first event in initiation of translation is the dissociation of the pre-existing 80S ribosomes into 40S and 60S subunits (Figure2). This is promoted by eIF3 and eIF1A, which bind to the 40S ribosomal subunit, and prevents its association with the 60S subunit. Another initiation factor, eIF6, has been shown to bind the 60S subunit to prevent association with the 40S subunit although the role of eIF6 in translation initiation has been questioned (*Si and Maitra, 1999*). An initiation-specific, aminoacylated Met-tRNA$_i$ from the cytoplasmic pool of tRNAs binds to eIF2-GTP. The eIF2-GTP-Met-tRNA$_i$ ternary complex then join the 40S subunit, together with eIF3 and eIF1A, to form the 43S pre-initiation complex.

Attachment of the 43S complex to the capped 5′ end of an mRNA requires a set of initiation factors termed eIF4F. This is a heterotrimeric complex consisting of eIF4E, eIF4G and eIF4A. eIF4G exist in two isoforms (eIF4GI and eIF4GII) that possess similar biochemical activities. The most abundant form (eIF4GI) has a predicted molecular mass of 171 kDa (*Gradi, et al.,*

1998) with binding sites for eIF4E, eIF4A, eIF3 and the cytoplasmic poly(A)-binding protein, PABPC. The carboxy-terminal (C-terminal) domain of eIF4G interacts with eIF4A, an RNA-dependent ATPase and RNA helicase, and a protein kinase specific for eIF4E, Mnk-1 (*Tarun et al., 1997*). Another binding site for eIF4A has been found in the central domain of eIF4G (*Imataka and Sonenberg, 1997*). eIF3, which binds the 40S ribosomal subunit, also interacts with the central domain of eIF4G *(Lomakin et al.,2000; Morino et al., 2000; Korneeva et al., 2000*). This interaction is thought to be involved in the delivery of the 40S ribosomal subunit near the 5′ cap on the mRNA. The binding-sites for eIF4E and PABPC reside in the amino-terminal (N-terminal) one-third part of the protein. Assembly of the eIF4F complex on mRNA is mediated by the cap-binding protein, eIF4E. However, the binding affinity of eIF4E to the cap-structure is weak but can be increased more than 10-fold by the interaction with eIF4G (*Haghihat and Sonenberg, 1997; Ptushkina et al., 1998*), indicating that the eIF4F complex might be formed before binding to the 5′-cap. The binding of PABPC to eIF4G explains how the poly(A)-tail and the cap synergistically can act in stimulating translation (*Gallie, 1991; Iizuka et al., 1994*). Because eIF4G is complexed to eIF4E, the PABPC-eIF4G interaction circularises the mRNA. In fact, addition of purified yeast eIF4G, eIF4E and Pab1p proteins to capped and polyadenylated mRNAs resulting in circularisation was observed by atomic force microscopy (*Wells et al., 1998*).

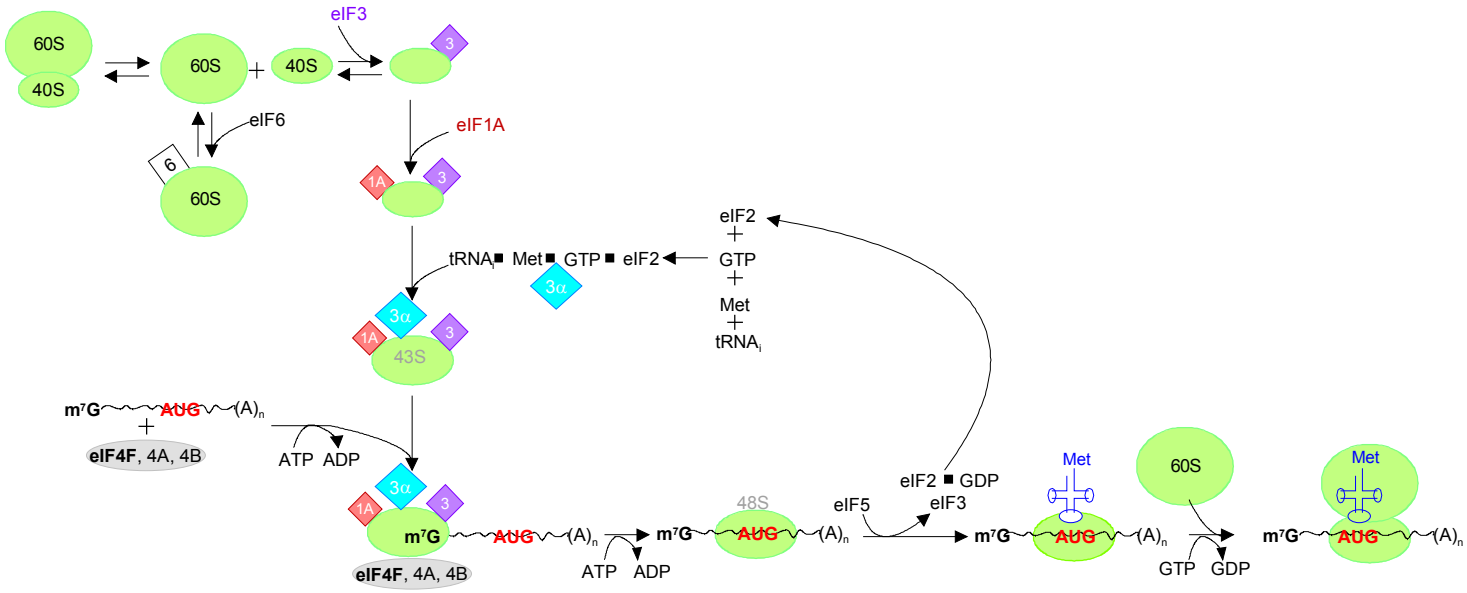

Figure 1.2. Mechanism of eukaryotic translation initiation. Adapted from Gingras et al., 1999; The role of the eIF4F complex in initiation is discussed in the text

Following binding of the 43S complex to the m^7G-cap proximal region of the mRNA, the ribosomal complex now moves in an ATP dependent manner from this initial binding site along the 5´-untranslated region (5´-UTR) until it locates an initiation codon in a favourable sequence context. This process is called scanning (*Kozak, 1989*). A 48S initiation complex is then formed with the Met-$tRNA_i$ positioned at the start codon. The associated initiation factors are released in a process mediated by a GTPase-activating protein (GAP), eIF5, which promotes GTP hydrolysis by eIF2. Dissociation of the initiation factors allows the joining of the large 60S ribosomal subunit to form an 80S ribosome, leaving the initiator tRNA in the P site of the ribosome ready to enter the elongation phase of translation (*Gingras et al., 1999; Hershey and Merrick, 2000; Pestova and Hellen; 2001*)

Elongation

The elongation phase works in a cyclic manner and adds one amino acid at a time to the growing polypeptide using the sequence of codons on mRNA as template. Three factors, eEF1A, eEF1B and eEF2 are controlling the elongation cycle. eEF1A complexed with GTP aids in positioning the aminoacylated tRNAs to the matching codons in the A site of the small ribosomal subunit. The tRNA is brought into the peptidyl-transferase centre where the new peptide bond is formed and eEF1A-GDP is recycled by the nucleotide exchange factor eEF1B. The last step of the elongation cycle involves eEF2-GTP, which controls the advance of the ribosome by exactly three nucleotides of the mRNA. The incoming tRNA is thereby moved into the P site, the deacylated tRNA is moved into the exit site (E site) and the next codon is exposed in the A site. (*Andersen and Nyborg, 2001*).

Termination

At least two proteins are necessary for efficient termination, class-1 release factor (eRF1) that recognises all three termination codons in eukaryotes and the class-2 release factor (eRF3), which binds guanine nucleotides and stimulates eRF1 activity. Based on the crystal structure, eRF1 was proposed to have a structurally anticodon-like loop by which it could to bind the A site of the ribosome and mediate a nucleophilic attack on the ester bond of the peptidyl-tRNA molecule in the P site, resulting in hydrolysis of the nascent polypeptide chain (*Song et al., 2000*). Peptide hydrolysis is followed by steps that involve removing the release factor(s) from the A site of the ribosome, separating the ribosomal subunits and dissociating the tRNA (*Frolova et al., 1996*). The Upf proteins are factors shown to be involved in the nonsense-mediated mRNA decay (see section 1.2.) and to interact with the release factors (*Czaplinski et*

al., 1995, 1998). Consequently Upf/RF complexes might be important for translation termination efficiency.

1.6. Deadenylation and translation

The rate limiting step of "normal" mRNA decay in eukaryotes seems to be the shortening of the poly(A) tail, as this process is slower than the subsequent decapping and degradation of the mRNA body. Because the presence of a poly(A) tail can enhance translation initiation, deadenylation also leads to a decreased rate of translation.

Deadenylation in somatic cells

For the eukaryotic translation apparatus, the mRNA 5′ cap is a recognition element that serves as a focal point for the assembly of initiation factors and ribosomes. For the cellular degradation machinery, the cap represents a barrier to the 5′-3′ exonuclease activity. Mutations in yeast translation eIFs increase the rate of deadenylation. Mutations in the translation initiation factor eIF4E, eIF4A, eIF4GI and a component of the eIF3 complex (Prt1) increase the deadenylation rate of PGK1 mRNA threefold over the wild-type strain. These observations indicate that the status of the translation initiation complex plays a role in modulating the deadenylation rate for yeast mRNAs (*Schwartz and Parker, 1999*). This conclusion is also supported by other observations. The insertion of a stem-loop into the PGK1 5′ UTR to inhibit ribosome assembly leads to a higher rate of deadenylation *(Muhlrad et al., 1995*). Alterations of the PGK1 5′ UTR and AUG context, which decrease the translation initiation rate, also increase the rate of deadenylation (*LaGrandeur and Parker, 1999*). AU-rich elements known to promote deadenylation in mammalian cells have also been observed to inhibit the translation initiation rate (*Kruys et al., 1989*). Moreover, the human ferritin L-chain mRNA shows changes in poly(A) tail length based on the translational status of the transcript. Translational repression by iron-regulatory proteins binding to the iron-responsive element of ferritin L-chain mRNA induces deadenylation. Furthermore, ribosome association with the ferritin L-chain mRNA seems to represent a determinant for induction of deadenylation since polyribosome release inhibitors are able to induce a shortening of the poly(A) tail but not translation inhibitors that preserve the ribosomal association (*Muckenthaler et al., 1997*).

Deadenylation during development

Early development relies mainly on post-transcriptional regulation. From oocyte maturation to the mid-blastula transition, no detectable transcription occurs and all proteins that are synthesized are the products of maternal mRNAs. Two mechanisms have been described that control mRNA translation in early development. The first mechanism is associated with regulated changes of the poly(A) tail. The second mechanism is independent of the poly(A) tail but depends on another sequence element named TIE (translational inhibitory element) (*Robbie et al., 1995*).

Usually, polyadenylation leads to an up-regulation of translation and deadenylation to a translational inactivation or reduced translation (*Standart and Jackson, 1990; Richter, 1999*). Maturation-specific deadenylation has little effect on the stability of the mRNA body until the mid-blastula transition (*Audic et al., 1997; Voeltz and Steitz, 1998*). Most mRNAs contain a conserved hexanucleotide sequence (AAUAAA) within their 3´ UTR, which directs polyadenylation of newly transcribed mRNAs in the nucleus (*Wickens et al., 2000*). Some mRNAs contain a cytoplasmic polyadenylation element, CPE ($UUUUA_{1-2}U$), which promotes poly(A) tail-lengthening in maturing oocytes. Initiation of oocyte maturation in *Xenopus laevis* coincides with a breakdown of the nuclear membrane and redistribution of a poly(A) specific ribonuclease, PARN. *Xenopus* PARN has been shown to be responsible for the so called default deadenylation of maternal mRNAs in *Xenopus* oocytes (*Körner et al., 1998; Copeland and Wormington, 2001*). Transcripts that do not contain a CPE are substrates for default deadenylation, an event that coincides with their translational quiescence (*Fox and Wickens, 1990; Varnum and Wormington, 1990*). A subclass of the CPE containing mRNAs is deadenylated after fertilisation. For example, the Eg mRNA family (Eg1-cdk2, Eg2, Eg5 and *c-mos*) contain another sequence element in the 3´ UTR named EDEN (embryo deadenylation element) which promotes their deadenylation following egg fertilisation (*Bouvet et al., 1994; Sheets et al., 1994*). An EDEN-binding protein has been identified and suggested to mediate the poly(A) tail-shortening by interacting with a deadenylase *(Paillard et al., 1998*). Furthermore, ARE sequences in the *c-mos* and *c-jun* mRNAs act to enhance EDEN-directed deadenylation in a position-dependent manner (*Ueno and Sagata, 2002; Paillard et al., 2002*).

Translational regulation of the *hunchback* (*hb*) mRNA is essential for *Drosophila* embryonic posterior patterning. Unlocalized maternal *hb* mRNA, with a Nanos response element (NRE) in the 3´ UTR, binds the Pumilio protein. Another protein, Nanos, associates with an assembled Pumilo-*hb* mRNA complex via protein-protein and protein-RNA interactions causing deadenylation and translational repression of the *hb* mRNA at the posterior pole of the embryo. This event restricts the Hunchback protein to the anterior half of the embryo (*Wharton et al., 1998; Sonoda and Wharton, 1999*). Similarly, the FBF protein in *C. elegans* is required for repression of the *fem-3* mRNA to achieve the hermaphrodite switch from spermatogenesis to oogenesis by binding to the *fem-3,* 3´ UTR (*Zhang et al., 1997*). In contrast, the *tra-2* mRNA must be repressed to permit spermatogenensis. Translational repression of *tra-2* mRNA is mediated by so-called TGE (tra-2 and GLI element) sequences in its 3´ UTR, that promote deadenylation (*Thompson et al., 2000*).

An *in vitro* extract system has recently been developed from *Xenopus* oocytes that recapitulated ARE-mediated mRNA deadenylation. This work resulted in the identification of a protein called embryonic poly(A)-binding protein (ePAB), which binds to AREs and is present in late oocytes and early embryos. The sensitivity of deadenylation to the level of ePAB suggests that this protein may be a potential regulator of mRNA deadenylation and translation during early development (*Voeltz et al., 2001*)

1.7. Deadenylating nucleases

Yeast

Two different deadenylating activities have been identified in *Saccharomyces cerevisiae*. The first activity to be found was a poly(A) nuclease complex named PAN. This activity requires the poly(A)-binding protein, Pab1p, for its activity *in vitro*. (*Sachs and Deardorff, 1992*). PAN is composed of two subunits, Pan2p and Pan3p, of which Pan2p is postulated to be the catalytic subunit since this protein is a member of the RNaseD family of exonucleases (*Boeck et al., 1996, Brown et al., 1996 and Moser et al., 1997*). PAN has been proposed to play a role in the nucleus by trimming nascent poly(A)-tails to a length of 50 to 90 nucleotides before export to the cytoplasm (*Brown and Sachs, 1998*) but might also participate in cytoplasmic deadenylation (*Tucker et al., 2001*). However, the two PAN subunits do not have an essential

function since both Δpan2 and Δpan3 yeast strains are viable. Moreover, these strains show only a minimal effect on deadenylation *in vivo* (*Boeck et al., 1996; Brown et al., 1996*).

The second deadenylating activity consists of two proteins that previously have been defined as transcriptional regulators. These are the carbon catabolite repression 4 (Ccr4) and the Ccr4-associated factor (Caf1) proteins. Database searches disclosed that both proteins have nuclease domains. The Ccr4 belongs to a magnesium dependent endonuclease-related family of nucleases and the Caf1p/Pop2p, may be a nuclease belonging to the RNaseD family of exonucleases (*Dlakic, 2000; Moser et al., 1997*). Pop2 homologues in mammalian cells and in *C. elegans* contain all three Exo motifs described by Moser et al., 1997 but yeast Pop2 is missing the third Exo motif. Nevertheless, Pop2p not only copurifies with a deadenylase activity in a Ccr4-dependent manner (*Tucker et al., 2001*), but also a ΔPop2p strain is defective in mRNA degradation and accumulates mRNAs with extended poly(A) tails (*Daugeron et al., 2001*). Both Ccr4p and Pop2p are required for normal rates of deadenylation in yeast although Ccr4p was suggested to be the catalytic subunit (*Tucker et al., 2002*). Even if Pop2p may have nuclease activity (*Daugeron et al., 2001*), over-expression of Pop2p does not suppress deadenylation defects in a Δccr4 strain (*Tucker et al., 2002*). Furthermore, Pop2p purified from a Δccr4 strain fails to show deadenylase activity *in vitro* (*Tucker et al., 2001*). Instead, it was proposed that Pop2p either directly or through additional protein-protein interactions acts to increase the activity of Ccr4p. Both Ccr4p and Pop2p are found in two large protein complexes that have been proposed to be involved in transcription (*Liu et al., 1998; Bai et al., 1999*). The core component of the smaller complex (~0.9 MDa) appears to be Not1p. Pop2p binds to the central region of Not1p and links Ccr4p to the rest of the NOT proteins. The larger complex (~1.9 MDa) includes, in addition to the five Not proteins, Ccr4p, Pop2p and several other proteins. The localisation of Not1p and Not2p in the cytoplasm and the finding that lesions in some of the NOT genes lead to defects in mRNA deadenylation rates, confirmed that the Ccr4p/Pop2p/Not complex is the cytoplasmic deadenylase in yeast (*Tucker et al., 2002*).

Mammals

cDNAs encoding human NOT2, NOT3, NOT4, CAF1 (POP2) and a CALIF (CAF-like factor) have been isolated. Interactions between the human proteins as well as between the human and yeast proteins have been demonstrated (*Bogdan et al., 1998; Albert et al., 2000; Dupressoir, 2001*). The conserved catalytic residues in yeast and human CCR4 related to the

Mg^{2+}-dependent endonuclease core and the ability to interact with the POP2 and NOT proteins suggested that a hCCR4/hPOP2/hNOT complex might be involved in mRNA deadenylation in mammals as well (*Dupressoir et al., 2001*). Furthermore, human CCR4, expressed in yeast did show deadenylating activity *in vitro* but failed to complement the phenotypes that are associated with ccr4p mutant yeast strains (*Chen et al., 2002*).

A bovine poly(A) specific 3´-exoribonuclease has been purified by C. Körner (*Körner and Wahle, 1997*). Based on the estimated deadenylation activity in extracts from calf thymus, a 140 000-fold purification was obtained. A 74 kDa polypeptide that co-purified with the activity was enriched during purification. The poly(A) degrading activity was named DAN, but was later renamed PARN (poly(A)-specific ribonuclease). Biochemical analysis showed that bovine PARN is a 3´-5´ exoribonuclease that releases 5´-AMP and requires a free 3´-hydroxyl group. This PARN activity has an absolute requirement for Mg^{2+} that cannot be replaced by Mn^{2+} or Ca^{2+}; a salt optimum of 120 mM potassium acetate or 100 mM potassium chloride; and a pH optimum at 7. In the presence of 120 mM potassium acetate, PARN degraded only poly(A). However, in the absence of salt, but with spermidine, poly(A) and poly(U) were degraded equally. Poly(A) was shortened in a synchronous manner indicating a distributive mode of action. Using HeLa cytoplasmic extract C. Körner showed that polyadenylated L3pre RNA was degraded with predominant decay intermediates that differed in length of about 30 nucleotides. The decay pattern was attributed to the binding of PABPC to the poly(A) tail based on two observations; first, the degradation intermediate pattern is consistent with the number of nucleotides that PABPC covers (~27 nt) and second, overexpression of PABPC in *Xenopus* oocytes protected mRNA from being deadenylated. Furthermore, the decay pattern could be reproduced with purified PARN and recombinant PABPC proteins (*Körner and Wahle, 1997*). More recent papers have shown that a proteolytic fragment of PARN was previously purified from HeLa cell nuclear extracts (*Åström et al., 1991; Åström et al., 1992; Martinez et al., 2000*).

Full-length human PARN (hPARN) cDNA has been cloned and sequenced. Database searches revealed that the predicted amino acid sequence of hPARN shows homology to the RNase D family of 3´-exonucleases. The amino acids known to be essential for catalytic activity are arranged in three clusters and are highly conserved within the protein family. Overexpression of hPARN in *Escherichia coli* showed that the recombinant protein has properties that are similar to the purified bovine PARN. Using affinity-purified antibodies, a diffuse staining in the cytoplasm of HeLa cells was observed but nuclear staining with a stronger signal in the

nucleoli was also detected, indicating that PARN is localised in both compartments. Furthermore, anti-PARN antibodies microinjected into *Xenopus* oocytes inhibits default deadenylation during progesterone-induced maturation. Ectopic expression of hPARN in enucleated oocytes rescues maturation-specific deadenylation showing that human PARN and the amphibian deadenylating activity are functionally equivalent (*Körner et al., 1998*).

Xenopus laevis

The default deadenylating activity in *Xenopus laevis* has been purified and identified as a homologue of hPARN. Full-length cDNA has been cloned and sequenced and it was found that human and *Xenopus* PARN (xPARN) share 72% overall identity but the C-terminal region shows more heterogeneity than elsewhere. xPARN belongs to the RNase D protein family, has a putative RNA recognition motif and contains a domain which is conserved among helicases known as minichromosome maintenance proteins. The deadenylating activity, purified from *Xenopus* ovary, copurified with two polypeptides of 74 kDa and 62 kDa, which both cross-react with anti-hPARN antibody. Subcellular localisation of xPARN showed that the p62 protein is cytoplasmic whereas p74 is localised in the nucleus (*Körner et al., 1998*). p74 is suggested to be a precursor of the p62 polypeptide since this species seem to be a proteolytic cleavage product of the larger protein. Interestingly, a putative nuclear localisation signal found in the C-terminal part of xPARN, suggests that this region may be required for nuclear localisation. Hence, proteolysis in this region may explain the subcellular localisation of the two xPARN species. xPARN is a 3′-5′exonuclease with 5′ AMP as products. Mg2+ is required for catalysis but not for RNA binding. Optimal salt concentration ranges from 50 to 100 mM KCl and the pH optimum is from 6.5 to 8. The presence of nonionic detergents or an RNase A inhibitor does not affect activity. xPARN degrades only poly(A) but the 3′most nucleotide does not have to be an A residue. (*Copeland and Wormington, 2001*).

A differential display screen designed to isolate rhythmic genes from *Xenopus laevis* retina identified a novel gene, nocturnin. The nocturnin mRNA is exclusively located in the rods and cones of the photoreceptor cell layer of the *Xenopus* retina. These cells are the location of the circadian clock that drives the rhythmic release of melatonin (*Green and Besharse, 1996*). Nocturnin homologues have been cloned from human, cow, chicken and *Drosophila*. Sequence database analyses revealed that nocturnin is a “novel” protein, similar in sequence only to the C-terminus of Ccr4p in *Saccharomyces cerevisiae*. Nocturin and Ccr4p belong to

the family of magensium-dependent nucleases with low overall sequence homology. However, the members of this protein family share pockets of similar amino acid residues. The conserved residues, including a magnesium-binding domain are important for catalysis (*Dupressoir et al., 2001; Whisstock et al., 2000; Diskic, 2000; Chen et al., 2002; Green, 2003*).

Recombinant GST-nocturnin was shown to be a poly(A) specific ribonuclease by several criteria: i) incubation with polyadenylated G52 RNA substrates produced an accumulation of poly(A)$^-$ substrate, ii) addition of cold polydeoxyadenylic acid (poly(dA)) had no effect on poly(A) tail removal, iii) an RNA substrate with a poly(G) tract at the 3′ end was not degraded and iv) a substrate containing three non-adenylate residues after the poly(A) tail is not degraded. In contrast to Ccr4p, which distributively degrades both ssDNA and *RNA (Chen et al., 2002*), nocturnin degrades only RNA and function in a processive manner. Retina extracts taken at different times throughout the day showed different levels of nocturnin protein with maximum at late night and early morning. In comparison, xPARN did not show such rhythmic expression but was present in equal amounts throughout the day, suggested that the nocturnin may deadenylate a different set of mRNAs (*Baggs and Green, 2003*).

1.8. Aim of this thesis

The poly(A) specific ribonuclease, PARN (formerly DAN) was purified from calf thymus and characterized by C. Körner (*Körner and Wahle, 1997*). The PARN cDNA from human (hPARN) was later cloned and sequenced, and was found to be a member of the RNaseD family of exonucleases (*Körner et al., 1998*). Purified recombinant hPARN, expressed in *E. coli* was able to rapidly degrade a capped and polyadenylated RNA in the presence of potassium salt. However, the activity under this condition was almost ten-fold lower than the nuclease activity purified from calf thymus (*Körner et al., 1998*). The activity of the bovine PARN (bPARN) preparation might be influenced by a post-translational modification, such as phosphorylation or glycosylation. Additionally, the nuclease preparation from calf thymus still contained other proteins and a possible activating factor might be associated with the purified nuclease in a substochiometric amount. One aim of this thesis is therefore to express and purify hPARN from eukaryotic cells and to characterize the recombinant nuclease. A m^7GpppG-cap at the 5′ end of RNA substrates appears to stimulate bPARN mediated deadenylation, whereas the activity of the recombinant enzyme does not seem to be affected

(*Körner, 1998b*). The nature of this stimulation will be investigated for the authentic as well as the recombinant nuclease. Furthermore, the significance of a 5´ cap on the processivity of PARN will be studied. A cap structure at the 5´ end of mRNA also plays an important role in initiation of translation and consequently, a possible interplay between translation initiation factors and PARN will be examined.

2. MATERIALS AND METHODS

2.1 Materials

2.1.1 Bacterial strains and cell lines

Bacteria

DH5α	*E.coli* K12, F^- *end*A1 *hsd*R17($r_{K-}m_{K+}$) *sup*E44*thi*-1 *rec*A1*gyr*A (Nal^r) *rel*A1 D(*lac*IZYA-*arg*F)U169 *deo*R [Φ80*dlac*D(*lacZ*)M15]
XL1 blue	*E.coli* K12, *rec*A1 *end*A1 *gyr*A96 *thi*-1 *hsd*R17 *sup*E44 *rel*A1 *lac*[F^- *pro*AB *lac*$I^qZ\Delta$M15 Tn*10* (Tet^r)]
BL21 (DE3) pUBS	*E. coli* B, F^- *dcm omp*T *hsd*S($r_{B-}m_{B-}$) *gal* λ(DE3) [pUBS]
BL21-CodonPlus®	*E.coli* B, F^- *omp*T *hsd*S($r_B^-m_B^-$) *dcm*+ Tet^r *gal* λ *end*A Hte [*arg*U *ilr*Y l*eu*W Cam^r]

Cell lines

HEK293-EBNA	permanent line derived from primary human embryonic kidney cells transformed by adenovirus type 5 (Ad 5) and consitutively expressing the Epstein-Barr nuclear antigen EBNA (Invitrogen)
Schneider 2 (S2)	permanent line derived from a primary culture of late stage (20-24 hours old) *Drosophila melanogaster* embryos (Schneider, 1972) (Invitrogen)

2.1.2 Culture media

LB (Luria Bertani)	1% (w/v) peptone, 0.5% (w/v) yeast extract,1% NaCl, pH 7
Schneider´s insect medium	(Sigma). Prepared as described by the manufacturer and sterile filtered through a OE 66 membrane (Schleicher&Schuell) in a pressure filter holder (Schleicher&Schuell)
SF-900 II SFM	(Gibco/BRL). Prepared as described by the manufacturer and sterile filtered through a OE 66 membrane (Schleicher&Schuell) in a pressure filter holder (Schleicher&Schuell)
Fetal calf serum (FCS)	(Biochrom)
Pluronic® F-68	(Gibco/BRL)

2.1.3. Proteins and enzymes

boPARN PS	from calf thymus	(*Körner and Wahle, 1997*)
His_6-huPARN MQ	from *E. coli*	C. Körner and this thesis
hPARN PS	from HEK293	this thesis
hPARN PS	from S2	this thesis
His_6-hPARN MQ	from S2	this thesis
eIF4E	from *E. coli*	S. Morley, Univ. of Sussex, UK
NFL eIF4GI	from Baculovirus	S. Morley and this thesis
p100 (C-terminal two-thirds of eIF4G)	from *E. coli*	S. Morley and this thesis
4GM (middle domain of eIF4G)	from *E. coli*	S. Morley and this thesis
PTB	from *E.coli*	this thesis
BSA Fraction V	Merck	
methylated BSA	E. Wahle (1991)	
yeast PAPΔ29	prepared by C. Körner	
capping enzyme	prepared by S. Meyer, MLU, Halle, Germany	
Taq DNA polymerase	A. Jenny	
SP6 RNA polymerase	Roche Diagnostics	
RNasin	Promega	
RNaseA	Roth	
RNaseP1	Amersham-Pharmacia	
ProteinaseK	Merck	
Alkaline Phosphatase	Roche Diagnostics	
Micrococcal Nuclease	MBI Fermentas	
T4-DNA ligase	New England Biolabs	
T4-Polynucleotidekinase	New England Biolabs	
restriction enzymes	New England Biolabs, MBI Fermentas	

2.1.4. Antibodies

rabbit anti-PARN (ser. 205 / ser. 1363)	M. Wormington, UVA, USA / this thesis
rabbit anti-PARN (affinity purified)	C. Körner
rabbit anti-eIF4G (WF)	S. Morley, Univ. of Sussex, UK
rabbit anti-eIF4G (APEd; affinity purified)	S. Morley. Univ. of Sussex, UK
rabbit anti-eIF4E	M. Muckentaler, EMBL, Heidelberg
swine anti-rabbit HRP	DAKO
rabbit anti-mouse HRP	DAKO

2.1.5. Nucleotides and Nucleic Acids

dNTPs	Amersham-Pharmacia
NTPs	USB
m^7GpppG	New England Biolabs
ApppG	New England Biolabs
GpppG	New England Biolabs
poly(A)	Roche Diagnostics
$polyA_{205}$ (13.6 µM)	S. Meyer
16S- and 23S-ribosomal RNA	Roche Diagnostics
[α–^{32}P] ATP, [α–^{32}P] UTP,	Amersham Pharmacia
[α–^{32}P] GTP, [λ–^{32}P] ATP	Amersham Pharmacia

2.1.6. Plasmids and vectors

pGMMCS645295	C. Körner (*Körner et al., 1998*)
pEAK 8	Edge BioSystems
pMT/V-HisC	Invitrogen
pGEM3	Promega
pQEPTB	Niepmann, JLU, Giessen, Germany
pET-28p100	S. Morley
pET-28 GM	S. Morley
pGEM β-globin3´-UTR	C. Körner
pBeloBAC 11	Genome Systems Inc.
pBeloBAC 251186	Genome Systems Inc.

2.1.7. Oligonucleotides

The following oligonucleotides were used for sequencing and PCR-analysis of mouse PARN.

Name	Length	Sequence
2065148 A	21-mer	5′-caggaatcagcaatggaccct-3′
rev′206 A	22-mer	5′-gagggtccattgctgattcctg-3′
2065148 B	23-mer	5′-gtatgaccacacagattccaagc-3′
rev206 B	23-mer	5′-gcttggaatctgtgtggtcatac-3′
1230578 C	23-mer	5′-ggatcagaagaagtttattgacc-3′
rev206 C	23-mer	5′-ggtcaataaacttcttctgatcc-3′
2065148 D	24-mer	5′-ccaactcaaagtctgataaataag-3′
reverse D	24-mer	5′-cttatttatcagactttgagttgg-3′
2065148 E	22-mer	5′-tgagacattagagactgaccag-3′
2065148 F	21-mer	5′-gtattagcaatggcatggatg-3′
1243352 G	20-mer	5′-cagagggaaggaaaaagtcc-3′
1243352 H	18-mer	5′-gtgtcagggacttcaaag-3′
2065148 I	22-mer	5′-ggaaagacatatagttatcagc-3′
3499571 K	20-mer	5′-ttgtgggacacaacatgctc-3′
reverse K	21-mer	5′-caagagcatgttgtgtcccac-3′
3499571 L	20-mer	5′-ccttaaaaggctgtgtgctg-3′
3499571 P	20-mer	5′-ttgcagagttggaaaagcgg-3′
875507 R	19-mer	5′-ccatggagatgaagcagag-3′
reverse R	20-mer	5′-ctctgcttcatctccatggc-3′
KR intron up	20-mer	5′-tttgggagggtcaaaaggtg-3′
3499571 S	21-mer	5′-aacttggaagggccagacttg-3′
reverse S	19-mer	5′-caagtctggcccttccaag-3′
3499571 T	22-mer	5′-aatgttaccgaaggcgctgaag-3′
reverse T	20-mer	5′-cagcgccttcggtaacattc-3′
2101477 V	22-mer	5′-cagaacagcacacaggcttgtc-3
2101477 X	22-mer	5′-catcagccttcgtttctctcag-3′
1243352 Y	21-mer	5′-ggacttttttccttccctctgg-3′
21014077 Z	19-mer	5′-gaaggaggtggacagaaag-3′
reverse Z	20-mer	5′-ctttctgtccacctccttcc-3′
mu 5′UTR	20-mer	5′-ccaaggttcggtctgcgccg-3′
M13 forward	17-mer	5′-gtaaaacgacggccagt-3′
T7 sequencing	16-mer	5′-aacagctatgaccatg-3′
ON-R	12-mer	5′-gggcggcgacct-3′
ON-L	12-mer	5′-aggtcgccgccc-3′

2.1.8. Kits

DNA fragment purification	QIAEX Gel Extraction Kit, QIAGEN
Western blot detection	Supersignal Substrate, Pierce
Protein assay	Biorad Protein Assay, BioRad
Cycle sequencing	ABI Prism BigDye Terminator Cycle Reaction Kit
Plasmid preparations	Qiagen Plasmid Midi/Mega Kit

2.1.9. Column materials

MonoQ-FPLC	Pharmacia
RecourceQ-FPLC	Pharmacia
Phenyl-Superose-FPLC	Pharmacia
Blue Sepharose	prepared as described by Bienroth et al., 1991
Ni^{2+}-NTA Agarose	Qiagen
Ni^{2+}-NTA Superflow	Qiagen
Glutathione Sepharose 4B	Amersham Pharmacia
7-Methyl-GTP Sepharose 4B	Amersham Pharmacia

2.1.10. Chemicals

Standard chemicals were purchased from either Merck or Roth.

40% Acrylamide (19:1)	Accugel, National Diagnostics
40% Acrylamide	BioRad
Agarose	Gibco/BRL
Agarose (PFGE grade)	BioRad
β-mercaptoethanol	Merck
Carbenicillin	Roth
Diethylpyrocarbonat (DEPC)	Sigma
Dithiothreitol (DTT)	Gerbu
Glycogen	Roche Diagnostics
Hygromycin B	Invitrogen
Isopropyl-β-D-thiogalactopyranoside (IPTG)	peQLab
Leupeptin	Roche Diagnostics
Nonidet P-40	Fluka
Pepstatin A	Boehringer (Roche)
Phenol, (ready to use)	Roth
Phenylmethansulfonylfluorid (PMSF)	Merck
Ponceau S	Sigma
N,N,N´, N´, Tetramethylethylendiamine(TEMED)	Merck
Tween® 20	Merck

2.1.11. Miscellaneous

DEAE paper	Whatman
Dialysis tubing	Serva
Nitrocellulose membrane	Protran® BA 83, Schleicher&Schuell
Scintillation cocktail	Lumasafe™Plus, Lumac.LSC
Storage Phosphor Screen	Molecular Dynamics
Tissue culture plastic wares	TPP
X-ray film	Kodak X-OMAT AR, Kodak
PEI Cellulose F, TLC plastic sheet	Merck

2.2 Methods

2.2.1. Standard methods

General microbiological methods like sterilisation of media and solutions, bacterial growth in medium or on agar plates, preparation of electro-competent *E. coli* cells and transformation by electroporation were performed according to standard protocols. General molecular biology techniques like restriction enzyme analysis, purification of DNA fragments, ligation, phosphorylation, dephosphorylation, polymerase chain reaction (PCR) and determination of DNA/RNA concentration were done according to the protocols supplied by the manufacturers or as described in Molecular Cloning: A Laboratory Manual (*Sambrook et al., 1989*) or in Current Protocols in Molecular Biology (*Ausubel et al.,1994*).

Agarose gel electrophoresis

Routine analysis of DNA molecules of 100 to 12,000 base pairs in size, was done by separation on agarose gels with 1 x TBE (90 mM Tris-Borate, pH 8, 1 mM EDTA) as running buffer.

Denaturing polyacrylamide gel-electrophoresis

Single stranded nucleic acids (e.g. RNA) were separated on 6 to 15 % polyacrylamide gels (polyacrylamide:bisacrylamide, 19:1) in 1 x TBE and 8.3 M urea. Running buffer was 1 x

TBE. Samples were resuspended in formamide loading buffer (100% formamide, 1 mM EDTA, 1 mg/ml bromophenol blue, 1 mg/ml xylene cyanol FF) and denatured at 95 ^{o}C for 2 minutes before loading. The gels were in general soaked onto Whatman 3MM paper and dried under vacuum before exposure to Phosphor screens (Kodak).

SDS gel electrophoresis

Proteins were separated by SDS-gel electrophoresis as described by Laemmli (1970). After separation, the proteins were routinely visualised by staining with Coomassie Brilliant Blue or transferred onto nitrocellulose membranes for Western blot analysis.

Silver staining

Minute amounts of proteins that were separated by SDS gel electrophoresis were visualised by silver staining. First the gel was fixed in 30 % ethanol and 10% acetic acid for 30 minutes and then for 30 minutes in 30% ethanol, 0.5 M sodium acetate, 0.5 % (v/v) glutaraldehyde and 0.2% (w/v) sodium thiosulfate. After washing with distilled H_2O (3 x 10 minutes), the gel was incubated with 0.1% (w/v) Ag_2NO_3 and 0.01% formaldehyde for 20 minutes. Following a short wash step to remove excess Ag_2NO_3, the gel was developed in 2.5% Na_2CO_3 and stopped with 0.05 M EDTA.

Western-blot analysis

Proteins separated by SDS gel-electrophoreses were transferred onto a nitrocellulose membrane (Schleicher & Schuell) by semi-dry blotting (*Harlow and Lane, 1988*) in 1 x transfer-buffer (2.9 g glycin, 5.8 g Tris, 0.37 g SDS and 200 ml methanol per litre). Following transfer, the membranes were incubated in TN-tween buffer (20 mM Tris-HCl, pH 7.5, 150 mM NaCl, 0.05 % (v/v) Tween 20™) for 10 minutes before visualising the transferred proteins by staining with Ponceau S (0.5 % (w/v) Ponceau S in 1 % (v/v) glacial acetic acid). After destaining in distilled water, the membranes were blocked in TN-tween over night. Before adding the primary antibody, the membranes were additionally blocked with 5 % (w/v) milk in TN-tween for 1 hour. Primary antibodies were diluted 1:1000-2000 in 0.5 % milk (for anti-PARN antibodies) or in 5 % milk (for other antibodies) and incubated with the membranes for 2-3 hours. Non-reacted antibodies were removed by a short wash-step (5 x 1

minute in TN-tween) prior to incubation with the secondary antibody (swine-anti-rabbit HRP, DAKO; diluted 1:4000-5000 in TN-tween) for 1 hour. After a second wash-step (6 x 1 minute in TN-tween), polypeptides that interacted with the primary antibody were visualised by incubation with the Super Signal Substrate (Pierce) and exposure to Kodak X-OMAT AR film. All incubation steps were performed at room temperature.

2.2.2. DNA methods

Preparation of plasmid DNA

Small scale plasmid DNA was done according to Birnboim and Doley, 1979. Preparation of plasmid DNA for transfections and sequencing was done with Qiagen Plasmid Midi Kit or the Plasmid Mega Kit (Qiagen) for transient transfection of HEK293-EBNA cells. Isolation of BAC DNA was with Qiagen Plasmid Midi Kit with the following modifications: resuspension, lysis and precipitation steps were adjusted to the Maxi protocol but the cleared lysate was applied to a Qiagen-tip 100 and the DNA was eluted with 5 x 1 ml QF buffer pre-warmed to 65^{o}C (see very low-copy plasmid/cosmid purification protocol in Qiagen plasmid purification handbook).

Sequence analysis

Plasmid constructs and the mouse PARN EST clone were sequenced by performing a fluorescence-based cycle sequencing with the ABI Prism BigDye Terminator Cycle Reaction Kit, based on the Sanger dideoxy sequencing procedure (*Sanger et al., 1977*). Fluorescent labelled DNA extension products were subsequently separated by capillary electrophoresis and analysed by the ABI PRISM® 310 Genetic Analyser (PE Applied Biosystems).

Construction of expression plasmids

To construct the expression plasmid pEAK8-PARN for transient transfection of HEK293 cells, a 2 kb *XhoI* fragment was excised from pEGFP-DAN (*Körner et al., 1998*) containing the PARN ORF and 35 nucleotides from the pEGFP-C_1 multiple cloning site (Clontech). The recessive ends were made blunt in a fill-in reaction with Klenow enzyme (Amersham) and

ligated into the EcoRV site of pEAK8 (Edge BioSystems, see Appendix). The pMT-PARN expression plasmid used to generate stable a S2 cell line, was made by excising a 2 kb *KpnI-SmaI* fragment from pEGFP-DAN (*Körner et al., 1998*) including the intrinsic PARN start and termination codons, and ligated into the *KpnI* and *EcoRV* sites of pMT/V5-HisC (Invitrogen, see Appendix). pMT-HisPARN was subsequently constructed by replacing a *XbaI* fragment from pMT-PARN with a *XbaI* fragment from pGMMCS 645295 (*Körner et al., 1998*). The 870 nt *XbaI* fragment from pGMMCS 645295 consists of an N-terminal Met-Ala-His_6-tag and 810 nt of the PARN coding sequence. The GST-tag in pGMMCS 645295:GST was cloned as a *NdeI* fragment (*Kühn et al., 2003*) into the corresponding site of pGMMCS 645295, in frame with the Met-Ala-His_6 tag. All constructs were sequenced.

Size determination of a mouse PARN genomic DNA insert in pBeloBAC 25186

The pBeloBAC 25186 clone was obtained from a PCR based BAC Mouse II library screen (Genome Systems Inc.) The size of the genomic insert was determined by linearizing the BAC clone at the cosN site in the pBeloBAC11 vector (Invitrogen, see Appendix) with λ-terminase (Epicentre Technologies). The digestion with λ-terminase resulted in the formation of unique 12 base 5´-overhangs to which radiolabelled ON-L and ON-R oligonucleotides were hybridised as described by the manufacturer. Separation of the digested DNA was carried out on a BioRad CHEF-DR III pulse-field gel electrophoresis apparatus for 20 hours at a field strength of 6 V/cm in a 1% agarose gel in 0.5 x TBE (45 mM Tris-HCl, pH 8, 45 mM boric acid, 0,5 mM EDTA) at 14^{o}C with a linear pulse time ranging from 1-12 seconds. A size marker ranging from 2-194 kb was purchased from New England Biolabs. The gel was stained in ethidium bromide to visualise the marker before vacuum dried and exposed to Kodak X-OMAT AR film.

2.2.3. Transfection of eukaryotic cells

Large-scale transient transfection of HEK293-EBNA cells

Cell growth and large-scale transfection was performed by Dr. Lucia Baldi at the Swiss Federal Institute of Technology (EPFL), Lausanne. The method has been described previously (*Meissner et al., 2001*). In brief: Suspension adapted HEK293-EBNA cells were resuspended

to 1 x 10^5 cells/ml in a DMEM-based medium containing 1% FCS and incubated for 2 hours at 37°C. 25 µg plasmid DNA per 10^5 cells was precipitated in a transfection mix containing 125 mM $CaCl_2$, 700 µM HEPES and 140 mM NaCl. The transfection mix was added to the cell suspension and incubated for 4 hours. After the incubation an equal volume of fresh medium was added in order to facilitate dissolution of the precipitate.

Transfection of *Drosophila* S2 cells and selection of stable transformants

The transfection procedure was performed as outlined in the "Drosophila Expression System" manual, version C (Invitrogen) with the following modifications.
Logarithmically growing *Drosophila* S2 cells (Invitrogen) were diluted to 1 x 10^6 cells/ml in fresh Schneider´s insect medium (Sigma) supplemented with 10% fetal calf serum (FCS) and 10% SF 900 II medium (Invitrogen). 3 x 10^6 cells were seeded into each well of a 6-well plate and incubated at 24°C for 20 hours. A transfection mix for each well was prepared as follows: Solution A (19 µg pMT-PARN or pMT-HisPARN, 1 µg pCoHYGRO, 240 mM $CaCl_2$ in 300 µl); Solution B 300 µl sterile 2 x HBS buffer (50 mM HEPES, 1.5 mM $NaHPO_4$, 280 mM NaCl; pH 7.1). Solution A was added dropwise to Solution B with continuous vortexing to assure the formation of a fine precipitate. After incubation at room temperature for 30 minutes, the transfection solution was mixed and added dropwise to the cells without disturbing the cell layer. One well was transfected with the selection plasmid, pCoHYGRO alone and two wells were not transfected as controls. After 20 hours of incubation the calcium phosphate solution was removed and the cells were washed twice in pre-warmed medium. Finally 3 ml fresh, complete medium (Schneider´s insect medium complemented with 10% FCS and 10% SF 900 II medium) was added to each well. Selection of resistant cells was initiated 3 days after transfection with 300 µg/ml hygromycin (Gibco) in complete medium. The selective medium was changed every 4 days. After the second selective medium change, floating, walnut-like cells were diluted in complete medium with 310 µg/ml hygromycin and transferred to a 24-well plate for expansion and expression test. 10 days after dilution, PARN-expressing cell populations were expanded and frozen. Adherent cells were further selected and hygromycin-resistant cells were growing out after 3 weeks in selective medium.

2.2. 4. Protein methods

2.2.4.1. Purification of recombinant proteins

Purification of recombinant proteins expressed in *E. coli*

The plasmids pGMMCS 645295 or pGMMCS 645295:GST encoding hPARN cDNA (*Körner et al., 1998* and section 2.2.2.) were transformed by electroporation into *E.coli* BL21 (DE3) pUBS or *E.coli* codon plus respectively. Transformed cells were grown in LB medium supplemented with 0.1 % glucose, 100 µg/ml carbenicillin and 50 µg/ml kanamycin (15 µg/ml tetracyclin for *E.coli* codon plus) at 37^{o}C and induced with 400 µM isopropyl-□-D-thiogalactopyranoside (IPTG) for 3 hours. The cells were harvested by centrifugation (4000 g for 20 minutes) and resuspended in buffer A [50 mM Tris-HCl, pH 7.9, 300 mM KCl, 0.1 mM MgAc, 1 mM imidazole, 1 mM β-mercaptoethanol, 0.4 µg/ml leupeptin, 0.7 µg/ml pepstatin and 0.5 mM phenylmethylsulfonyl fluoride (PMSF)]. The cells were disrupted by sonication on ice with a Branson Sonifier (15 seconds constant duty cycle, output 4 and 30 seconds on ice) until a stable $O.D._{600}$ was reached. Cell debris and high molecular weight DNA were removed by centrifugation at 10,000 g for 30 minutes and the supernatant was incubated with 2.5 ml of a 50 % Ni^{2+}-NTA slurry (Quiagen) on a rotating wheel at +8-12^{o}C over night. The resin was packed by gravity force into a column (Econo-Column, BioRad), washed once with 25 ml buffer A and twice with 25 ml of buffer B (50 mM Tris-HCl, pH 7.9, 300 mM KCl, 10 % glycerol, 0.02 % Nonidet P40, 20 mM imidazole, 1 mM β-mercaptoethanol, 0.4 µg/ml leupeptin, 0.7 µg/ml pepstatin and 0.5 mM PMSF). The proteins were eluted with 5 x 1 ml buffer B containing 300 mM imidazole and dialysed for 5 hours against protein dialysis buffer (50 mM Tris-HCl, pH 7.9, 50 mM KCl, 1 mM EDTA, 10 % glycerol, 1 mM DTT, 0.5 mM PMSF 0.02 % Nonidet P40) with one buffer change. After centrifugation at 15,000g for 30 minutes proteins were further purified by anion exchange chromatography on FPLC (Fast Protein Liquid Chromatography, Amersham Pharmacia). The Ni^{2+}NTA-eluates were applied on a 1 ml MonoQ column (Amersham Pharmacia) equilibrated with dialysis buffer. The column was washed with 10 bed volumes equilibration buffer and the proteins were eluted with a 50-500 mM KCl gradient over 40 ml at 1 ml/min.

p100 and eIF4GM proteins were purified as described by Pestova et al. (1996). The first purification step over Ni^{2+}-NTA agarose was performed as outlined above with an additional purification on heparin sepharose.

Purification of recombinant NFL-eIF4G expressed in baculovirus-infected cells

A high titer virus stock (10^9 p.f.u./ml) of a recombinant baculovirus expressing full length eIF4G was obtained from Dr. S. Morley (University of Sussex, U.K.). Sf 21 cells in SF 900 II medium supplemented with 1% Pluronic F-60 solution (Invitrogen) were adapted to suspension growth in Erlenmayer-flasks, shaking in an orbital shaker with 135 r.p.m. at 24-26^{o}C. At a density of 1 x 10^6 cells/ml the cells were infected with the recombinant baculovirus at a M.O.I. (multiplicity of infection) of 1 and incubated for another 72 hours. The following procedure was adapted from a purification protocol developed in Dr. Morley´s lab: The cells were harvested by centrifugation and resuspended in 10 ml buffer A (40 mM MOPS (KOH) pH 7.2, 300 mM NaCl, 2 mM benzamidine, 20 mM imidazole, 3.5 mM β-mercaptoethanol, 0.5 mM PMSF, 0.7 µg/ml pepstatin, 0.4 µg/ml leupeptin). For lysis, 1 % Nonidet P40 was added and the cell suspension was vortexed and incubated on ice for 10 minutes. Cell debris and high molecular weight DNA was removed by centrifugation at 11,000g for 20 minutes. The supernatant was incubated on a rotating wheel with 0.5 ml packed Ni^{2+}-NTA resin per litre of cells at +4^{o}C for 1 hour and packed into an Econo-column (BioRad) by gravital force. The resins were washed twice with 12.5 ml of each of the following buffers: buffer A (40 mM MOPS (KOH) pH 7.2, 300 mM NaCl, 2 mM benzamidine, 20 mM imidazole, 3.5 mM □-mercaptoethanol, 0.5 mM PMSF, 0.7 µg/ml pepstatin, 0.4 µg/ml leupeptin); buffer B (buffer A plus 1 % Nonidet P40); buffer C (buffer B containing 500 mM NaCl) and buffer D (buffer A without protease inhibitors). The protein was eluted with 5 x 200 µl buffer E (40 mM MOPS (KOH) pH 7.2, 300 mM NaCl, 2 mM benzamidine, 250 mM imidazole, 3.5 mM β-mercaptoethanol). The eluates were pooled and diluted to 100 mM NaCl with ice-cold buffer F (40 mM MOPS (KOH) pH 7.2, 2 mM benzamidine) and mixed with 250 µl packed anti-M2 FLAG agarose (Sigma) resin and incubated on a rotating wheel at +4^{o}C for 1 hour. The slurry was packed into a column and washed 2 x 10 ml with ice-cold buffer G (40 mM MOPS (KOH) pH 7.2, 100 mM NaCl, 2 mM benzamidine) and 2 x 10 ml with buffer H (5 mM MOPS (KOH) pH 7.2, 100 mM NaCl, 2 mM benzamidine) at room temperature. The protein was eluted with 5 x 200 µl of 10 mM glycine pH 2.5. Fractions with a pH below 5 were collected and neutralised with 1 M Tris-HCl, pH 8. Each fraction was assayed for protein content by the Bio-Rad Protein-Assay (Bradford assay) system and dialysed against protein dialysis buffer (50 mM Tris-HCl, pH 7.9, 50 mM KCl, 1 mM EDTA, 10 % glycerol, 1 mM DTT, 0.5 mM PMSF 0.02 % Nonidet P40) for 4 hours. The protein was quick frozen in liquid nitrogen and stored in aliquots at –80^{o}C until use.

Purification of PARN from HEK293-EBNA

Three separate spinner flasks each with 1 L HEK-293 EBNA cell-suspension were transfected (Dr. L. Baldi) as described (*Meissner et al., 2001*) with 80% pEAK8-PARN, 2% pEGFP-N1 (*Pick et al., 2002*) and 18% carrier DNA. Harvesting was done at 55 hours post-transfection. The cell pellets were washed once with 150 ml cold PBS (Na_2HPO_4, KH_2PO_4 , NaCl, KCl) and frozen at –80°C. Cytoplasmic extracts were made as described by Dignam (*Dignam, 1990*). The cell pellet was resuspended in five volumes buffer A (10 mM Hepes(NaOH) pH 7.9, 1.5 mM $MgCl_2$, 10 mM KCl, 0.5 mM DTT, 0.5 mM PMSF) and incubated on ice for 10 minutes. Cells were lysed with 15 strokes in a glass-glass Dounce homogenizer with piston B or until lysis could be observed by inspection in a microscope. Nuclei were collected by centrifugation at 1300g for 10 minutes and retained for preparation of nuclear extract. To the supernatant from this step 0.11 volumes of buffer B (0.2 mM Hepes(NaOH) pH 7.9,1.4 M KCl, 30 mM $MgCl_2$) was added and incubated at +4°C for 15 minutes with gentle stirring followed by centrifugation at 100,000g for 1 hour. The supernatant fraction from this step (S100) was then dialysed in protein dialysis buffer (20 mM Tris-HCl, pH 7.9, 50 mM KCl, 1 mM EDTA, 10 % glycerol, 1 mM DTT, 0.5 mM PMSF 0.02 % Nonidet P40).

After dialysis, precipitated material was removed by centrifugation at 15,000 g for 30 minutes, and the supernatant was applied on a 1 ml Resource Q FPLC column (Amersham Pharmacia). The column was washed with 20 ml dialysis buffer and the protein was eluted with a 50-500 mM KCl gradient over 40 ml at 1 ml/min. Eluted fractions were tested for activity by the TCA-precipitation assay (*Körner and Wahle, 1997*) and the presence of the PARN polypeptide was investigated by Western blot analysis.

Active PARN fractions were combined and diluted with dialysis buffer without KCl to the same conductivity as the BS equilibrating buffer (see protein dialysis buffer). An empty Econo-column (BioRad) was packed with 3 ml Blue Sepharose (Amersham Pharmacia). The packed column was equilibrated with 10 bed volumes of BS equilibration buffer and pooled fractions were applied by gravity force. After a 9 ml wash step with 250 mM KCl the protein was eluted with 8 ml of 1 M KCl and collected in 10 fractions.

At this point, active fractions were dialysed against PS equilibration buffer (20 mM Tris-HCl, pH 7.9, 50 mM KCl, 1 mM EDTA, 10% glycerol, 2 mM DTT, 25% ammonium sulfate, 0.5 mM PMSF) followed by centrifugation at 10,000g for 20 minutes to remove precipitated material. The supernatant was applied on a 1 ml Phenyl Superose FPLC column equilibrated with PS equilibration buffer. The column was washed with 10 column volumes of PS

equilibration buffer and developed with a descending gradient from 25% to 0% ammonium sulphate over 20 ml at 0.1-0.2 ml/min.

Purification of PARN from *Drosophila* S2 cells

The stable PARN:S2 A4 cell line was expanded in hygromycin selective Schneider´s insect medium and adapted to suspension growth in 500 ml SF 900 II medium without hygromycin. Induction of PARN expression was made with 500 µM copper sulfate at a cell density of 10 x 10^6 cells/ml and cells were harvested after 26 hours (cell count: 14 x 10^6 cells/ml). The cells were washed once with PBS and an S100 extract was prepared as described for the HEK293-EBNA cells. PARN was purified as described, with fractionations over Resource Q FPLC, Blue Sepharose and Phenyl Superose FPLC columns.

Purification of His_6-PARN from *Drosophila* S2 cells

Schneider 2 cells were transfected with pMT-HisPARN and selected for stable transformants as described. Cells expressing the polyhistidine-PARN (His_6-PARN) fusion protein were expanded in selective medium and adapted to suspension growth in 500 ml SF 900 II medium without hygromycin. Induction of His_6-PARN expression and harvesting of the cells were as described for the PARN:S2 A4 cell line. The cell pellet was resuspended in buffer A [50 mM Tris-HCl, pH 7.9, 300 mM KCl, 0.1 mM MgAc, 10 mM imidazole, 1 mM □-mercaptoethanol, 0.4 µg/ml leupeptin, 0.7 µg/ml pepstatin and 0.5 mM phenylmethylsulfonyl fluoride (PMSF)] and the cells were lysed by freeze-thawing in liquid nitrogen and in a 42°C water bath. Lysis was monitored by inspection in an inverted microscope. The DNA was shared by sonication and cell debris were removed by centrifugation at 30.000g for 20 minutes. The cleared lysate was applied on a XK1626 FPLC column (Pharmacia) packed with Ni^{2+}-NTA Superflow (Qiagen). After washing the column with 2 bed volumes with buffer A the protein was eluted with a 145 ml gradient from 10 mM imidazole to 400 mM imidazole at a flow rate of 1 ml/min. Active fractions were pooled and dialysed against protein dialysis buffer (50 mM Tris-HCl, pH 7.9, 50 mM KCl, 1 mM EDTA, 10 % glycerol, 1 mM DTT, 0.5 mM PMSF 0.02 % Nonidet P40) followed by anion exchange chromatography on FPLC as described earlier for purification of proteins expressed in *E.coli*.

2.2.4.2. m^7GTP-Sepharose affinity chromatography

A 100 µl aliquot of a side fraction (Phenyl-Superose fraction 34) from the bovine PARN purification (*Körner and Wahle, 1997*) was diluted with 500 µl wash buffer (50mM Tris-HCl, pH 7.9; 100 mM KCl; 0.02% NP-40; 1 mM EDTA; 0.5 mM PMSF; 0.4 ug/ml leupeptin, 0.7 ug/ml pepstatin; 1 mM DTT). Half of the sample (300 µl) was mixed with 75 µl of packed m^7GTP-Sepharose beads (Amersham Pharmacia) pre-washed with wash buffer and incubated on a rotating wheel at +8-12^oC for 2 hours. The rest of the sample was used as loading control. After incubation, the beads were pelleted by a quick centrifugation and washed successively twice with 300 µl wash buffer and once with 300 µl wash buffer containing 0.1 mM GTP (Sigma) and finally, eluted with 300 µl wash buffer plus 0.1 mM m^7GTP (Sigma). A 150 µl aliquot each of the loaded material and the first supernatant and the entire volume of each of the wash fractions were precipitated in 12% TCA with 10 µg yeast ribosomal RNA (Roche Diagnostics) as carrier. After a wash with ice-cold acetone and drying, the pellets were resuspended in 15 µl SDS gel-loading buffer, separated on a 9% SDS-polyacrylamide gel and silver stained.

2.2.4.3. GST pull-down assay

200 µl packed Gluthathione-Sepharose beads were washed three times with 1 ml CLPD wash buffer (20 mM HEPES, pH 7, 0.01% Nonidet P40, 100 mM KCl, 4 mM MgAc, 1mM EDTA, 1 mM DTT) and resuspended in 200 µl CLPD binding buffer (20 mM HEPES, pH 7, 0.01% Nonidet P40, 100 mM KCl, 4 mM MgAc, 1mM EDTA, 1 mM DTT and 200 µg/ml BSA). Half of the suspension was mixed with 40 µg GST-PARN (MonoQ fraction 41) diluted in 600 µl CLPD binding buffer and incubated on a rotating wheel at room temperature for 1 hour. The resin was pelleted by centrifugation at 510g for 5 minutes. Unbound protein was removed by washing the resin three times with 1 ml ice-cold CLPD wash buffer and finally resuspended with 100 µl CLPD binding buffer. Four 30 µl aliquots of the protein-bound Gluthathione-Sepharose suspension was incubated with 3 µg of either eIF4GM or p100 in 600 µl CLPD binding buffer on a rotating wheel for 1 hour. In order to elucidate a possible protein-RNA-protein interaction, one aliquot each with either eIF4GM or p100 was treated with 600 units Micrococcal nuclease (MBI Fermentas) for another 30 minutes. Following incubation the resins were washed five times with 1 ml ice-cold CLPD wash buffer. Bound

proteins were eluted with 15 µl SDS gel-loading buffer, separated on a 9% SDS-polyacrylamide gel and analysed by Western blot.

2.2.4.4. m^7GTP pull-down assay

The binding of recombinant PARN to m^7GTP-Sepharose beads was performed in 600 µl CLPD binding buffer at +8-12°C for 1 hour on a rotating wheel but the following steps were identical to the GST pull-down assay.

2.2.4.5. UV-cross-linking

^{32}P-cap-labelled and polyadenylated β-globin RNA (~3fmol, 30,000 c.p.m.) was incubated with recombinant eIF4E and NFLeIF4G (S.Morley) in 10 µl CLPD buffer for 15 minutes at 30°C. The mixtures were transferred to 96-well plate and irradiated on ice for 20 minutes with a UV Stratalinker (Stratagene) at a distance of 15 cm, followed by digestion with RNase A (1 µg per reaction) for 15 minutes at 37°C. Cross-linked proteins were separated by SDS-12% PAGE and analysed by PhosphorImager (Molecular Dynamics).

2.2.5. Preparation of substrate RNA

Preparation of homogeneously radiolabelled poly(A)

The reaction conditions for nonspecific polyadenylation were described by Lingner et al., 1991. A 50 µl reaction mixture containing: 3.12 µM oligoA_{26-30}, 390 µM ATP, 50 µCi [α-^{32}P]ATP (Amersham), in yPAP buffer (20 mM Tris-HCl, pH 7, 60 mM KCl, 0.7 mM $MnCl_2$, 0.2 mM EDTA, 10% glycerol, 0.5 mM DTT and 0.8 mg/ml methylated BSA), was pre-incubated for 2 minutes at 30°C before the reaction was started by addition of 1.4 µg yPAPΔ1 (a deletion mutant of yeast poly(A) polymerase Δ1). After 1 hour of incubation the reaction was stopped with 50 µl 2 x PK buffer and 30 µg Proteinase K (Sigma), incubated for another 1 hour at 37°C and precipitated with ethanol. The RNA was resuspended in 100 µl 2.5 M ammonium acetate and precipitated again to remove unincorporated nucleotides, washed twice with 70% ethanol and resuspended in 100 µl DEPC treated water.

in vitro transcription

pSP6L3pre and pSP6glob (*Körner and Wahle, 1997*) were linearized with *RsaI* or *EcoRI* respectively, and transcribed *in vitro* by SP6 RNA polymerase (Roche) in the presence of 50 μCi [α-^{32}P]UTP (Amersham), 600 μM of either ApppG, m^{7}GpppG or GpppG (New England Biolabs, NEB), 100 μM GTP and UTP, 500 μM CTP and ATP for 1 hour at 37°C. pSP6L3preA$_{110}$ (*U. Kühn, personal communication*) was linearized with *BbsI* and transcribed as above but at 39°C to increase the yield of transcripts with a comparable poly(A) tail length. Non-radioactive transcripts were made as described above but with 500 μM of each ribonucleotide triphosphate for non-capped RNAs or with a reduced concentration of GTP in the presence of a cap-analogues (New England Biolabs) and incubated for 3 hours at 39°C. Transcription products were separated on 6-8% denaturing polyacrylamide gels, full-length RNA was excised and eluted in 1 ml elution buffer (0.5 M ammoniumacetate, 10 mM magnesium acetate, 1 mM EDTA , 0.1% SDS and 30 μl phenol) in a Thermomixer (Eppendorf) over night. After a phenol-extraction, the RNA was precipitated with ethanol, resuspended in DEPC treated water and stored at –20°C until use.

Polyadenylation of *in vitro* transcribed RNAs

Polyadenylated transcripts were prepared under conditions for nonspecific polyadenylation (*Lingner et al., 1991*) with a 125 fold molar-excess of ATP over transcript and 1.4 μg yPAP□1 per 1-3 pmol RNA and incubation at 30°C for 1 hour. Non-radioactive transcripts with homogeneously labelled poly(A) tails were made in the same way but in the presence of 50 μCi [□-^{32}P]ATP (Amersham). Polyadenylated transcripts were fractionated on a 6% denaturing polyacrylamide and eluted as described.

Post-transcriptional capping of RNA

Non-radioactive transcripts were radiolabelled in the cap structure with [α-^{32}P] GTP and recombinant guanylyltransferase. A typical 25 μl reaction mixture consisted of 10-15 pmol RNA transcript, 40 units RNasin (Promega), 20-25 pmol (60-75 μCi) [α-^{32}P] GTP (Amersham), 100 μM S-adenosyl-L-methionine (Sigma) and 0.24-0.3 μg of a partially purified fraction of recombinant guanylyltransferase (S. Meyer) dialysed against the reaction buffer (50 mM Tris-HCl, pH 8, 1.25 mM $MgCl_2$, 6 mM KCl, 0.4 mg/ml methylated BSA, 2.5

mM DTT). The capping reaction was incubated at 37°C for 1 hour, stopped by the addition of SDS and incubation with Proteinase K (Sigma) followed by an ethanol precipitation. Non-methylated cap structures were made by omitting S-adenosyl-L-methionine in the reaction. In general, 30-60% of the RNA molecules were labelled by this procedure.

2.2.5.1. Cap analysis

The fraction of methylated to unmethylated ^{32}P-labelled capped RNA, was analysed by RNase P1 digestion followed by thin-layer chromatography. Substrate RNA or fully deadenylated RNA was extracted from the denaturing polyacrylamide gel shown in Figure 3.16, section 3.4 and incubated with 0.6 units RNase P1 (Amersham Pharmacia) in 10 µl 0.1 M sodium acetate for 1 hour at 37°C. The entire reaction volume was spotted in 1 µl portions onto a PEI Cellulose F thin-layer sheet (Merck). 10 µmoles m^{7}GpppG (NEB), GpppG (NEB) and GMP (Sigma) were spotted in adjacent lanes. The thin-layer sheet was immersed in a TLC chromatography tank containing 80% (v/v) saturated ammonium sulphate, 18% (v/v) 1M sodium acetate and 2% (v/v) 2-propanol and developed by ascending chromatography. After drying, the TLC sheet was illuminated with UV and the positions of the control compounds were marked. The migration of the radioactive degradation products were analysed by a PhosphorImager (Molecular Dynamics)

2.2.6. PARN activity assays

TCA-precipitation assay

Poly(A)-degrading activity was assayed by the release of TCA-soluble products from homogeneously labelled poly(A) (*Körner and Wahle, 1997*). In assays used to monitor purification, 5 ng homogeneously labelled poly(A) and 1 µg unlabelled poly(A) were mixed with 50 µl PARN reaction buffer (20 mM Hepes pH 7.05, 1 mM magnesium acetate, 0.02% Nonidet P-40, 0.2 mg/ml methylated BSA, 10% (v/v) glycerol). The reaction was started by the addition of protein and incubation at 37°C for 15 minutes, thereafter quenched by the addition of 150 µl ice-cold 13.3% (w/v) trichloroacetic acid supplemented with 100 mM KCl. After a short incubation on ice, the samples were centrifuged at 20,800 g for 15 minutes at +8-

10°C. 100 µl of the supernatant was neutralised with 100 µl 1 M Tris base, mixed with 2 ml scintillation cocktail and counted in a scintillation counter (Liquid Scintillation Analyzer, Packard). One unit was defined as the activity that releases 1 nmol of nucleotides/min (*Körner and Wahle, 1997*).

In assays where reaction kinetics were determined, 80 to 100 fmol labelled, *in vitro* transcribed RNA was used without additional unlabelled poly(A).

Gel-assays

Non-quantitative deadenylation assays were performed essentially as described (*Körner and Wahle, 1997*) except that reaction mixes were assembled on ice. Salt, substrate and enzyme concentrations are indicated in the figure legends. Reactions were started by the addition of purified protein or HeLa cytoplasmic extracts and incubation at 37°C. Aliquots were removed at indicated times and the reactions were stopped by incubation with 20 µg Proteinase K in a buffer consisting of 100 mM Tris-HCl, pH 7.9, 150 mM NaCl, 1% SDS, 12.5 mM EDTA, 2 µg yeast rRNA (Roche) and 4 µg glycogen (Roche Diagnostics) as carrier. Following protein digestion, reaction products were ethanol precipitated, separated on denaturing urea-polyacrylamide gels and analyzed with a Phosphorimager (Molecular Dynamics).

2.2.7. Sedimentation equilibrium

Sedimentation equilibrium analysis was performed by Dr. H. Lilie (MLU, Halle, Germany), using a Beckman Optima XL-A/I analytical ultracentrifuge. Recombinant hPARN, expressed in *E. coli*, was dialysed for 15 hours in dialysis buffer (50 mM Tris-HCL, pH 7.9, 100 mM KCl, 1 mM DTT, 0.02% Nonidet P-40, 10% glycerol) and centrifuged at 10,000 g for 20 minutes to remove precipitated material. The cells were loaded with 300 µl of protein diluted in dialysis buffer to a concentration of 0.35 mg/ml. Sedimentation equilibrium absorbance data were acquired at 290 nm. The rotor speed was 8000 rpm at a rotor temperature of 10°C. A global nonlinear regression analysis was performed using the data analysis software package provided by Beckman-Coulter (Version 4.0 and ORIGIN Version 4.1).

The obtained sedimentation coefficient was converted to

$$S^{o}_{20,w} = s(1-\nu\rho)_{20,w}\eta_{T,b} / (1-\nu\rho)_{T,b}\eta_{20,w}$$

where $S^{o}_{20,w}$ refers to the sedimentation coefficient at 20°C in water, with η being the viscosity of the water at 20°C, or the viscosity of buffer b at temperature T, ν partial specific volume of the protein (average 0.73 cm^3/g) and ρ the density of the solution (10% glycerol, 0.767 cm^3/g). The molecular mass, M, in g mol-1 of the protein can be calculated by

$$M = RT\, s_{20,w} / D(1-\nu\rho_w)$$

Where D is the diffusion coefficient, R is the gas constant and T is the temperature

Knowing the molar mass and the sedimentation coefficient, the frictional coefficient f can be calculated from

$$f = M(1-\nu\rho) / s_{20,w}\, N_{av}$$

where N_{av} is Avogadro´s number (6.022×10^{23})

The degree of asymmetry is described by f/f_0 where f_0 is the calculated frictional coefficient of a sphere having the same volume as the protein and can be calculated from Stokes equation

$$f_0 = 6\pi\eta R_S$$

where η is the viscosity of water (0.0100 g cm^{-1} g^{-1}) and R_s can be calculated from

$$R_s = [3M\nu / 4\pi N_{av}\, (\nu_p + \delta H_2O\, \nu^{o}H_2O)\,]^{1/3}$$

where δH_2O is g of water bound for every g of protein, this value varies with the method used to obtain it but an average may be around 0.35, and ν^o is 1.00 cm^3 g^{-1}

3. RESULTS

3.1. Cap-dependent deadenylation by purified bovine PARN.

3.1.1. The 7-methyl guanosine cap stimulates deadenylation in HeLa cell extracts

In agreement with previous results, a polyadenylated RNA with a 7-methyl guanosine cap (m^7GpppG) at its 5´end was deadenylated upon incubation with a HeLa cell cytoplasmic extract. A characteristic pattern of decay intermediates, due to partial protection of the poly(A) tail by the binding of PABPC, can be seen in Figure 3.1 A (lanes 3-5) and has been described earlier (*Körner and Wahle, 1997*). In contrast, the decay intermediates were not produced when the RNA substrate was carrying a ApppG-cap (Figure 3.1. A, lanes 7-10). Moreover, the full-length polyadenylated ApppG-capped RNA disappeared with a twofold lower rate than the RNA with a methylated cap. RNA lacking a cap structure behaved like the one with an ApppG cap (Figure 3.1. B). The absence of deadenylation intermediates and the decreased degradation rate suggest that uncapped RNA or RNA with an ApppG-cap may be degraded by a different pathway or in another mode of action.

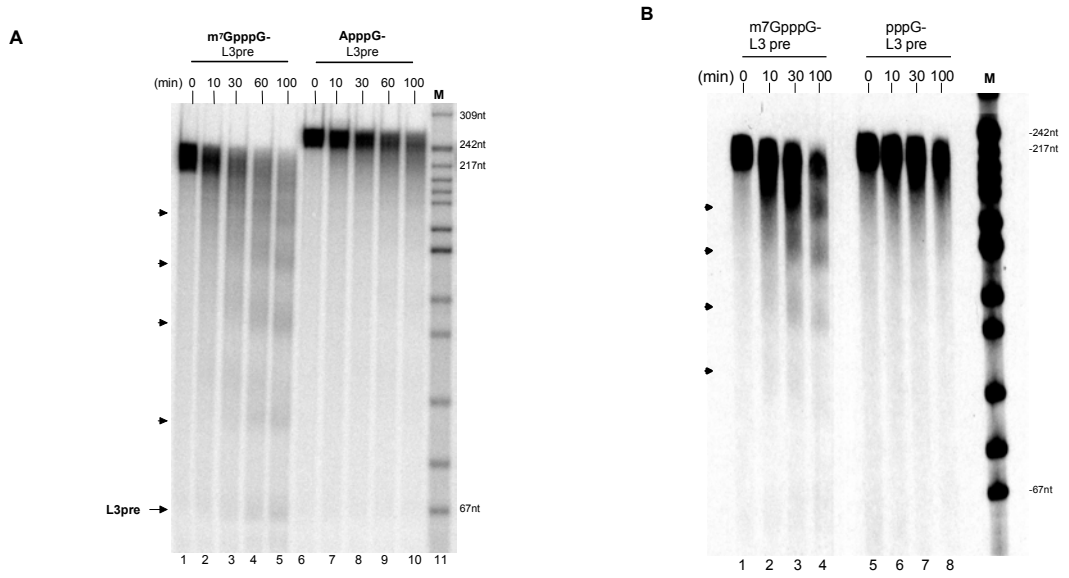

Figure 3.1: Cap-dependent deadenylation in a HeLa cytoplasmic extract.
A. Two reaction mixtures were assembled on ice, containing 36 fmol of m^7GpppG-capped or ApppG-capped and polyadenylated L3pre-RNA in 70 µl of reaction buffer supplemented with 120 mM KAc. The reactions were started by the addition of HeLa CXT and incubation at 37°C. 1.7 µl HeLa CXT for the m^7GpppG-capped RNA and with 2.3 µl HeLa CXT for the ApppG-capped RNA were used due to the difference in length of the poly(A)-tails and PABPC binding sites. Aliquots were taken at the indicated times and analysed on a 8% denaturing polyacrylamide gel. **B.** Two reaction mixtures containing 26 fmol m^7GpppG-capped or non-capped L3 pre A(160) RNA in 50 µl reaction buffer plus 120 mM KAc were assembled on ice. Both reactions were started by the addition of 1.3 µl HeLa CXT and incubation at 37°C. Aliquots were removed at the indicated times and analysed on a 8% denaturing polyacrylamide gel. The arrowheads indicate intermediate decay products.

The requirement for a 7-methyl guanosine cap in deadenylation was also investigated by an inhibition experiment. The addition of free m^7GpppG inhibited the deadenylation of m^7GpppG-L3 preA_{160} RNA in the HeLa cytoplasmic extract at the lowest concentration tested, 20 µM, whereas roughly 300 µM free GpppG was required to achieve the same effect (Figure 3.2). Thus, deadenylation in HeLa cell extracts depends on the authentic cap structure, m^7GpppG. An unmethylated cap is recognized with much lower affinity.

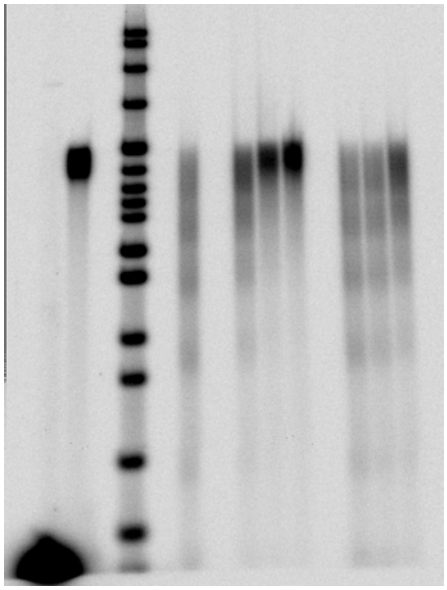

Figure 3.2. Competition with free cap structure analogs in HeLa CXT.
20 µl reaction mixtures with 10 fmol m^7GpppG-capped and polyadenylated L3 pre RNA, 0.5 µl HeLa CXT and 0, 20, 100, and 330 µM m^7GpppG or GpppG were assembled on ice. The deadenylation reactions were incubated at 37°C for 80 min and the products were separated on a 8% denaturing polyacrylamide gel. Lane 1, L3 pre RNA without poly(A) tail and lane 2, polyadenylated L3 pre (A_{160}); lane 4, a DNA size marker with the sizes of two of the fragments indicated on the left and decay intermediates are indicated with arrowheads.

3.1.2. A m^7GpppG-capped RNA is the preferred substrate for bPARN

If PARN is responsible for the observed deadenylation in HeLa cytoplasmic extracts, it is plausible that the protein purified from calf thymus, bPARN (*Körner and Wahle, 1997*), would exhibit a similar cap-dependence. When this protein was allowed to act on

polyadenylated RNA substrates with different 5´-ends (Figure 3.3 A), an accelerated reaction was clearly to be seen for the m^7GpppG-capped RNA. In fact, the accumulation of fully deadenylated RNA plotted against the incubation time revealed a four fold higher rate of product formation for the m^7GpppG-capped RNA than RNA substrates with other 5´-ends (Figure 3.3: B). Interestingly, RNA degradation beyond the poly(A) portion by about 20 nucleotides, was also facilitated by the cap structure.

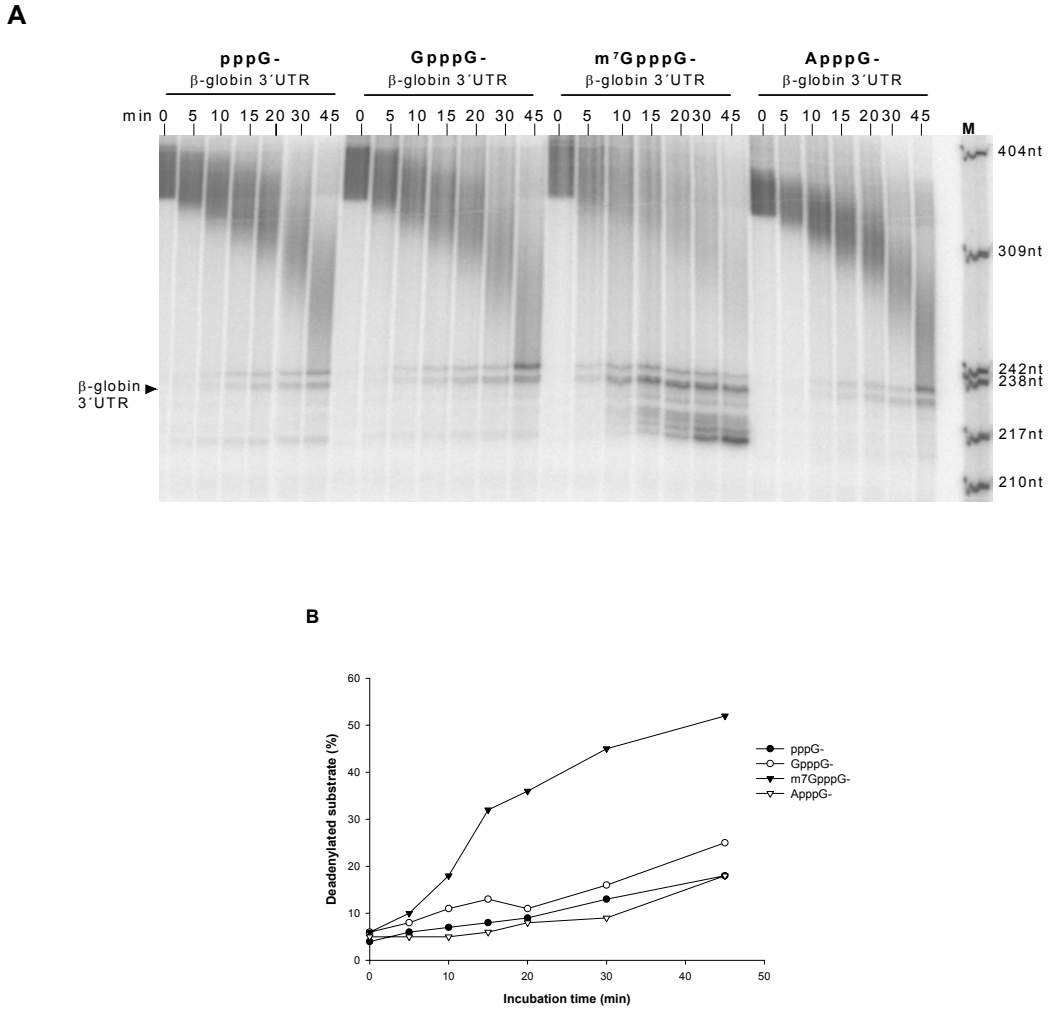

Figure 3.3. RNA with a methylated-cap structure is the preferred substrate for bPARN.
A. Reaction mixtures were assembled in ice, containing 40 fmol polyadenylated (A130) ß-globin 3´-UTR RNA with an m7GpppG, GpppG, ApppG dinucleotide or pppG at the 5´-end of the transcript in 50 µl reaction buffer supplemented with 10 mM KCl. The reactions were started by the addition of 15 fmol boPARN and incubation at 37°C. Aliquots were withdrawn at the indicated times and the decay products were separated on a 6% denaturing polyacrylamide gel. Fully deadenylated ß-globin RNA is indicated by an arrowhead, and the sizes of the DNA are shown at the side of the M lane. **B.** The accumulation of fully deadenylated RNA was quantified by Phosphorimager (Molecular Dynamics) analysis. The appearance of deadenylated substrate at each time point, as part of the total radioactivity in each lane, was plotted against the incubation time.

Combined in the same reaction mixture, will bPARN prefer a RNA substrate with a methylated cap to non-methylated capped RNA? This question was addressed by attaching a m^7GpppG-cap to a 5´-extended L3pre RNA and a GpppG-cap to L3pre RNA. These transcripts and their degradation products could thus be distinguished by size in a denaturing gel. The RNAs, each carrying a poly(A) tail of similar length (80-100 nt), were added to a deadenylation reaction in equal concentrations and incubated with bPARN for the indicated times. Again, the RNA with a methylated cap at the 5´-end was deadenylated faster and upon an extended incubation time, the enzyme was able to invade the non-polyadenylated part of the RNA (Figure 3.4, left panel). A similar result was obtained when the cap on the short L3pre RNA was carrying the methyl-group (Figure 3.4, right panel). It should be noted that fully deadenylated L3pre RNA could not be detected on this gel since the separation of polyadenylated and deadenylated L3preL RNA required a longer gel run.

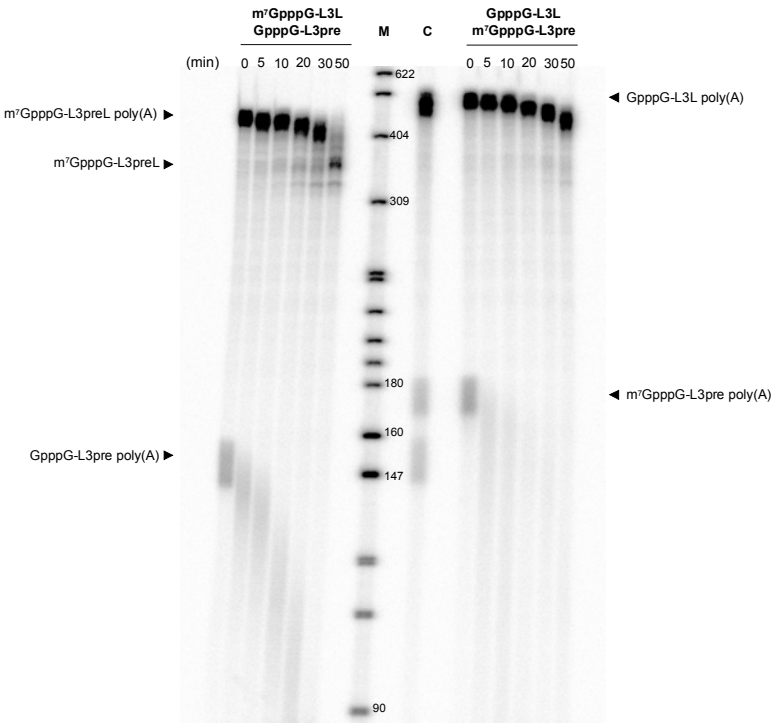

Figure 3.4. Preference for RNA with a m^7GpppG-cap over GpppG-capped RNA in the same reaction. Two 50 µl reaction mixtures were assembled on ice containing (*Left*): 25 fmol each of polyadenylated m^7GpppG-L3preL and GpppG-L3pre RNA and (*Right*):25 fmol each of polyadenylated GpppG-L3preL and m^7GpppG-L3pre RNA. The deadenylation reactions were started by the addition of 15 fmol bPARN and incubation at 37°C. 8 µl aliquots were withdrawn at indicated time points and the reactions were stopped by Proteinase K digestion. Degradation products were separated on a 8% denaturing polyacrylamide gel. RNA substrates incubated for 45 minutes in the absence of bPARN (lane C). DNA size marker with the sizes in nucleotides indicated to the right (lane M).

The initial rate of deadenylation by bPARN was assayed by the release of acid-soluble nucleotides (*Körner and Wahle, 1997*). ß-globin 3´-UTR RNA with a radiolabelled poly(A) tail and with or without a methylated cap were used as substrates. Also in this assay, the m^7GpppG-RNA was deadenylated at a fourfold higher rate compared to the RNA without a methylated cap (Figure 3.5). Furthermore, the initial deadenylation rate is independent of the length of the poly(A) tail on the RNA substrates (compare open and filled symbols).

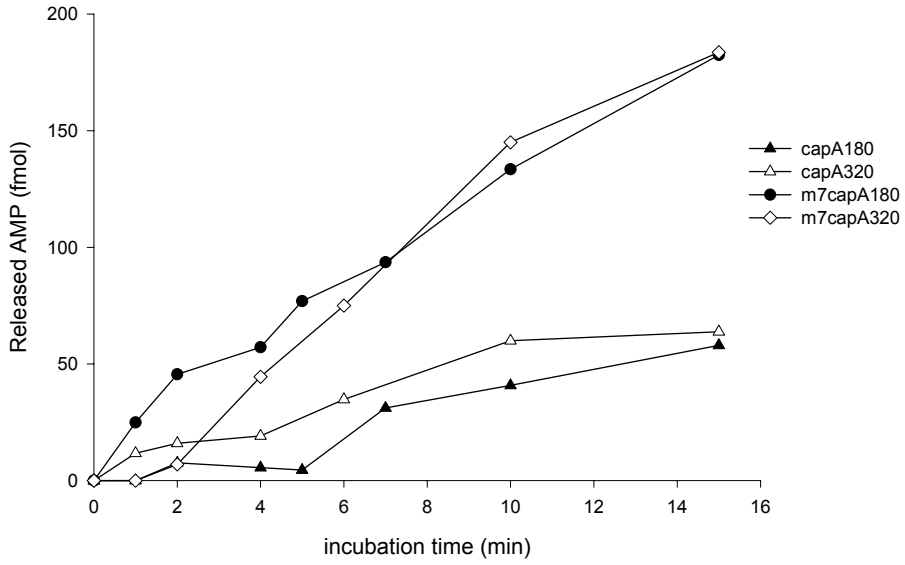

Figure 3.5: Initial rates of cap-dependent deadenylation.
The poly(A)-degrading activity of bPARN was assayed by the release of TCA-soluble nucleotides from radiolabelled poly(A)-tails on m^7GpppG-capped and GpppG-capped ß-globin 3´-UTR RNAs. Reaction mixtures containing 7.5 fmol size fractionated RNA substrate in 10µl reaction buffer plus 100 mM KCl were pre-warmed at 37°C for 5 min. and the reactions started by the addition of 2 fmol bPARN. The reactions were stopped at indicated times with 30 µl ice-cold stop mix, containing 13.3% TCA, 5 µg glycogen and 0.1% SDS. After precipitation by centrifugation, 20 µl supernatant was counted in a scintillation counter and the released acid soluble AMP was plotted versus incubation time. RNAs with a poly(A) tail length of 180 nt are indicated with filled symbols and poly(A) tails of 320 nt are indicated with open symbols.

Together, these results indicate that a bona fide cap structure on the RNA substrate stimulates the deadenylating activity in both HeLa cell extracts and of the purified bPARN.

3.1.3. Bovine PARN is a cap-binding protein

Cap dependence of deadenylation in HeLa cell extracts (Figures 3.1. and 3.2.) could be mediated by a cap-binding protein acting as a co-factor or reflect an intrinsic cap-binding activity of the nuclease itself. Although the bovine PARN preparation still contained other proteins none of the known cap-binding proteins (eIF4E and the 20 kDa subunit of the nuclear cap binding complex) were detectable in this preparation (*C. Körner,1998b*). However, it could not be excluded that an additional protein, being present in sub-stoichiometric amounts, was responsible for the cap-recognition. In order to determine if bPARN itself had a cap-binding activity, a partially purified side fraction (Phenyl-Superose fraction 34, *Körner and Wahle, 1997*) of bPARN was examined for its capability to bind to m^7GTP-Sepharose. By comparing the load and the flow-through fractions, in a silver-stained SDS-polyacrylamide gel, a significant depletion of PARN could be observed (Figure 3.6. A). In the two following washing steps a small amount of PARN was released from the m^7GTP-Sepharose resin. At the washing step with GTP only insignificant quantities of PARN were eluted. Most of the protein, however, was eluted with 0.1 mM m^7GTP and the rest by boiling the resin in SDS. A small amount of a 60 kDa protein was co-eluted with PARN but if binding to the beads was mediated by an associated cap-binding factor, one would expect stoichiometric amounts of this protein to be present in the eluate.

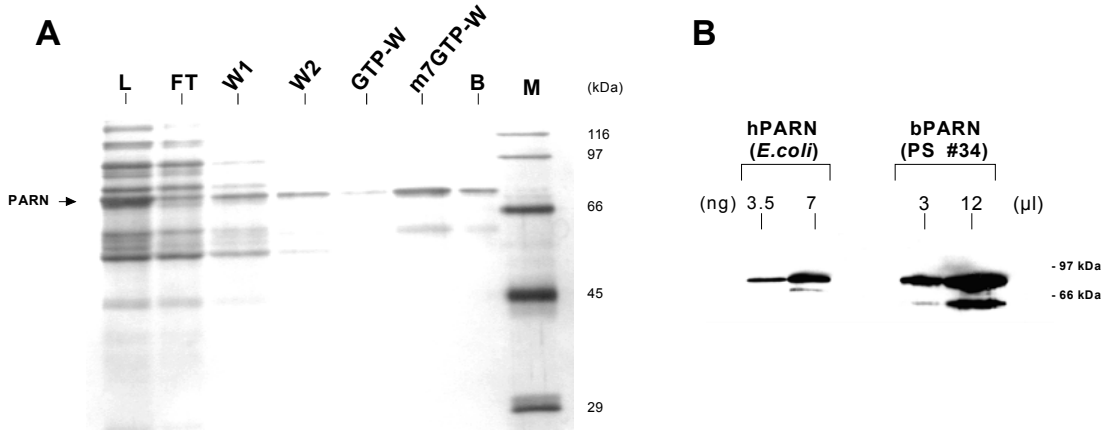

Figure 3.6: Binding of bPARN to m^7GTP-Sepharose. A. A partially purified fraction of bPARN (Phenyl-Superose fraction 34) was incubated with m^7GTP-Sepharose at 8-12 °C for 2 hours. Lane L (load), starting material; lane FT (flow-through), unbound proteins; lanes W1 and W2, washes with nucleotide-free buffer; lane GTP-W, wash with 0.1 mM GTP in the buffer; m7GTP-W, wash with 0.1 mM m^7GTP in the buffer; lane B, beads; lane M, molecular weight marker. 50% of the sample was loaded on the gel in lanes L and FT whereas the entire samples were loaded in the other lanes. The proteins were separated on a 9% SDS-polyacrylamide gel and silver stained. **B.** Western blot analysis of the PARN preparation used in A probed with anti-PARN antibodies.

Western blot analysis of the PARN preparation used for the experiment revealed, that a 60 kDa polypeptide reacted with the anti-PARN-antibody (Figure 3.6. B). Consequently, the only other protein binding to m^7GTP-Sepharose in this PARN preparation was likely to be a proteolytic fragment of PARN itself. In conclusion, PARN does not only show a strong cap dependence in catalyzing deadenylation but has also an inherent cap binding property. The direct binding of PARN to m^7GTP and m^7GpppG is therefore likely to increase the affinity of the enzyme to RNAs carrying an authentic cap structure.

3.2. Cap-dependent deadenylation by recombinant human PARN

Human PARN (hPARN) cDNA, expressed in *E.coli* as a fusion protein with a N-terminal His_6-tag (*Körner et al., 1998*) proved to possess similar catalytic properties as PARN purified from calf thymus. However, the specific activity of the recombinant protein under physiological salt conditions was eight-fold lower than that of bovine PARN (*Körner et al., 1998*). Furthermore, while the bovine enzyme seemed to be highly stimulated by m^7GpppG-capped RNA, the recombinant hPARN did not show a significant preference for 7-methyl G-capped RNAs (*C. Körner, 1998b*).

A new protein preparation of bacterially expressed recombinant hPARN was assayed with polyadenylated RNA carrying either a methylated or unmethylated cap. To assure that the observed substrate was correctly capped, the RNA was post-transcriptionally radiolabelled in the cap structure using ^{32}P-GTP and recombinant guanylyl transferase (see section 2.2.5.). The degradation products were separated by denaturing gel electrophoresis and analysed on a PhosphorImager (Molecular Dynamics). Figure 3.7 shows, that hPARN deadenylates RNAs with a GpppG-cap at a slower rate than m^7GpppG-capped RNA. However, the difference in deadenylation rate is less pronounced compared to that of the purified bovine PARN (Figure 3.7. (right) and Figure 3.3. B). Furthermore, the *E. coli* expressed nuclease invaded the non-adenylate portion of both m^7GpppG- and GpppG-capped RNA (Figure 3.7. (left) and Figure 3.3. A).

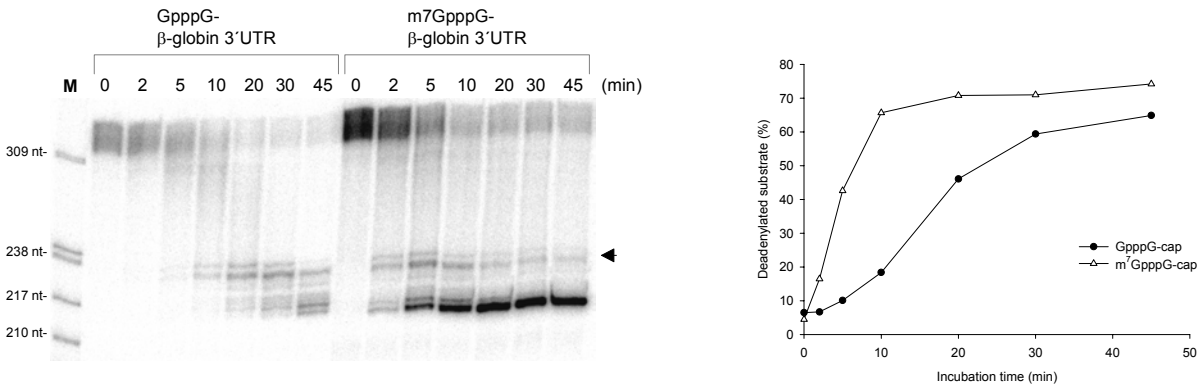

Figure 3.7. Cap dependence of recombinant hPARN. (Left) Deadenylation assay. Two 50 µl reactions with 80 fmol of either m^7GpppG- or GpppG-capped and polyadenylated β-globin 3´-UTR RNA in PARN reaction buffer with 100 mM KCl, were assembled on ice. The deadenylation reactions were started by the addition of 5 fmol recombinant hPARN. Aliquots of 7 µl were taken at the indicated time points and stopped by Proteinase K digestion. After ethanol precipitation, degradation products were separated on a 8% urea-polyacrylamide gel and analysed on a PhosphorImager. The position of fully deadenylated β-globin RNA is indicated by an arrowhead (Right) Quantitation of the accumulation of fully deadenylated RNA in the gel assay. The appearance of deadenylated substrate at each time point, as part of the total radioactivity in the lane, was calculated by the ImageQuant 5.0 program and plotted versus incubation time.

The higher specific activity under physiological salt conditions and the discrimination between methylated and non-methylated capped RNA that was observed with purified bovine PARN might be the result of a post-translational modification which is lacking in *E. coli* expressed proteins. In addition, hPARN was expressed as a His_6-fusion protein and although this peptide-tag is small, it might influence the activity of the protein. To test this possibility, hPARN with and without His_6-tag, was expressed in *Drosophila* Schneider 2 (S2) cells. The expression vector, pMT/V5-HisC allowed inducible expression from the metallothionein promoter (*Bunch et al., 1988*) and a stable cell line was generated by co-transfection with the selection vector, pCoHYGRO. As there is no endogenous *Drosophila* homologue to PARN, the S2 cells provide a null background

3.2.1. Over-expression of hPARN in Schneider 2 cells

Schneider 2 cells were co-transfected with the expression plasmid pMT-HisPARN and the selection plasmid pCoHYGRO to establish a stable cell line for expression of hPARN (see Materials and Methods). Cells, that appeared to be hygromycin resistant after one week in selection medium were diluted by seeding into a 24-well plate (~10^5 cells/well). After an additional 3 days of growth in selection medium, half of the cells from each well were re-seeded into 6-well plates for an expression test. PARN expression was induced with 500 µM copper sulfate for 24 hours. Whole cell lysates were prepared, separated by SDS-PAGE and transferred to a nitrocellulose membrane. Western blot analysis revealed that PARN was expressed in 11 of the 24 wells (Figure 3.8). A pronounced 60 kDa polypetide cross-reacted with the anti-PARN antibody in all induced extracts (compare non-induced cell control). Interestingly, this peptide cannot be seen in induced cells carrying the empty vector (Western blot, data not shown). Hence, this peptide may be derived from the PARN plasmid and is either a protein degradation product or reflect a deletion of the PARN cDNA. Cells expressing full-length PARN protein (PARN:S2 A4) were expanded for large scale production. A time course for induction of PARN in these cells revealed a maximum protein production between 24-38 hours post-induction (data not shown). A stable cell line expressing His_6-PARN fusion protein was established in a similar way (data not shown).

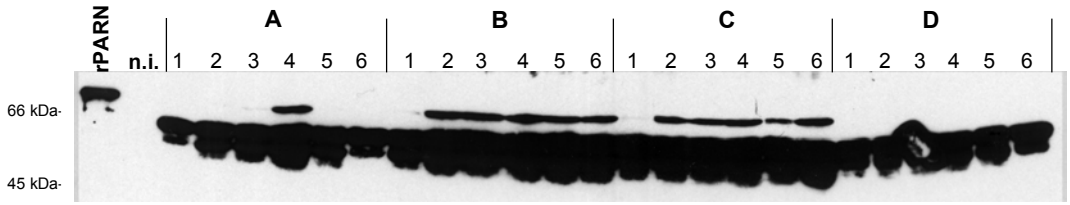

Figure 3.8. Expression of hPARN in transfected S2 cells. Western blot analysis of different populations of hygromycin-resistant S2 cells after co-transfection with pMT-HisPARN and pCoHYGRO. PARN expression was induced with copper sulfate for 24 hours and whole cell lysates were separated on a 9% SDS-polyacrylamide gel and transferred onto nitrocellulose membrane. PARN expression was detected with anti-PARN antibodies. Capital letters indicate the rows and numbers indicate the wells in the 24-well tissue culture dish. Lysate from non-induced cells is indicated with n.i. and rPARN is recombinant hPARN purified from *E. coli*.

To establish the conditions for large scale production of PARN, S2 cells were adapted to suspension growth in serum free medium. The cells were grown in a shaker culture, since oxygen is not rate limiting under these conditions (*Richardson, 1995*). A 100 ml culture with an initial density of 2x10 ^{6} cells/ml in a 250 ml Erlenmayer flask was monitored for 6 days. Living cells were counted and the cell density was plotted against time (Figure 3.9). Since these cells are able to grow logarithmically up to 2x10^{7} cells/ml as a batch culture, a suitable cell density for induction of PARN expression would be about 10^{7} cells/ml.

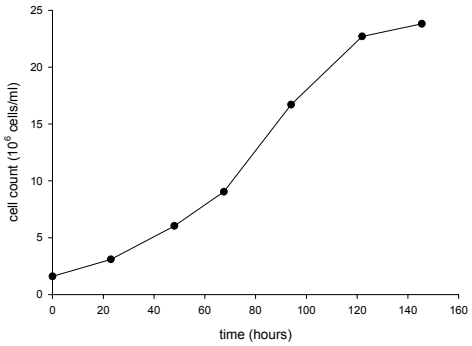

Figure 3.9. Growth of S2 cells in shaker culture. 100 ml SF 900 II medium in a 250 ml Erlenmayer flask, with a loosened metal cap, was inoculated with 2x10^{8} suspension adapted S2 cells. The culture was incubated at room temperature in an orbital shaker at 135 r.p.m. Cells were counted using the trypan blue exclusion assay and the viable cell count was plotted against time.

3.2.2. Purification of hPARN from Schneider 2 cells.

The stable, PARN expressing cell line was induced with copper sulphate and the cells were harvested after 26 hours of induction. After lysing the cells with a Dounce homogenizer, a S100 extract was prepared and hPARN was further purified by successive Resource Q, Blue Sepharose and Phenyl-Superose chromatography. An activity peak, estimated by the TCA-precipitation assay (see section 2.2.6), was observed after fractionation over a Resource Q column at 0.2 M KCl and the active fractions were applied on a Blue Sepharose column. The recovery after this step was about 50% (load: 550 U, flow through: 8 U and elution: 244 U) (see also section 3.4.2.). Such a loss of activity was not observed in the purification of bovine PARN from calf thymus (*Körner and Wahle, 1997*). However, deadenylation activity during the two first steps of that purification was assayed in the presence of an excess of rRNA to

suppress unspecific nucleolytic activity. Since no competitor was added in these assays, the low recovery on Blue Sepharose in this purification might be explained by the elimination of other nuclease activities at this step. PARN was eluted in the last fractions of the descending $AmSO_4$-gradient in the Phenyl-Superose fractionation (Figure 3.10.) which might explain that only 65% of the activity (158 U) was recovered (see also section 3.4.2.). A single polypeptide of about 74 kDa, corresponding to the size of PARN, co-migrated with the activity in a silver stained SDS-polyacrylamide gel.

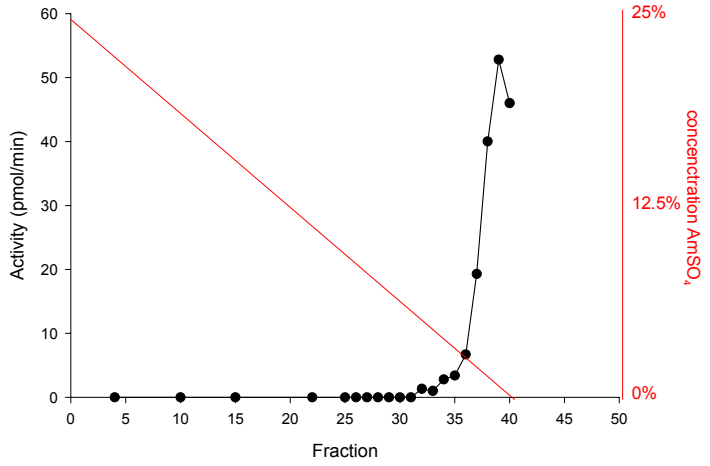

Figure 3.10. **Activity profile of the final Phenyl-Superose column**. 2 µl of each fraction was analysed by the TCA-precipitation assay. The activity, as released pmol AMP/min, is plotted versus fraction number. The concentration of ammonium sulphate in each fraction is indicated in red.

The purified protein was examined for its preference for RNAs with a methylated cap in a deadenylation assay with m^7GpppG-capped and ApppG-capped β-globin RNA as substrates. Figure 3.11. shows that hPARN expressed in Schneider 2 cells is indeed stimulated by a m^7G-cap (compare Figures 3.3. and 3.7.)

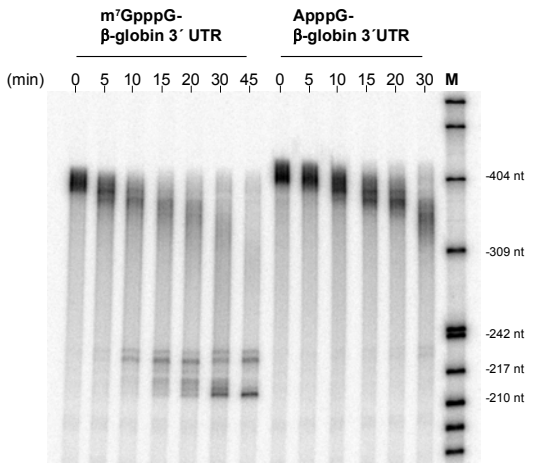

Figure 3.11. Recombinant hPARN expressed in S2 cells prefers correctly capped RNA. Two 100 µl reaction mixtures were assembled on ice containing 120 fmol of co-transcriptionally m^7GpppG- or ApppG-capped and polyadenylated β-globin RNA in PARN reaction buffer with 100 mM KCl. The deadenylation reaction was started by the addition of 30 fmol S2 PARN (Phenyl-Superose fraction 39) and incubation at 37°C. 20 µl aliquots were removed at the indicated times and stopped by Proteinase K digestion. The reaction products were separated on a 8% denaturing polyacrylamide gel. The sizes (in nucleotides) of the DNA marker are indicated on the right.

3.2.3. Purification of recombinant 6xHis-tagged hPARN

The stable S2 cell line expressing the His_6-PARN fusion protein was induced with 500 µM copper sulphate and harvested 26 hours post-induction. Lysis of the cells was done by freezing and thawing in lysis buffer (see section 2.2.4.1.) followed by centrifugation to remove cell debris. The supernatant was fractionated by FPLC Ni^{2+}-NTA affinity chromatography and eluted with a imidazole gradient. Active fractions were subsequently applied on a MonoQ FPLC column. Interestingly the activity, as assessed by the TCA-precipitation assay, was divided into two peaks (Figure 3.12 A). The activity peak fractions were co-migrating with two polypeptides of 74 kDa and 60 kDa (Figure 3.12. B). A Western blot analysis of the fractions revealed that both polypeptides reacted with anti-PARN antibodies (Figure 3.12 C). The shorter polypeptide may therefore be a proteolytic fragment of the full-length PARN-protein. A deletion mutant lacking the 193 C-terminal amino acids of hPARN showed full nucleolytic activity (C. K*örner, 1998b*). Furthermore, a 54 kDa PARN fragment, purified from a HeLa nuclear extract and shown to be a C-terminal truncation of the full-length protein, was also found to have deadenylating activity *(Åström, 1992 and*

Martinez, 2000). As the Exo I-III motifs, which are important for catalytic activity, are located within the N-terminal two thirds of the protein, it is reasonable to assume that the shorter polypeptide is a C-terminal truncation of PARN. Interestingly, in the Western blot analysis of the hPARN expression test, a prominent polypeptide of similar size was observed in induced cells that must have originated from PARN (see Figure 3.8).

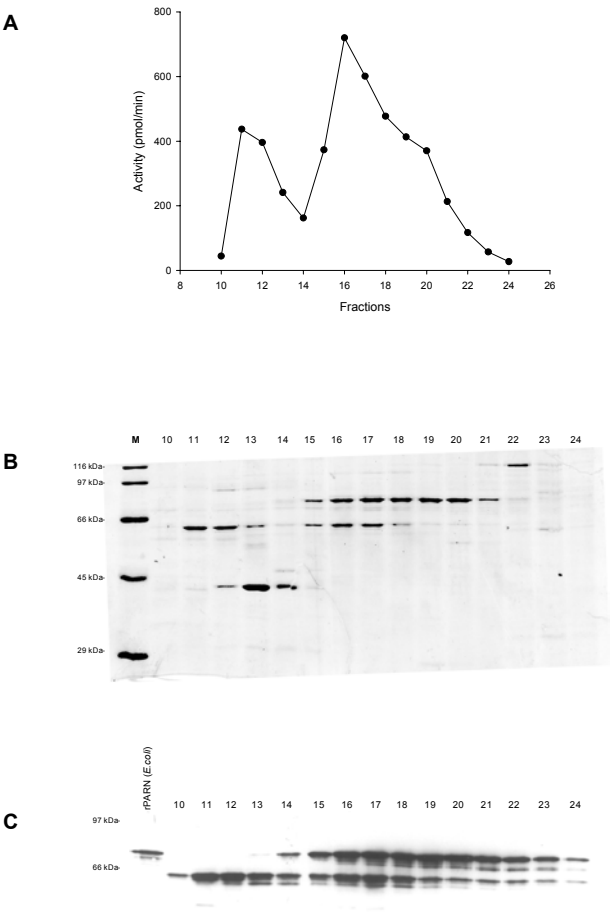

Figure 3.12 A. Activity profile after MonoQ fractionation of His_6-hPARN. The activity (pmol AMP/min) in 1µl of the fractions, monitored by the TCA-precipitation assay in PARN reaction buffer with 120 mM KAc. **B**. **Comassie stained gel** of the active MonoQ fractions. 5 µl of the indicated fractions were separated on a 9% SDS-polyacrylamide gel. **C**. **Western blot analysis** of the corresponding MonoQ fractions probed with anti-PARN antibodies.

3.2.4. The N-terminal His_6-tag does not influence the m^7cap-preference of hPARN.

The difference between purified bovine PARN and bacterially expressed hPARN, with respect to preference for m^7-capped RNA substrates, might also be due to the presence of a N-terminal His_6-tag on hPARN. In order to test this possibility, His_6-hPARN was expressed in

Schneider 2 cells (see section 3.2.4.). Polyadenylated β-globin RNAs with a m^7GpppG-cap or a GpppG-cap were subjected to deadenylation by recombinant hPARN with or without His_6-tag. Deadenylation of methylated capped RNA was more rapid and fully deadenylated substrate appeared earlier than for the RNA without a methylated cap regardless if the enzyme carried a His_6-tag or not (Figure 3.13. A and B). The N-terminal His_6-tag on recombinant hPARN does not influence the preference for a correctly capped RNA substrate. Thus, it is likely that a post-translational modification makes the enzyme cap dependence.

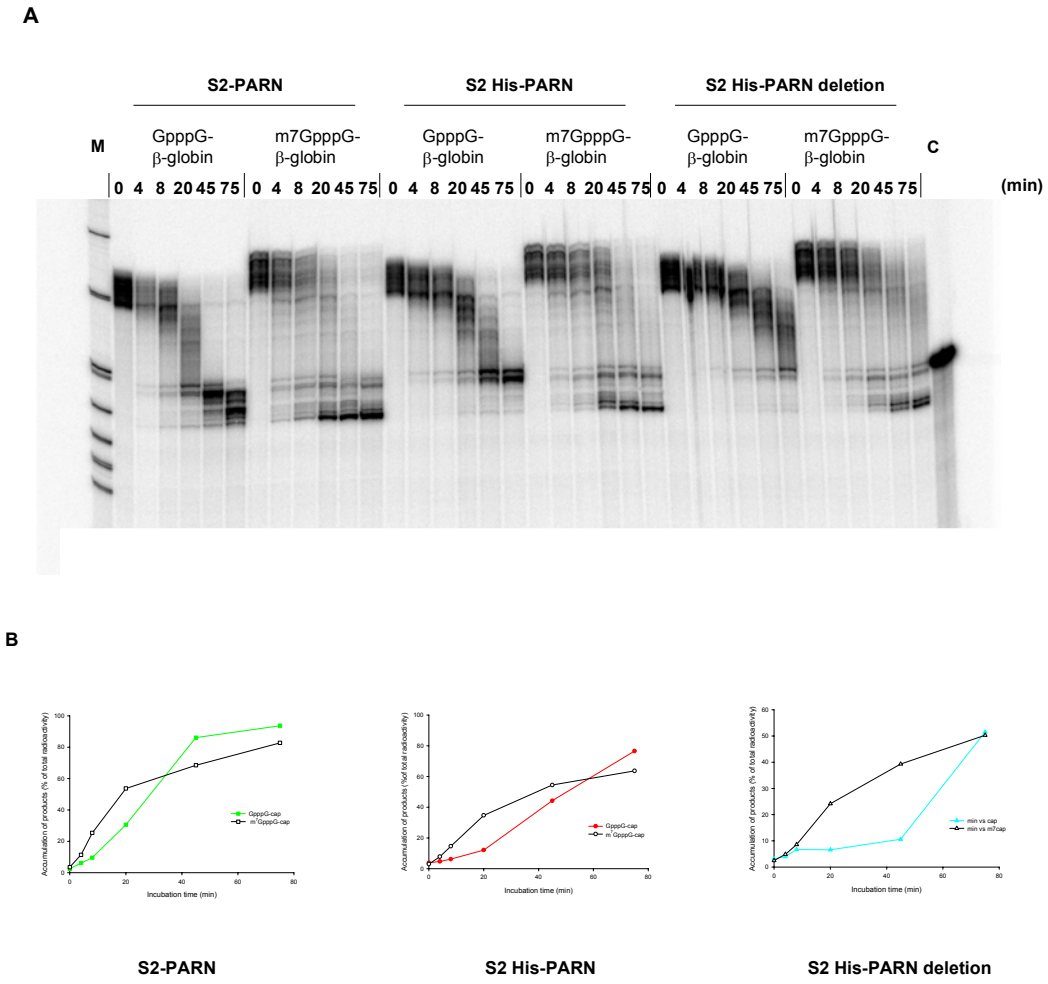

Figure 3.13. Effect of the N-terminal His_6-tag on recombinant hPARN cap-dependence. A. Deadenylation assay. Reaction mixtures containing 150 fmol m^7GpppG- or GpppG-capped and polyadenylated β-globin RNA in 50 µl PARN reaction buffer, supplemented with 100 mM KCl, were assembled on ice. The reactions were started by addition of 5 fmol hPARN (S2-PARN: PS fraction 39, S2 His-PARN: MQ fraction 19, S2 His-PARN deletion: MQ fraction 11) and incubation at 37°C. At indicated times, 7 µl aliquots were withdrawn and the reactions were stopped by Proteinase K digestion. The degradation products were separated on a 8% denaturing polyacrylamide gel and analysed on a PhosphorImager. **B.** Accumulation of fully deadenylated RNA at each time point, as part of the total radioactivity in the lane, was plotted against the incubation time.

The nucleolytically active PARN fragment (section 3.2.4.) was also tested for its preference for m^7GpppG-capped RNA in this experiment. The PARN fragment shortened the poly(A) tails of both methylated and unmethylated capped RNA at a slower rate than the full-length proteins, despite the fact that the specific activities of the fragment and the full length His_6-fusion protein were identical. Still, RNA with a methylated cap seemed to be the preferred substrate

3.3. The effect of the 7-methyl group in the 5´ cap structure on hPARN reaction mechanism

3.3.1. Transient transfection and expression of hPARN in HEK293-EBNA cells

We employed a large scale transient gene expression system in mammalian cells (*Wurm and Bernard, 1999; Meissner et al., 2000*) for purifying recombinant hPARN. One advantage of such a system is that a toxic protein can be expressed during a short time-period at a high cell density. It is also less time consuming than an expression system based on stable integration of the gene of interest into the chromosome. Moreover, co-transfecting a GFP-expressing vector allows to directly monitor transfection efficiency *in vivo* and to correlate fluorescence intensity with protein expression (*Hunt et al, 1999*).

In order to establish optimal conditions for a large scale transfection of HEK293-EBNA cells (Invitrogen) with the pEAK8-PARN plasmid construct, a DNA titration and a time course were performed (Dr. Lucia Baldi, EPFL, Lausanne). $5x10^5$ adherent HEK293-EBNA cells were transfected with a total of 4µg DNA consisting of carrier DNA, 10% pEAK8-EGFP plasmid and 10-90% pEAK-PARN plasmid. The cells were harvested between 21h to 117h post-transfection and the content of PARN protein at different time-points was analysed by Western blot. Figure 3.14 shows a correlation between protein content and the proportion of pEAK8-PARN plasmid to total DNA in the transfection mixture. A longer exposure revealed a weak signal corresponding to the expected size of PARN in the mock transfected cells. This polypeptide reacting with the anti-PARN antibodies probably reflects endogenous PARN in the HEK293 cells. Maximum PARN expression appears to occur at 44-74h post-transfection.

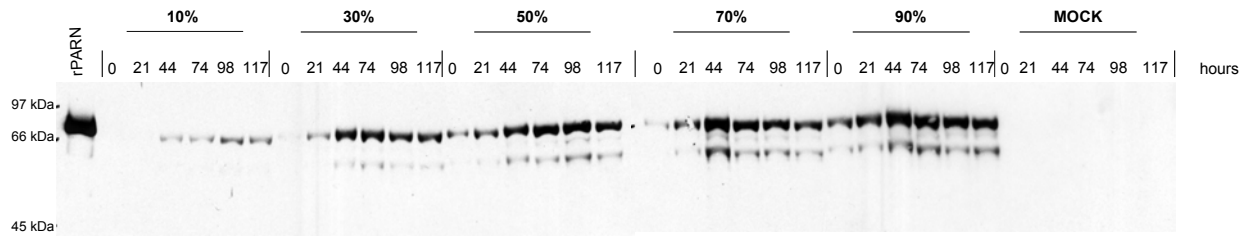

Figure 3.14. Expression of PARN after transient transfection of HEK293-EBNA cells. Whole cell lysates from 10^4 cells per time point were assayed for expression of hPARN in a Western blot using anti-PARN antibodies. The cells were harvested at indicated times after transfection.

A dose-dependent, toxic effect of the pEAK8-PARN vector could be observed after 5 days (Figure 3.15.). Consequently, a high concentration of the pEAK8-PARN plasmid in the transfection mix and harvesting the cells 2 days post-transfection to avoid the toxic effect. was chosen for the large-scale production of PARN.

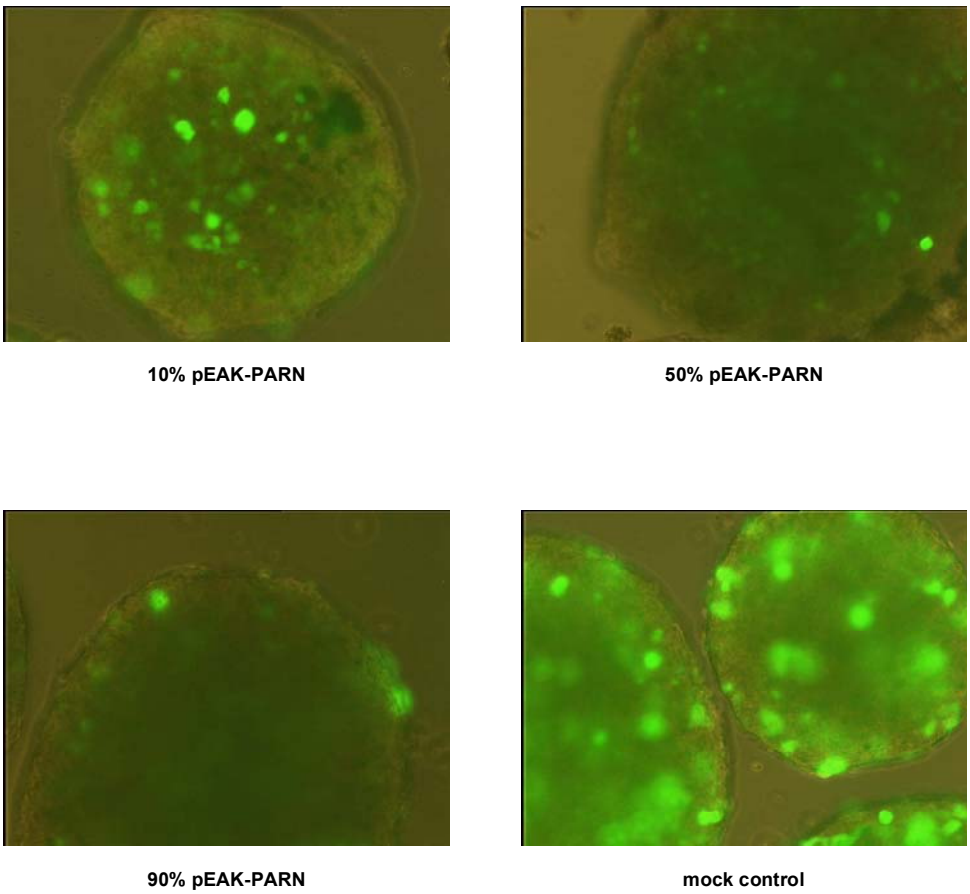

Figure 3.15. Cytotoxic effect of PARN expression. $5x10^5$ HEK293-EBNA cells were transfected with 4 μg DNA consisting of carrier DNA, 10% pEAK8-EGFP plasmid and 10%, 50% and 90% pEAK8-PARN plasmid. At 117 h post-transfection the EGFP fluorescent signals in the transfected cells were examined in a confocal microscope.

3.3.2. Purification of recombinant hPARN expressed in HEK293-EBNA cells

HEK293-EBNA cells, transiently transfected with the pEAK8-PARN expression plasmid (Dr. L. Baldi, EPFL, Lausanne) (section 2.2.4.1.), were used for purification of recombinant hPARN. Cytoplasmic and nuclear extract were made (section 2.2.4.1.) and assayed for deadenylating activity using the TCA-precipitation assay described in section 2.2.6. Most of the activity was found in the cytoplasmic extract (CXT), and this was used for further purification. The purification was performed with two batches of cells (P1 and P2) and is summarised in Table 3.1. It is worth mentioning that the P1 cells were contaminated with bacteria which could explain the very low yield for this preparation. Bacterially derived nucleases may have contributed to the activity in the cytoplasmic extract and the S100 fraction, thus explaining the poor recovery after the Resource Q and the Blue Sepharose columns (see also section 3.2.3). Moreover, some protein may have been retained in the Blue Sepharose column as the enzyme was eluted in one step with 1M KCl.

Step	**Protein (mg)**		**Activity (U)**		**Specific activity (U/mg)**		**Yield (%)**		**Purification (-fold)**	
	P1	**P2**	**P1**	**P2**	**P1**	**P2**	**P1**	**P2**	**P1**	**P2**
Homogenate	60	72.8	1140	5096	19	70	100	100	-	-
CXT	45.5	42.5	1547	6205	34	146	136	122	1.8	2.1
NXT	8	8.1	178	200	22	25	17	4	-	-
S100	21.6	18.4	2230	2723	49	148	196	53	2.6	2.1
Resource Q	6	4.2	623	1772	104	422	55	35	5.5	6
Blue Sepharose	0.65	0.48	124	842	191	1754	11	17	10	25
*Phenyl-Superose	*0.22		*805		*3657		*13		*50	

Table 3.1. Purification of hPARN from HEK293-EBNA cells. Purification was monitored by the TCA-precipitation assay described in section 2.2.6. One unit is defined as the activity that releases 1 nmol of nucleotides/min (*Körner and Wahle, 1997*). CXT is cytoplasmic extract after a low spin centrifugation, NXT is crude nuclear extract after lysis of nuclei, S100 is the supernatant of CXT after centrifugation at 100,000 g for 1 hour. * indicates, that the active fractions from both preparations were pooled before this step and the final activity was compared to the sum of the activities in the homogenates for both preparations.

The activity profile of the final Phenyl-Superose column and a Comassie stained SDS-polyacrylamide gel with the active fractions are shown in Figure 3.16. As PARN was eluted in the 6 last fractions of the descending $AmSO_4$ gradient, collecting a few more fractions at the wash step would probably have increased the yield. However, most of the activity was eluted. With an approximately 50-fold purification, the enzyme was more than 90% pure (Figure 3.16. B) and the only other polypeptide that co-purified with PARN is a proteolytic fragment of PARN itself (Western blot analysis, data not shown)

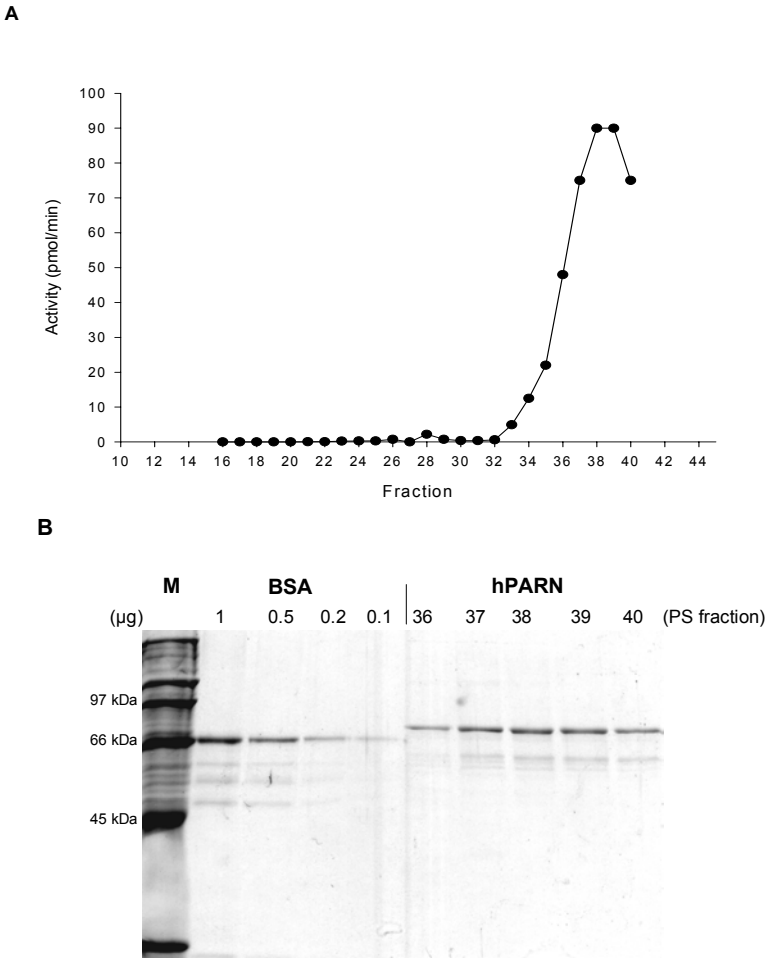

Figure 3.16. Final column of the purification of recombinant hPARN from HEK293-EBNA cells. A. Activity profile of the Phenyl-Superose (PS) column. The activity in 2 µl of each fraction was assayed by the TCA-precipitation assay. **B** Comassie stained gel of active fractions. 5 µl from each fraction were separated on a 9% SDS-polyacrylamide gel. 0.1, 0.2, 0.5, and 1 µg BSA , were applied on the same gel to estimate the protein concentration in the PS fractions.

3.4. The m^{7}GpppG-cap induces a processive reaction mechanism.

The observed deadenylation patterns of m^{7}GpppG-capped RNAs, where full-length substrate and completely deadenylated products co-exist (Figures 3.3, 3.11, and 3.12), may be indicative for a processive reaction mechanism. However, the RNA substrates were likely to be heterogeneous, due to e.g. some modification of the 3´-end making the RNA resistant to 3´-exonucleolytic digestion (*Körner and Wahle, 1997*) or incomplete capping. In the above-mentioned experiments, the RNAs were co-transcriptionally capped by the use of cap-analogues, such as m^{7}GpppG, GpppG and ApppG. The dinucleotides will be incorporated by the phage polymerase at the 5´-end of RNA, as the first nucleotide in the transcript is a guanosine. Many of the RNA molecules will not be capped due to competition between the cap-analogous and the GTP in the transcription reaction. Furthermore, the m^{7}G-nucleotide is separated from the RNA body by a tri-phosphate bridge in normal caps, but when m^{7}GpppG is used for transcription, about 40% of the RNA has the cap incorporated in the "wrong" orientation (*Pasquinelli, 1995*).

To overcome these problems, the cap structure was added post-transcriptionally by the use of recombinant guanylyl transferase (protein preparation, Dr. S. Meyer). With ^{32}P-labelled GTP in the capping reaction, it was possible to label the RNAs at their 5´-ends. The fate of capped RNA that is degraded from the 3´-end could therefore selectively be followed. In addition, S-adenosyl-methionine in the reaction mix would be used for methylation of the cap in a subsequent step of the reaction so the methyl group would always be in the correct position.

Recombinant hPARN, purified from transiently transfected HEK293-EBNA cells, was used in a processivity assay (Figure 3.17. A) with polyadenylated m^{7}GpppG-capped and GpppG-capped β-globin RNA as substrates. At two minutes incubation time a very small portion of the full-length m^{7}GpppG-capped RNA was degraded, but completely deadenylated RNA products were already detectable with few visible intermediates (Figure 3.17. A, right). Deadenylation of almost all RNA molecules was achieved after about 60 min incubation time, at which an invasion of the non-poly(A) region could be observed. The GpppG-capped RNA was apparently deadenylated much slower and almost all molecules was deadenylated at the same rate (Figure 3.17.A, left). This means that the enzyme binds and dissociates from these substrate molecules several times before deadenylation is completed. However, in this assay, a small fraction of fully deadenylated RNA was observed at 20 min of incubation whereas the majority of the substrate molecules were still intact. These RNAs may carry a methylated cap as the capping enzyme might have carried along S-adenosyl-methionine during the

purification. To investigate this possibility, the full-length substrate and the completely deadenylated RNA fractions from the 30, 40, 60 and 80 minute time points were isolated and subjected to cap analysis by RNase P1 digestion and polyethyleneimine (PEI) thin-layer chromatography. As RNase P1 hydrolyses RNA to 5´-mononucleotides but leaves the cap-dinucleotide intact and because the RNA substrates were ^{32}P-labelled in the 5´-cap, methylated and unmethylated cap structures could be separated and quantified on a PhosphorImager. Indeed, the portion of m^{7}GpppG-capped RNA on the completely deadenylated substrate was 20-fold higher compared to the full-length RNA fraction (compare lanes A and C in Figure 3.17 B). Moreover, the full-length RNA with a methylated cap contained less than 0.5% non-methylated RNA (lane B).

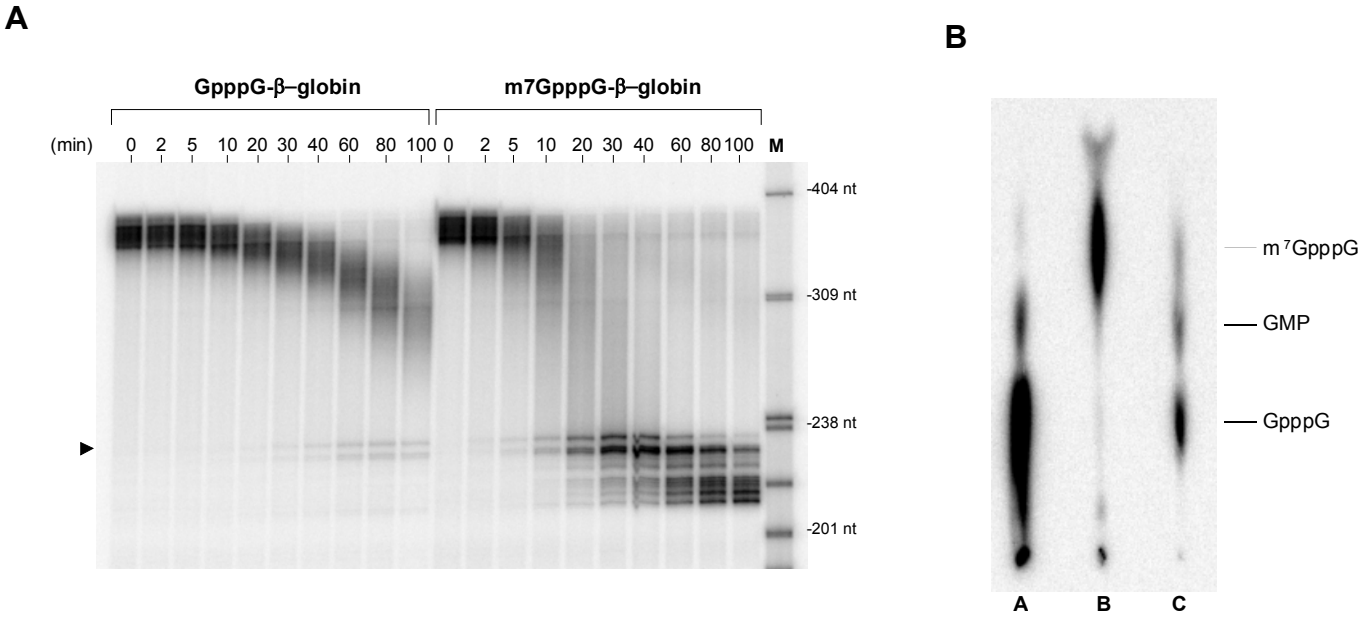

Figure 3. 17. The methyl-group on the cap structure confers a processive mode of action to PARN.
A. Polyadenylated ß-globin 3´-UTR RNA with a m^{7}GpppG-cap or a GpppG-cap was subjected to deadenylation by hPARN. The cap structures were added post-trascriptionally by recombinant guanylyl-transferase with the radiolabel on the cap and the efficiency of capping was estimated by the incorporation of ^{32}P-GTP. Reaction mixtures with 100 fmol RNA with a m^{7}GpppG-cap (68% labelled) or 508 fmol RNA with a GpppG-cap (6.5% labelled) in 50 µl reaction buffer plus 100 mM KCl were assembled on ice and the reactions were started by the addition of 5 fmol hPARN and incubation at 37^{o}C. Aliquots were withdrawn at the indicated times and digested with Proteinase K. The degradation products were ethanol precipitated and separated on a 8% denaturing polyacrylamide gel. Fully deadenylated β-globin RNA is indicated with an arrowhead. **B.** RNase P1 analysis of the capped RNA substrates and fully deadenylated GpppG-ß-globin 3´-UTR RNA. Full-length GpppG capped RNA (lane A) and the fully deadenylated RNA products (lane C) were excised from the gel in A and eluted. The recovered RNA was later digested with RNase P1 for 1 h at 37^{o}C, spotted on a PEI cellulose chromatography paper and analysed on a Phosphorimager (Molecular Dynamics). RNase P1 digestion of the m^{7}GpppG–capped β-globin RNA substrate is shown in lane B. GpppG, m^{7}GpppG and GMP were spotted in an extra lane, visualised by UV and are indicated on the right.

When the enzyme is distributive, the appearance of fully deadenylated substrates will be more delayed if more substrate is added above the saturation level of the enzyme. In contrast, if the enzyme is processive, the earliest time point when fully deadenylated products appear is independent of the RNA concentration provided the enzyme is working close to its V_{max} value. Due to the poor capping efficiency (6.8%), a large proportion of the unmethylated capped RNA substrate was lacking a cap structure at all in the experiment shown in Figure 3.17. To confirm the difference in reaction mechanism between RNA substrates carrying a methylated or unmethylated cap, the experiment was repeated with uniformly labelled RNAs and co-transcriptionally coupled cap structures (Figure 3.18). In this case, the concentrations of capped substrate RNAs were comparable since both of the cap analogues (m^7GpppG and GpppG) are incorporated equally. In principle, the same result was obtained but in contrast to Figure 3.17, a fraction of the m^7G-capped RNA was degraded in a more distributive fashion. This is possibly uncapped RNA which, due to the label in the RNA body, was visible in this assay.

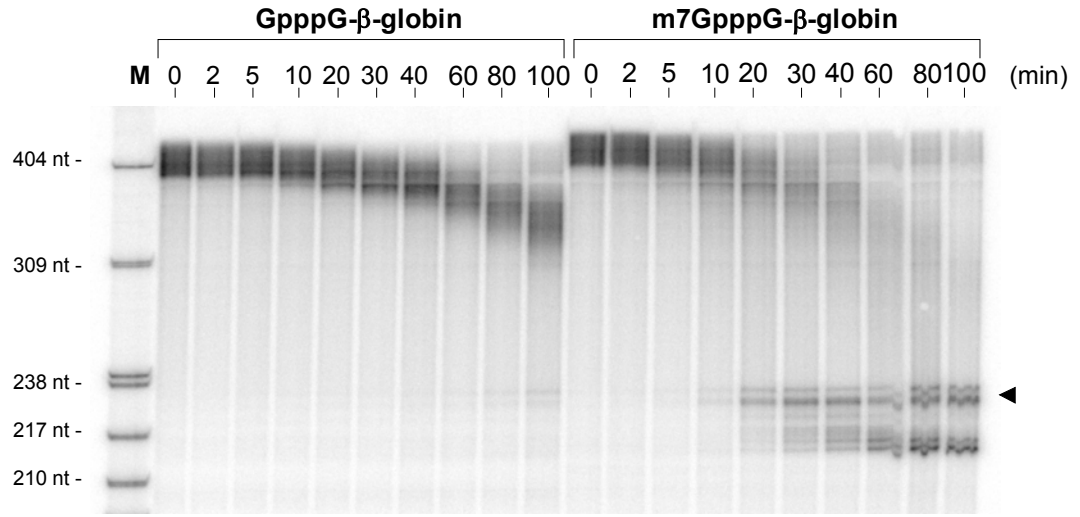

Figure 3.18. RNA with a non-methylated cap is deadenylated by a distributive reaction mechanism. Two 50 µl reaction mixtures with 150 fmol polyadenylated and GpppG-capped or m^7GpppG-capped β-globin RNA in PARN reaction buffer with 100 mM KCl were assembled on ice. The reactions were started by the addition of 5 fmol HEK PARN and incubation at 37°C. 5 µl aliquots were withdrawn at the indicated times and the reactions were stopped by Proteinase K digestion. Degradation products were separated on a 8% denaturing urea-polyacrylamide gel Fully deadenylated β-globin is indicated by an arrowhead and the sizes of the DNA molecular weight marker are indicated on the left.

A titration of hPARN, expressed in HEK293 cells, (Figure 3.19) revealed that a 5 to 10-fold higher concentration of PARN was needed to fully deadenylate all non-methylated-capped RNA molecules compared to methylated-capped RNA within the same incubation time.

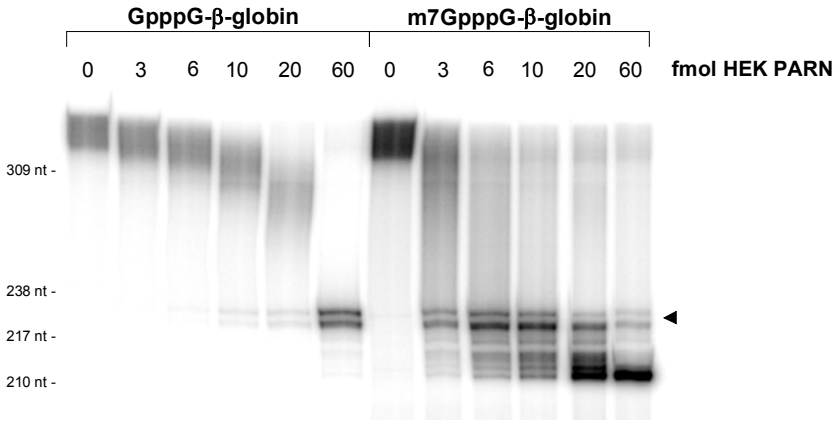

Figure 3.19. Titration of HEK expressed recombinant PARN. Polyadenylated and post-transcriptionally m^7GpppG- and GpppG-capped β-globin RNA were incubated with increasing concentrations of hPARN. 20 µl reaction mixes containing either 91 fmol (5.8 fmol labelled) GpppG-capped or 51 f mol (35 fmol labelled) m^7GpppG-capped and polyadenylated β-globin RNA in PARN reaction buffer with 100 mM KCl were assembled on ice. The deadenylation reactions were started by the addition of hPARN at the indicated concentrations and incubated at 37^0C for 7 minutes and stopped by digestion with Proteinase K. The degradation products were separated on a 8% denaturing gel and analysed on a PhosphorImager. The sizes, in nucleotides, of a DNA marker are shown on the left.

In conclusion, a methylated cap on the RNA substrate changes the reaction mechanism of PARN from a distributive to a processive mode.

3.5. HEK PARN has a higher affinity to the m^{7}G-cap than *E.coli* expressed PARN

The discrepancy between recombinant human PARN and purified bovine PARN described in section 3.2.1 might be related to a different affinity of the enzymes to the cap structure on the RNA. Recombinant hPARN, purified from HEK293 cells to near homogeneity, showed the same degree of cap dependence as bPARN. The specific activity under physiological salt conditions was 45 % of that of the purified bovine PARN but four-fold higher than the recombinant enzyme expressed in *E. coli* (*Körner et al., 1998* and section 3.4.2.) Free m^{7}GpppG cap analogue inhibits PARN-dependent deadenylation in a HeLa cytoplasmic extract (see Figure 3.2) and the activity of purified bovine PARN (results by C. Körner published in *Dehlin et al., 2000*) at about the same concentration. Therefore, inhibition by free cap analogue could be used to estimate the affinity to m^{7}GpppG of the different enzyme preparations. Furthermore, I wanted to investigate if RNA substrates carrying either a methylated or non-methylated cap were affected equally, that is, if the RNA context would influence binding of PARN to the cap. For this purpose, the deadenylation activity was assayed by the release of acid-soluble nucleotides.

The activities, plotted against the concentration of m^{7}GpppG cap analogue in the reactions, are shown in Figure 3.20 and summarised in Table 3.2. Free m^{7}GpppG inhibits HEK PARN at all concentrations tested (Figure 3.19 A), which is consistent with the previous results obtained with bovine PARN and HeLa cytoplasmic extracts (*C. Körner, 1998b*). However, the inhibition of HEK PARN activity was almost identical whether the RNA substrates were carrying a methylated or unmethylated cap structure (Table 3.2). The measured activities probably reflect the binding affinity of the enzyme to free m^{7}GpppG rather than a competition for binding to the RNA substrate.

In contrast, the activity of recombinant hPARN, purified from *E. coli*, was stimulated by low concentrations (10-50 µM) of free m^{7}GpppG (Figure 3.20 B). Interestingly, deadenylation of substrates with an unmethylated cap seemed to be more stimulated than substrates with a methylated cap. PARN catalysed deadenylation of non-methylated capped substrates were nevertheless inhibited by 40% at 300 µM of the methylated guanosine dinucleotide whereas deadenylation of substrates with a methylated cap basically remained unaffected. A similar activation by low concentrations of free cap analogue was observed with the purified 54 kDa-fragment of PARN both in a gel assay and by analysis of released AMP (*Martinez et al., 2001*)

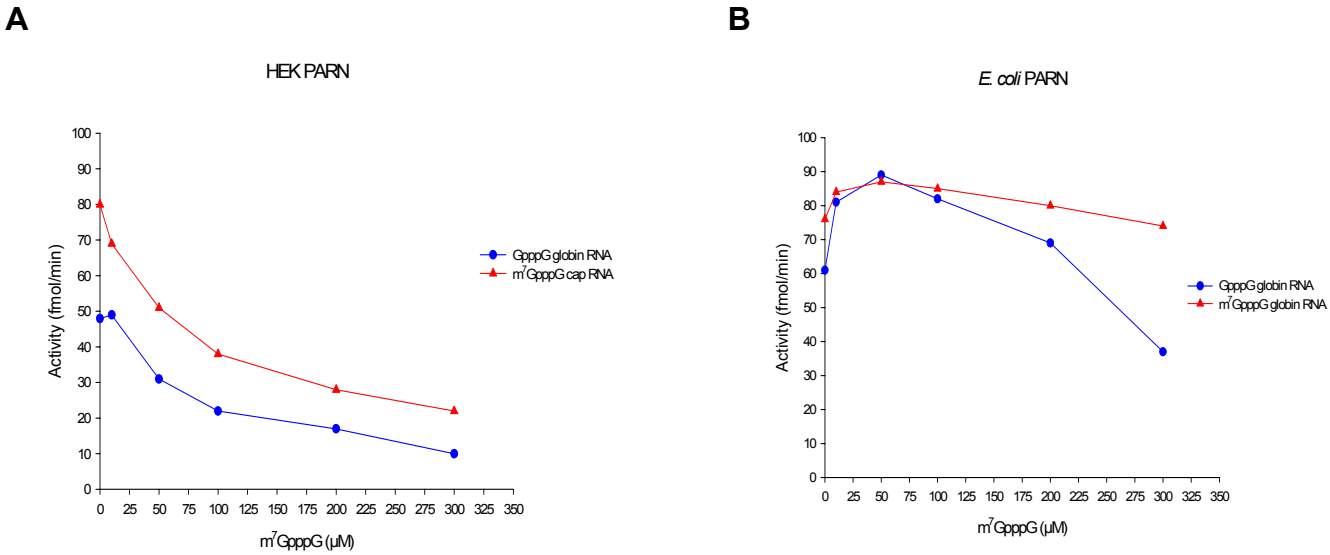

Figure 3.20. The effect of m^{7}GpppG added in *trans* on deadenylation of capped RNA substrates.
A. Deadenylation by HEK PARN. **B.** Deadenylation by *E. coli* PARN. 100 fmol m^{7}GpppG- or GpppG-capped β-globin RNA with radiolabelled poly(A_{105}) tails were mixed with PARN reaction buffer supplemented with 120 mM KAc in a 50 µl reaction. m^{7}GpppG cap analogue was added at final concentrations of 0, 10, 50, 100, 200 or 300 µM and the deadenylation reactions were started by the addition of 5 fmol HEK PARN or 5 fmol E. coli PARN. The reactions were incubated at 37°C and stopped after 15 minutes with 150 µl 13.3% TCA plus 100 mM KCl. High molecular weight molecules were collected by centrifugation and 100 µl of the supernatants was counted in a scintillation counter. All reactions were made in duplicates.

RNA substrate	Inhibition constant (K_i) **HEK PARN**	Inhibition constant (**K_i**) ***E. Coli* PARN**
GpppG-β-globin A_{105}	80 µM	~300µM
m^{7}GpppG-β-globin A_{105}	100 µM	>>300 µM
Poly(A)	10-15 µM	120 µM

Table 3.2. Inhibition of deadenylation activity by free m^{7}GpppG cap analogue. The inhibition constant K_i was defined as the concentration of m^{7}GpppG that reduced PARN activity with 50%.

In order to compare the cap dependence for HEK PARN and *E. coli* PARN, without taking the binding of PARN to a cap structure in *cis* in consideration, the experiment was repeated with straight poly(A) as substrate. Figure 3.21 shows, that the HEK PARN deadenylation activity is inhibited by 50% at 10-15 µM of free m^7GpppG-cap analogue whereas a 10-fold higher concentration was required to inhibit the *E. coli* activity to the same extent. The different concentrations, at which the activity of the two PARN preparations is inhibited, are therefore likely to represent a difference in the affinity for m^7GpppG. To which extent the two different proteins are discriminating between a methylated and a non-methylated cap on the RNA remains to be evaluated.

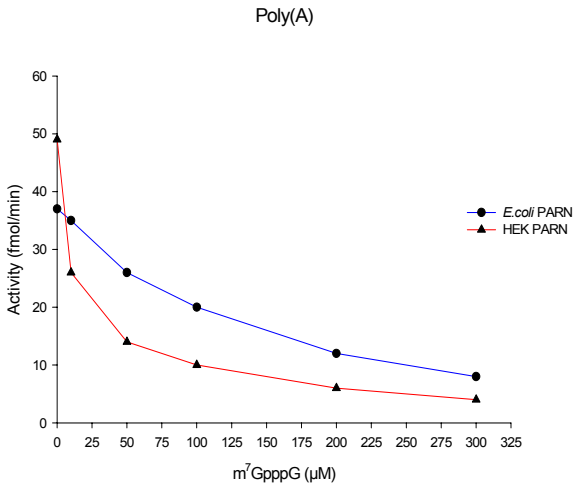

Figure 3.21. Inhibition of HEK PARN and *E. coli* PARN deadenylation activity by m^7GpppG. 50 µl reaction mixes were assembled with 150 fmol labelled poly(A) in PARN reaction buffer and 120 mM KAc. m^7GpppG cap analogue was added to final concentrations of 0, 10, 50, 100, 200 and 300 µM before the deadenylation reactions were started by addition of 5 fmol of either HEK PARN or *E. coli* PARN and incubation at 37°C. After 15 minutes the reactions were stopped by TCA and 50% of the acid soluble fraction was counted in a scintillation counter. All reactions were made in duplicates. The activity plotted against the concentration of the cap analogue is the average of two experiments.

3.6. Deadenylation and translation

3.6.1. PARN-mediated deadenylation is inhibited by translation initiation factors

Deadenylation of mRNA *in vitro* is stimulated by a m^7G-cap structure in both a HeLa cytoplasmic extract and with recombinant hPARN (see sections 3.1-3.4). In fact, a configuration in which the 5´cap and the 3´ poly(A) tail are close to each other seems to be the optimal substrate for PARN-dependent deadenylation. A "closed loop" formation also plays an important role in translation initiation where the cap and the poly(A) tail are connected by multiple interactions through their respective binding proteins, eIF4E and PABPC. Consequently one would expect translation to protect mRNA against the attack of PARN by preventing the enzyme´s access to the cap and by stabilising the binding of PABPC to the poly(A) tail.

The periodic pattern of intermediate degradation products, observed in gel assays under physiological conditions (*Körner and Wahle, 1997*; and section 3.1.1), has been attributed to partial inhibition by PABPC. Furthermore, since the m^7G-cap accelerates deadenylation but is not absolutely required, binding of the translation initiation complex may be expected to regulate the rate of deadenylation. To investigate if binding of eIF4E/eIF4G to the 5´ cap would further inhibit PARN-mediated deadenylation, recombinant PABPC and increasing concentrations of eIF4E/eIF4G were allowed to assemble on m^7GpppG-L3preA_{80} RNA before deadenylation was started by addition of recombinant HEK PARN. As saturating concentrations of PABPC alone completely inhibits PARN (*Körner and Wahle, 1997; Wormington, 1996*), the experiment was performed at a concentration that allowed deadenylation to occur. That PABPC partially inhibits deadenylation at this concentration can be seen in Figure 3.22, lane 5 (compare lanes 3-4 with PARN alone). A graphic representation of the distribution of radioactivity in the lanes for the 10 minutes incubation time points shows that with increasing concentrations of translation initiation factors (TIFs), the intermediates become less pronounced and full-length substrate accumulates. Hence, PARN-mediated deadenylation is further inhibited by eIF4E/eIF4G, possibly due to a circularization of the substrate RNA by interaction with PABPC. The inhibition of deadenylation by the translation initiation complex is likely to be underestimated in this experiment, as a fraction of the RNA substrate probably is deficient of bound protein because of insufficient capping (see figure legend).

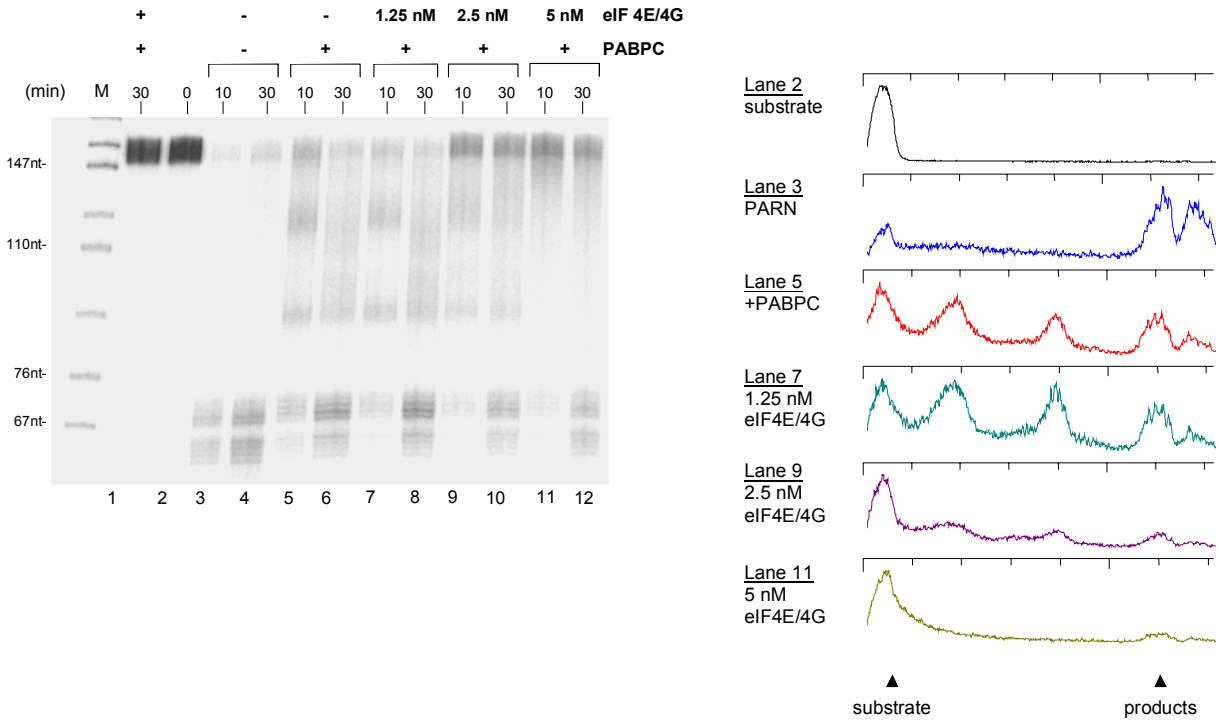

Figure 3.22. Inhibition of PARN-mediated deadenylation by translation initiation factors. 10 µl reaction mixtures were assembled on ice containing 2.5 nM m^7GpppG-L3preA_{80} (of which 2 nM is radiolabelled in the cap) and 2.5 nM recombinant hPABPC in PARN reaction buffer supplemented with 100 mM KCl. Recombinant eIF4E and eIF4G were added at indicated concentrations and the reaction mixtures were pre-incubated at room temperature for 5 minutes. Deadenylation was started by addition of 0.25 nM HEK PARN and incubation at 37°C. Aliquots were withdrawn at indicated times and the reactions were stopped with SDS and proteinase K digestion. The degradation products were separated by 8% urea-PAGE and exposed to a Phosphor screen. Lane 1: m^7GpppG-L3preA_{80} RNA incubated with 2.5 nM each of eIF4E, eIF4G and PABPC. Lane 2: non-treated m^7GpppG-L3preA_{80} RNA. The sizes of the DNA marker are indicated to the left. The distribution of radioactivity in the lanes of the 10 min. time-points were analysed with the ImageQuant 5.0 software and are shown as graphs to the right.

3.6.2. Inhibition of deadenylation by translation initiation factors is independent of the cap structure

PARN activity does not require access to a free 5´-end on the RNA (*U. Klösgen, personal communication*) implying that, even if the eIF4E/eIF4G complex is bound to the cap structure, PARN could still act on the poly(A) tail but at a slower rate. The translational status of a messenger RNA might therefore regulate PARN mediated deadenylation. eIF4E, eIF4G and PABPC were tested, individually and in combination, for their ability to inhibit PARN activity. Polyadenylated and m^7GpppG-capped L3pre RNA was incubated with the TIFs prior to addition of PARN and the reaction kinetics were monitored by removing aliquots at indicated times. At 5 minutes of incubation, 10 nM eIF4E did not inhibit deadenylation

(Figure 3.23, lanes 5-7). Even when combined with PABPC, a further inhibition of PARN activity could not be observed (lanes 18-20; see also graphs showing the radioactivity distribution in the lanes). Moreover, a titration of eIF4E up to 1 µM did not influence PARN mediated deadenylation (data not shown). In contrast, when 10 nM eIF4G was added to the deadenylation reaction, accumulation of fully deadenylated products was reduced after 5 minutes incubation (lane 8 and graph) indicating a decreased deadenylation rate.

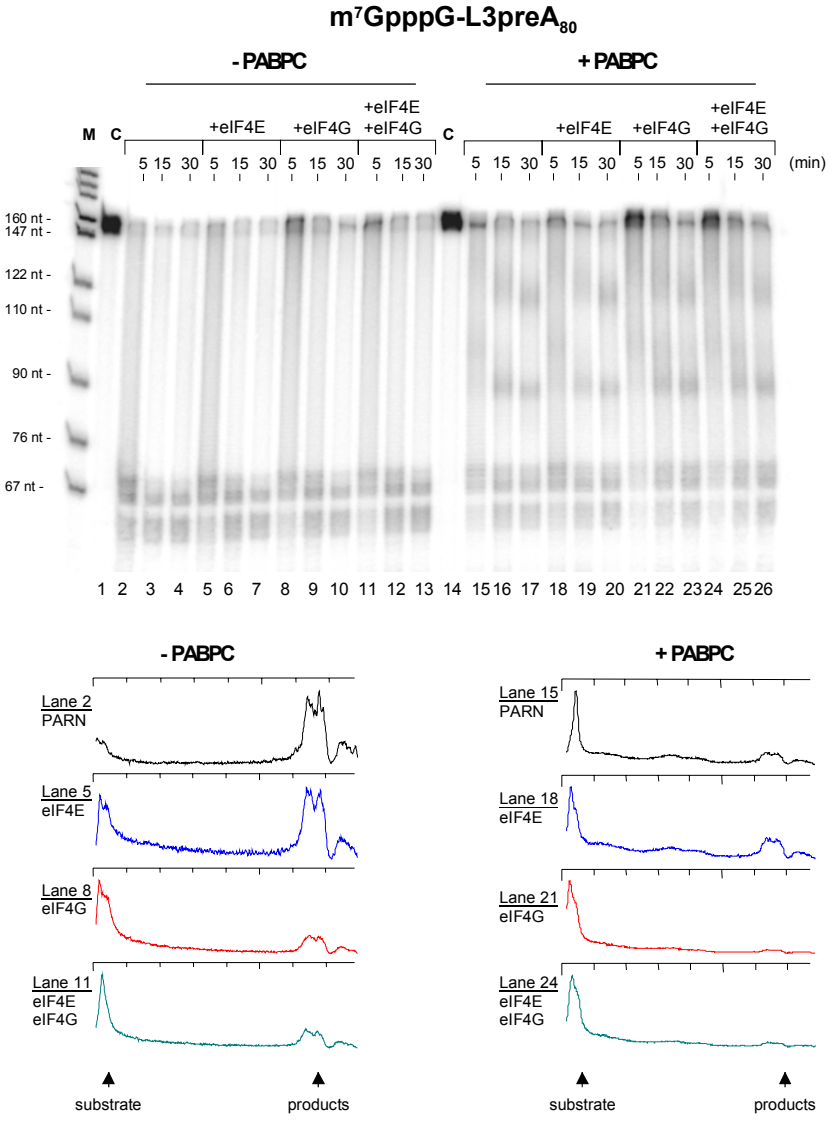

Figure 3.23. PARN activity is decreased in the presence of eIF4G. Reaction mixtures, containing 2.5 nM post-transcriptionally m^7GpppG-capped L3preA_{80} RNA in 20 µl PARN reaction buffer with 100 mM KCl, were assembled on ice. After addition of 10 nM of eIF4E and/or eIF4GI the reactions were divided and 2.5 nM PABPC was added to half of the reactions. The RNA was pre-incubated with the translation initiation factors for 5 minutes at room temperature before addition of 0.25 nM HEK PARN. 2.5 µl aliquots were withdrawn after 5, 15 and 30 minutes incubation at 37°C and stopped with SDS and Proteinase K digestion. Reaction products were separated on a 8% denaturing polyacrylamide gel and exposed to a Phosphor screen. The control lanes show RNA incubated with eIF4E/eIF4G with and without PABPC for 30 minutes. The sizes of the DNA marker are indicated to the left. The distribution of radioactivity in the lanes of the 5 minutes time-points are shown as graphs on each side of the gel.

A similar reduction of deadenylation products by eIF4G was observed in the presence of PABPC (lane 21 and graph). Furthermore, the degradation rate did not change significantly when both eIF4E and eIF4G were allowed to assemble on the RNA substrate before initiating deadenylation (lanes 11 and 24).

As a m^7G-cap structure on the RNA substrate promotes a processive reaction mechanism, binding of the eIF4E/eIF4G complex to the cap would be expected to result in a distributive mode of action. But by eye, a change in reaction mechanism could not be detected.

Although the cap binding protein, eIF4E, binds the cap with a relatively low affinity, 0.3-0.7 µM (*Hsu et al., 2000*) the affinity is increased 10-fold by interaction with eIF4G (*Haghighat and Sonenberg, 1997*). It is therefore surprising that there was no additional inhibition when eIF4E and eIF4G were combined in the deadenylation reaction. This could be explained if the reaction conditions for deadenylation were inappropriate for binding of eIF4E to the cap or for interaction with eIF4G. The ability of eIF4E to bind a m^7GpppG cap was therefore investigated by a crosslinking assay.

The eIF4E protein used in these experiments could be crosslinked to an RNA with a radiolabelled 5´ cap at a concentration of 4µM (Figure 3.24). This agrees with published data (*Haghihat and Sonenberg, 1997*) and indicates that the eIF4E protein is also able to bind the cap under deadenylation reaction conditions. Moreover, a weak crosslink signal with 40 nM eIF4E in the presence of eIF4G demonstrates the ability of eIF4E to bind the cap structure at a concentration close to the one used in the deadenylation experiments.

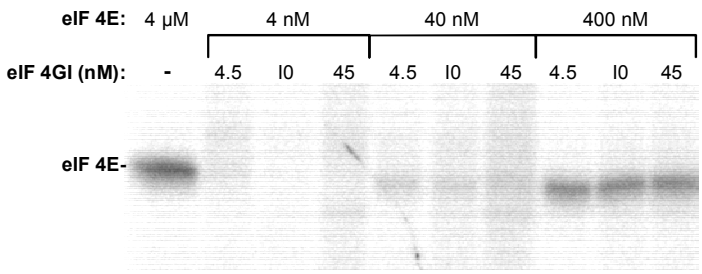

Figure 3.24. Recombinant eIF4E binds the 5´ cap structure of β-globin RNA. Reaction mixtures of 10 µl each with 0.3 nM polyadenylated β-globin RNA, ^{32}P-labelled in the cap, and recombinant eIF4E (4 µM, 400 nM, 40 nM or 4 nM) were combined with NFL-eIF4G (4.5 nM, 10 nM or 45 nM) in CLPD buffer were incubated at 30°C for 15 minutes and crosslinked in a Stratalinker on ice for 15 minutes (Materials and Methods). After digestion with RNaseA the proteins were separated on a 12% SDS-polyacrylamide gel and exposed to a Phosphor screen.

The association constant of eIF4E to different cap analogues differs by orders of magnitude with the highest affinity for m^7GpppG (*Niedzwiecka et al., 2002*). If the observed obstruction of PARN activity in Figure 3.22 is independent of the cap structure and the ability to form a "closed loop" configuration of the RNA, a similar effect would be seen with ApppG-capped L3preA$_{80}$ RNA which eIF4E cannot bind at these concentrations. The deadenylation of this RNA substrate followed a distributive reaction mechanism, which can be seen in Figure 3.25,

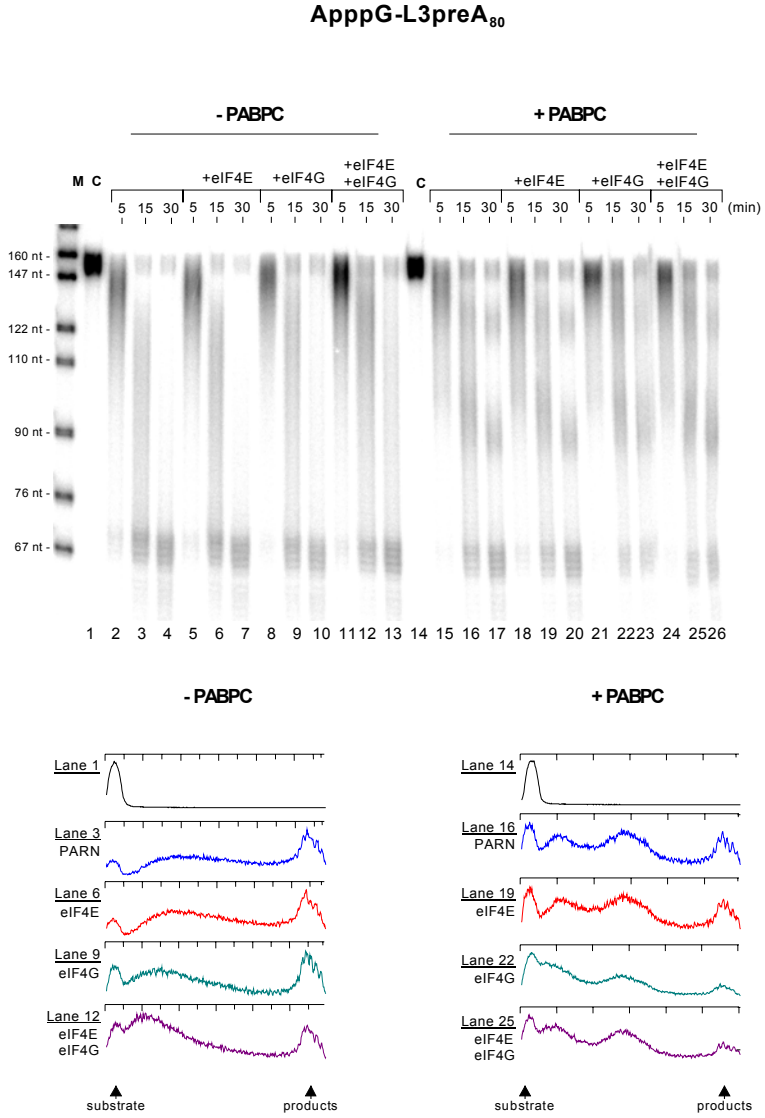

Figure 3.25. Inhibition of PARN activity by eIF4G is independent of the cap structure. Reaction mixtures, containing 2.5 nM co-transcriptionally ApppG-capped L3preA$_{80}$ RNA in 20 µl PARN reaction buffer with 100 mM KCl, were assembled on ice. After addition of 10 nM of eIF4E and/or eIF4GI the reactions were divided and 2.5 nM PABPC was added to half of the reactions. The RNA was pre-incubated with the translation initiation factors for 5 minutes at room temperature before the deadenylation reaction was started by the addition of 0.25 nM HEK PARN. 2.5 µl aliquots were withdrawn after 5, 15 and 30 minutes incubation at 37^{o}C and stopped with SDS and Proteinase K digestion. Reaction products were separated on a 8% denaturing polyacrylamide gel and exposed to a Phosphor screen. The control lanes show RNA incubated with eIF4E/eIF4G with and without PABPC for 30 minutes. The distribution of radioactivity in the lanes of the 15 minutes time-points are shown as graphs on each side of the gel.

lanes 2-4 (compare Figure 3.23, lanes 2-4). Pre-incubation of the RNA with eIF4E had no effect on PARN activity (Figure 3.25; lanes 5-7 and graph). However, a shift to longer degradation intermediates was seen in the presence of eIF4G (lanes 8-10 and 21-23 see also graphs). A modest accumulation of the longer degradation intermediates was observed with both eIF4E and eIF4G in the reaction mixture (lanes 11-13; lanes 24-26 and graphs) although the formation of fully deadenylated RNA did not change significantly (lanes 11-13 and 24-26).

The observed inhibition of PARN activity seems to be caused by eIF4G, at least to some degree, and does not depend exclusively on a "closed loop" configuration of the RNA. I wanted to know if deadenylation of straight poly(A) without a 5´cap would be inhibited by eIF4G as well. Furthermore, the central domain of eIF4G (4GM), which is lacking the binding sites for eIF4E and PABPC, was examined for its ability to impede PARN activity. Figure 3.26, shows that 4GM did indeed inhibit PARN-mediated deadenylation but at a concentration of 50 nM.

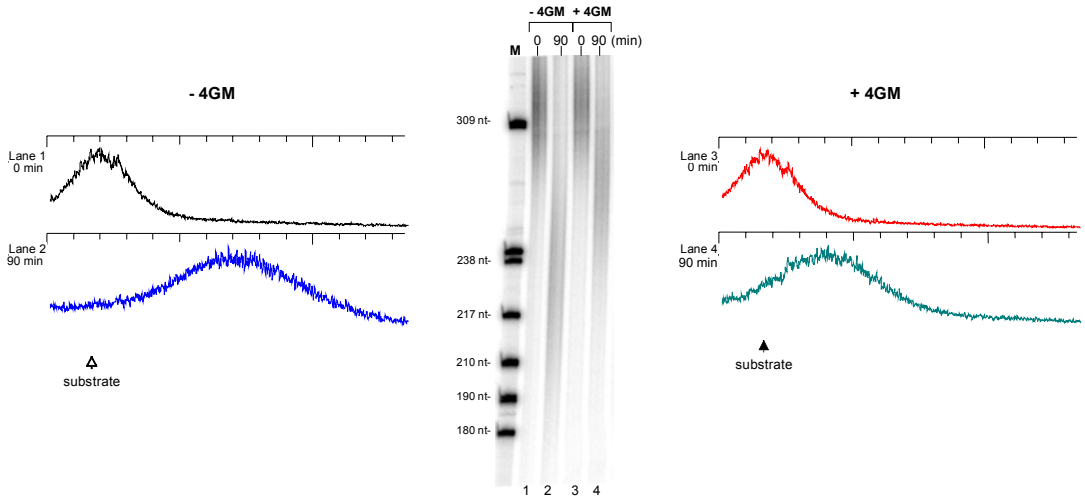

Figure 3.26. Deadenylation of poly(A) is inhibited by the central domain of eIF4G. Two reaction mixtures containing 25 fmol poly(A) in 25 µl PARN reaction buffer with 100 mM KCl were assembled on ice. One of the reaction mixtures was pre-incubated with 50 nM 4GM at room temperature before the deadenylation reactions were started by addition of 10 fmol HEK PARN and incubation at 37°C. The reactions were stopped by Proteinase K digestion and the degradation products were separated on a 6% urea-polyacrylamide gel. The distribution of radioactivity in each lane is shown as graphs.

4GM contains two putative RNA recognition motifs which are thought to interact with RNA in a non-specific manner to stabilize the binding of eIF4E to the RNA cap (*Gingras et al.,*

1999). Hence, the inhibition of PARN activity by eIF4G alone might simply be that the RNA is protected by bound eIF4G.

3.6.3. The inhibitory effect on deadenylation does not depend on the RNA binding property of eIF4G.

General RNA binding proteins, such as the pyrimidine tract binding protein (PTB), are promoting cap-dependent translation by binding to mRNAs in a sequence-non-specific way. Coating of the mRNAs with RNA-binding proteins is thought to prevent translation initiation at aberrant start sites by masking potential internal ribosome binding sites. An eIF4G-RNA interaction, is proposed to be accompanied by a displacement of the RNA-associated proteins to promote cap dependent translation. (*Svitkin et al., 1996*).
If PARN is inhibited by an eIF4G-RNA contact close to the 5´ cap, bound PTB on the RNA would prevent this contact. Recombinant PTB, eIF4E and/or eIF4G were pre-incubated with m^7GpppG-capped β-globin(A_{80}) RNA before deadenylation was started by HEK PARN.

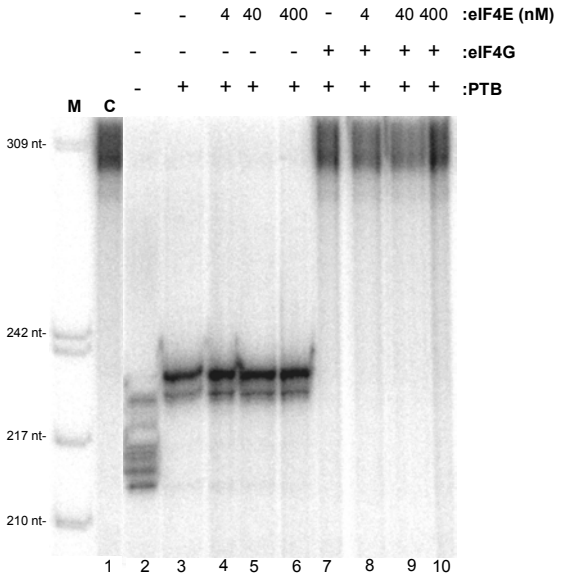

Figure 3.27. PTB. a general RNA-binding protein, does not prevent inhibition of PARN by eIF4G. Reaction mixtures of 25 µl containing 0.6 nM m^7GpppG-capped β-globin(A_{75}) RNA and 20 nM PTB in PARN reaction buffer supplemented with 100 mM KCl were assembled on ice. eIF4G at 50 nM and eIF4E at indicated concentrations were added and the reaction mixtures were preincubated at room temperature for 5 minutes before the deadenylation reactions were started by addition of 0.2 nM HEK PARN. The reactions were incubated at 37°C for 45 minutes and stopped by SDS and Proteinase K digestion. Degradation products were separated on a 8% urea-polyacrylamide gel and exposed to a Phosphor screen. Lane M is a DNA size marker with the sizes indicated to the right and C is non-treated RNA substrate.

Invasion of the non-adenylate portion of the RNA was prevented by PTB, Figure 3.27 (compare lanes 2 and 3), indicating that the RNA body was covered by bound PTB. Still eIF4G alone as well as in complex with eIF4E prevented PARN mediated deadenylation to occur (lanes 7-10). Thus, it is not likely that eIF4G blocks PARN activity by binding to RNA close to the 5´ cap. Since PTB does not bind to the poly(A) tail (Figure 3.27, lanes 2 and 3), there is still a possibility that eIF4G would inhibit PARN activity by binding to the poly(A) tail. However, the binding affinity of PARN to RNA is in the nanomolar range (data not shown and *Martinez et al., 2001*, unpublished data) whereas eIF4G binds RNA with an affinity that was measured to 1 µM for wheat (*Sha et al., 1995*). It is therefore unlikely that eIF4G would inhibit PARN activity by binding to the poly(A) tail under these conditions.

3.6.4. eIF4G interacts with PARN

If eIF4G does not intervene with PARN activity by preventing its access to the RNA substrate, the inhibition might be a consequence of a protein-protein interaction. To test for an interaction between PARN and eIF4G, a glutathione S-transferase (GST)-pulldown assay was carried out. A GST-tag was therefore cloned in frame with the Met-Ala-His_6 tag of the hPARN expression plasmid pGMMCS645295 (*Körner et al., 1998*). The fusion protein, expressed in *E. coli,* was purified by Ni^{2+}-NTA affinity chromatography and FPLC Mono before being immobilised on glutathione-Sepharose. Translation competent cytoplasmic S30 extract from HeLa cells (*Striegler, Diploma thesis, 2002*) was incubated with the immobilised PARN. Bound proteins were eluted with SDS-loading buffer and separated on a 9% SDS-polyacrylamide gel. A Western blot analysis with affinity purified antibodies directed against eIF4G (see Materials and Methods section), showed that cytoplasmic eIF4G could bind to GST-PARN (Figure 3.28; lanes 4-6) but not to glutathione-Sepharose (lane 1).

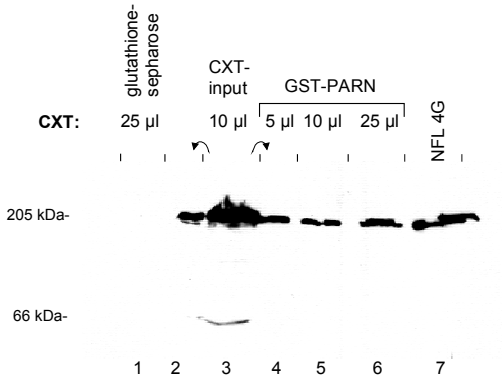

Figure 3.28. GST-pulldown assay. Interaction of PARN and eIF4G in HeLa cytoplasmic extract. GST-His_6-PARN immobilised on glutathione-Sepharose was incubated with indicated volumes of HeLa cytoplasmic extract (S30) at RT for 30 minutes. Associated proteins were recovered by boiling the resin in 15 µl SDS-loading buffer, separated on a 9% SDS-polyacrylamide gel and subjected to Western blot analysis using affinity purified anti-eIF4G antibody (APEd). CXT: S30 HeLa cytoplasmic extract. NFL4G: recombinant eIF4G expressed in Baculovirus-infected insect cells (S. Morley). Arrows indicate a possible spill-over since lane 2 was left empty.

The central domain of eIF4G (4GM), see section 3.5.2, seemed to be the smallest fragment that was capable to inhibit PARN activity. Therefore this fragment (4GM) and a larger fragment (p100), containing the C-terminus of eIF4G, were examined for a possible interaction with PARN. His_6-fusions of the eIF4G fragments were expressed in *E. coli.* The purified fusion-proteins were then incubated with and without GST-PARN coated glutathione–Sepharose. After extensive washing steps, bound protein was eluted with SDS-loading buffer, separated by SDS-PAGE and analysed by Western blotting.

The GST-pulldown assay revealed that 4GM and p100 were specifically bound to GST-PARN but not to glutathione-Sepharose (Figure 3.29). The recovery was increased when extra non-GST tagged PARN was added (panel A). This result is unclear but could be a result of a PARN-PARN-4GM interaction. The larger fragment including the C-terminus of eIF4G was also capable of binding to GST-PARN as can be seen in panel B. The protein was partially degraded since the eIF4G antibody (WF, see Materials and Methods), reacted with two additional polypeptides. Interestingly, also the predominant 60 kDa degradation fragment interacted with PARN in this assay whereas the larger fragment did not. The recovery of the eIF4G polypeptides was not reduced when the protein mixtures were treated with micrococcal nuclease, suggesting that the interactions were not mediated by RNA binding.

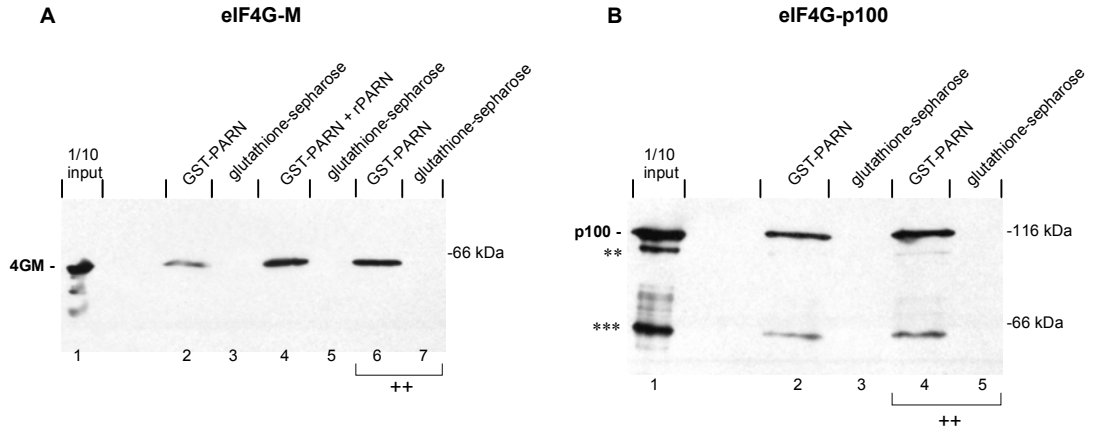

Figure 3.29. Interaction of PARN with eIF4G fragments. GST-pulldown assay. GST-His_6-PARN, immobilised on glutathione-Sepharose (30 µl packed beads) was incubated with 3 µg of either eIF4G-M or p100 for 30 minutes at room temperature. After removing unbound proteins the beads were boiled in SDS. Eluted proteins were separated by 8% SDS-PAGE and analysed by Western blot using antibodies directed against the expressed C-terminus of eIF4G. **A.** Lane 1: 0.3 µg purified 4GM. Lanes 2, 4 and 6: 4GM bound to immobilised GST-PARN. Lanes 3, 5 and 7: glutathione-Sepharose bound proteins. **B**. Lane 1: 0.3 µg purified p100. Lanes 2 and 4: p100 bound to immobilised GST-PARN. Lanes 3 and 5: glutathione-Sepharose bound proteins. ** and *** denote proteolytic fragments of p100. ++ indicates that these samples were treated with micrococcal nuclease.

The interaction between PARN and the eIF4G fragments was also confirmed by a m^7GTP-Sepharose pulldown assay. The ability of PARN to bind m^7GTP (see section 3.1.3.) was used to attach recombinant PARN without a GST-tag to a solid matrix. The p100 and 4GM fragments were then incubated with immobilised PARN as described (see Materials and Methods). Associated proteins were separated by SDS gel-electrophoresis and analysed by Western blot. Again, an interaction between PARN and the eIF4G peptide fragments was detected (Figure 3.30, lanes 7 and 8). Also PABPC was recovered (lane 6) however to a lesser degree. The significance of this interaction may be questioned because p100 also bound to naked m^7GTP-sepharose and might therefore reflect unspecific binding. Interestingly, the anti-eIF4G antibody reacted with recombinant PABPC, that was expressed in *E. coli*. As there was no PABPC bound to m^7GTP-Sepharose the observed interaction might still be specific.

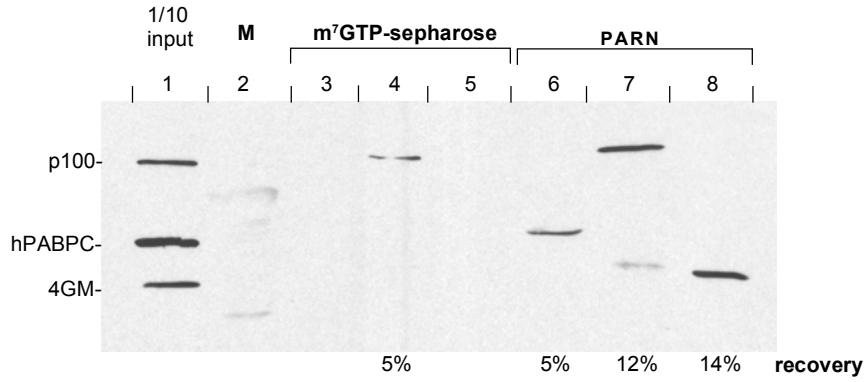

Figure 3.30. m7GTP pulldown assay. Interaction between PARN and the eIF4G fragments, 4GM and p100. Recombinant hPARN immobilised on m^7GTP-Sepharose (20 µl packed beads) was incubated with 3 µg of either 4GM or p100 and 6 µg of hPABPC in a final volume of 600 µl at room temperature for 45 minutes. Unbound proteins were removed by several washings in ice-cold CLPD buffer. Bound proteins were eluted in SDS-loading buffer and subjected to Western blot analysis using anti-eIF4G antibodies (WF). Lane 1: 0.3 µg p100, 0.6 µg hPABPC and 0.3 µg 4GM. Lane 2:SDS-6H molecular weight marker. Lanes 3-5: recovered protein on naked m^7GTP-sepharose and lanes 6-8: bound proteins on rPARN coated m^7GTP-sepharose.

Taken together, these experiments suggest that eIF4G and PARN are able to interact, however, further experiments have to be done to show that this interaction also takes place in the cell.

3.7. PARN is a homodimer

In the Diploma thesis of Thorsten Meyer (*Meyer, Diploma thesis, 1997*), the native molecular mass of bPARN was estimated to be 257 kDa using gel filtration chromatography. However the molecular mass estimated by SDS-gel electrophoresis is 74 kDa. Consequently, the native form of bPARN is either a multimer or a filamentous protein, as the determination of molecular mass by gel filtration is based on the assumption that the protein has a globular shape. Furthermore, the protein preparation contained a substantial amount of other proteins, which raised the question if PARN would exist as part of a complex with other proteins.
As recombinant hPARN was purified to near homogeneity this protein preparation was used in a sedimentation equilibrium experiment to re-examine the native molecular mass of PARN.

Sedimentation equilibrium allows a more accurate estimation of the molecular mass since this method is independent of the shape of the protein. The sedimentation equilibrium absorbance versus radial position data and the deviations from the global fit are shown in Figure 3.31.

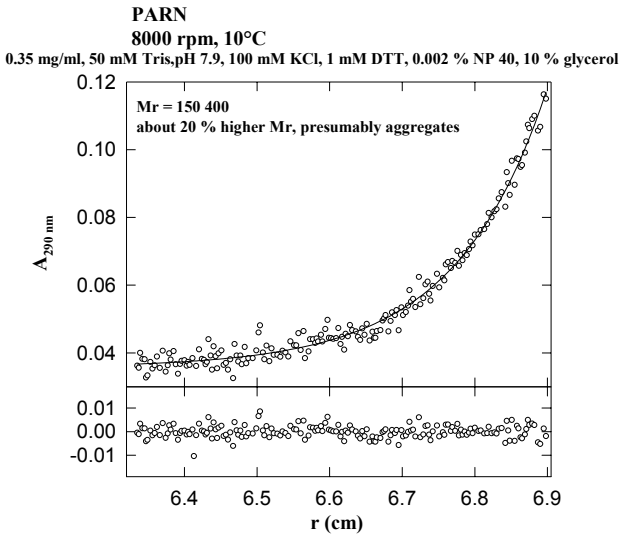

Figure 3.31. Sedimentation equilibrium concentration profile of recombinant hPARN. The solid line shows the best-fit distribution after global modelling of data obtained at a rotor speed of 8,000 rpm. (*Lowe*r) Residuals of the fitted line to the experimental data

The molecular mass of hPARN determined by this analysis is 150.4 kDa with a sedimentation coefficient of 4.8 x10^{-13} s.

Shape asymmetry can be deduced from the ratio f/f_0, which is the quotient between the measured frictional coefficient of the protein and the frictional coefficient it would have if its mass were distributed to form a hard sphere of the same partial specific volume. For most spherical proteins the values are 1.1-1.2, for example, Ribonuclease A has a f/f_0 ratio of 1.066 whereas the f/f_0 ratio for fibrinogen is 2.336 (*Smith, 1970*).

Knowing the molecular mass and the sedimentation coefficient, the f/f_0 ratio can be calculated. The f/f_0 ratio for PARN is fairly high (see section 2.2.7) which is an indication that PARN has an extended shape and might explain the higher molecular weight that was estimated by gel filtration.

Together, these results indicate that PARN is an extended protein consisting of two subunits.

3.8. Identification of a mouse PARN homologue and investigation of its genomic organization.

The reaction mechanism for PARN could be elucidated by *in vitro* experiments, but the physiological function of the enzyme has to be resolved *in vivo*. By knocking out the gene, a loss of function effect could perhaps be assigned. Generating a knockout mouse involves several steps, (i) mapping the genomic organisation of the gene and isolation of genomic clones, (ii) construction of a targeting vector with a selective marker that interrupts the gene, (iii) transfection of embryonic stem (ES) cells with the targeting vector, (iv) a blastocyst injection or morula aggregation with the antibiotica-selected ES clones, (v) implantation into a pseudo-pregnant mouse and producing chimeric offspring followed by the production of a homozygous mutant.
During the progress of this work a new method was introduced for gene silencing in mammalian cells. It was found that 21-nucleotide small interfering RNA (siRNA) duplexes could repress the expression of both endogenous and heterologous genes in different mammalian cell lines (*Elbashir et al., 2001*) and proved to be a more convenient way to study PARN function *in vivo*.

A mouse homologue of human PARN was identified in a database search of mouse expressed sequence tags (ESTs). The IMAGE clone 2101477 (Accession number: AW209831) was obtained from the IMAGE Consortium, RZPD (Germany), and the 2.4 kb cDNA insert was sequenced (Figure 3.32). A set of 9 PCR primers (section 2.1.6.) were designed to examine mouse embryonic stem cell chromosomal DNA for a specific PCR product. This resulted in one reproducible 1.2-1.3 kb product with a primer pair at the 5´end of the coding region. The fragment was sequenced and found to contain, in addition to the cDNA sequence, a 1.1-1.2 kb putative intron sequence. This primer pair (2065148 A, pos. 94-114 and 2065148 B. pos. 224-246) was subsequently used in a BAC Mouse II library screen by PCR (Genome Systems Inc.) and the pBeloBAC 25186 clone was identified.
The size of the inserted genomic mouse DNA was determined by linearizing the plasmid with λ-terminase at the *cos* site (see Appendix), annealing the radiolabelled ON-R and ON-L oligonucleotides (see section 2.1.7.) to the generated 12-base 5´-overhangs and separation by

mouse ATGGAGATAA TCCGGAGCA▼A TTTTAAGATT AATCTTCACA AAGTGTACCA GGCCATAGAG GAGGCTGACT TCTTCGCCAT 80
human ATGGAGATAA TCAGGAGCA▲A TTTTAAGAGT AATCTTCACA AAGTGTACCA GGCCATAGAG GAGGCCGACT TCTTCGCCAT 80

mouse CGATGGGGAG TTTTCAGGAA TCA▼GCAATGG ACCCTCAGTA ACAGCATTAA CAAGTGGTTT TGACACCCCA GAAGAGAGAT 160
human CGATGGGGAG TTTTCA▲GGAA TCAGTGATGG ACCTTCAGTC TCTGCATTAA CAAATGGTTT TGACACTCCA GAAGAGAGGT 160

mouse ATCAGAAGCT TAAAAA▼GCAT TCCATGGACT TTTTGCTGTT TCAGTTTGGC CTTTGTGCTT TTAAGTATGA CCACACAGAT 240
human ATCAGAAGCT TAAAAA▲GCAT TCCATGGACT TTTTGCTATT TCAGTTTGGC CTTTGCACTT TTAAGTATGA CTACACAGAT 240

mouse TCCAA▼GCATG TAACGAAGTC ATTTAACTTC TATGTTTTCC CCAAGCCTTT CAGTAGGTCC TCACCAGATG TCAAGTTTGT 320
human TCAAA▲GTATA TAACGAAGTC ATTTAACTTC TATGTTTTCC CGAAACCCTT CAATAGATCC TCACCAGATG TCAAATTTGT 320

mouse TTGCCA▼GAGC TCCAGCATTG ACTTCCTGGC GAGCCAAGGA TTTGACTTTA ATAAAGTGTT TTGCAGTG▼GG ATTCCATATC 400
human TTGTCA▲GAGC TCCAGCATTG ACTTTCTAGC AAGCCAGGGA TTTGATTTTA ATAAAGTTTT TCGAAAT▲GGA ATTCCATATT 400

mouse TGAATCAGGA AGAAGAAAGG CAGCTGAGAG AGCAATTCGA TGAAAAACGG TCTCAAGCCA ATGGGGCAGG AGCTCTGGC* 479
human TAAATCAGGA AGAAGAAAGA CAGTTAAGAG AGCAGTATGA TGAAAAACGT TCACAGGCGA ATGGTGCAGG AGCTCTGTCC 480

mouse ********** ********** AAAATGTCCT GTGACCATCC CTGAGGATCA GAAGAAGTTT ATTGACCAAG TAAT▼AGAGAA 539
human TATGTATCTC CTAACACTTC AAAATGTCCT GTCACGATTC CTGAGGATCA AAAGAAGTTT ATTGACCAAG TGGTA▲GAGAA 560

mouse GATAGAGGAT TTCCTACAAA GTGAAGAGAA GAGGAGCCTG GAACTTGACC CATGCACTGG ▼GTTCCAAAGA AAACTTATTT 619
human AATAGAGGAT TTATTACAAA GTGAAGAAAA CAAGAACTTG GATTTAGAGC CATGTACCGG ▲GTTCCAAAGA AAACTAATTT 640

mouse ATCAGACTTT GAGTTGGAA▼G TATCCTAAAG GCATTCATGT TGAGACATTA GAGACTGACA AG▼AAGGAAAG ACATATAGTT 699
human ATCAGACTTT GAGCTGGAA▲G TATCCGAAAG GCATTCATGT TGAGACTTTA GAAACTGAAA AG▲AAGGAGCG ATATATAGTT 720

mouse ATCAGCAAGG TGGATGAAGA AGAACGCAAA AGGAGAGAGC AGGAGAAGTA CACAAAGGAG CAG▼GAGGAGC TGAATGATGC 779
human ATCAGCAAAG TAGATGAAGA AGAACGCAAA AGAAGAGAGC AGCAGAAACA TGCCAAAGAA ▲CAGGAGGAGC TGAATGATGC 800

mouse TGTGGGATTT TCAAGAGTCA TCCATGCCAT TGCTAATTCG▼ GGGAAGCTGG TTGTGGGACA CAACATGCTC TTGGATGTCA 859
human TGTGGGATTT TCTAGAGTCA TTCACGCCAT TGCTAATTCG▲ GGAAAACTTG TTATTGGACA CAATATGCTC TTGGACGTCA 880

mouse TGCATACGAT TCATCAGTTC TACTGCCCCC TGCCTGCG▼GA CCTGAATGAG TTTAAGGAGA TGGCAATATG TGTCTTCCCC 939
human TGCACACAGT TCATCAGTTC TACTGCCCTC TGCCTGCG▲GA CTTAAGTGAG TTTAAAGAGA TGACAACATG TGTTTTCCCC 960

mouse AG▼ACTCTTGG ATACTAAGTT GATGGCCAGC ACACAGCCTT TTAAG▼GATAT CATTAACAAC ACATCCCTTG CAGAGTTGGA 1019
human AG□ACTCTTGG ATACTAAATT GATGGCCAGC ACACAACCTT TTAAG▲GATAT CATTAACAAC ACATCCCTTG CGGAATTGGA 1040

mouse AAAGCGGTTG AAAGAGACAC CTTTTGACCC TCCCAAAGTT▼ GAAAGTGCAG AAGGCTTTCC AAGCTACGAC ACAGCTTCTG 1099
human AAAGCGGTTA AAAGAGACAC CTTTCAACCC TCCTAAAGTT▲ GAAAGTGCCG AAGGTTTTCC AAGTTATGAC ACAGCCTCTG 1120

mouse AGCAGCTTCA TGAGGCGGGG TACGATGCCT ACATCACAGG GCTCTGCTTC ATCTCCATGG CAAATTACTT AG▼GTTCTTTA 1179
human AACAACTCCA CGAGGCAGGC TACGATGCCT ACATCACAGG GCTGTGCTTC ATCTCCATGG CCAATTACCT AG▲GTTCTTTT 1200

mouse CTCAGTCCTC CAAAAATGTG TGTGTCTGCC AGATCAAAGC TCATTGAACC CTTTTTTAAC AA▼GTTATTTC TTATGAGGGT 1259
human CTCAGCCCTC CAAAAATTCA TGTGTCTGCC AGATCAAAAC TCATTGAACC TTTTTTTAAC AA▲GTTATTTC TTATGAGGGT 1280

mouse CATGGATATT CCCTATTTAA ACTTGGAAGG GCCAGACTTG C▼AGCCTAAGC GGGACCATGT TCTCCACGTG ACCTTCCCCA 1339
human CATGGATATC CCCTATCTAA ACTTGGAAGG ACCAGACTTG C▲AGCCTAAAC GTGATCATGT TCTCCATGTG ACATTCCCCA 1360

mouse AAGAGTGGAA AACCAGCGAC CTGTACCAGC TCTTCAGCGC CTTCG▼GTAAC ATTCAGATAT CCTGGATTGA TGATACATCA 1419
human AAGAATGGAA AACCAGCGAC CTTTACCAGC TTTTCAGTGC CTTTG▲GTAAC ATTCAGATAT CCTGGATTGA TGACACATCA 1440

mouse GCCTTCGTTT CTCTCAGCCA GCCAGAACAA GTACAAATT▼G CCGTTAATAC CAGCAAGTAC GCTGAAAGTT ATCGGATCCA 1499
human GCATTTGTTT CCCTTAGCCA GCCCGAGCAA GTAAAGATT▲G CTGTCAATAC CAGCAAATAT GCAGAAAGCT ATCGGATCCA 1520

mouse GACCTATGCT GAGTATGTGG GAAAGAAGCA GAAAGGCAAG CAGGTCAAGA GGAAGTGGAC AGAAGACAGT TGGAAGGAGG 1579
human AACCTATGCT GAATATATGG GGAGAAAACA GGAAGAGAAG CAGATCAAAA GAAAGTGGAC TGAAGATAGC TGGAAGGAGG 1600

mouse TGGACAGAAA GCGG****** CCCCA***** ********** CATGCAGGGC CCCTGTTACC ACAGCAACAG▼ CTTCACAGCC 1638
human CTGACAGCAA ACGGTTAAAC CCCCAGTGCA TACCCTACAC CCTGCAGAAT CACTATTACC GCAACAATA▲G TTTTACAGCT 1680

mouse GCTGGAGTGC TTGGAAAGAG GACGCTGAGT CCCGACCCAA GGGAAGCTGC CTTGGAGGAC AGAGAATCAG AGGAGGTATC 1718
human CCCAGCACAG TAGGAAAGAG AAATTTGAGT CCTAGTCAAG AGGAAGCTGG CCTGGAGGAC GGAGTGTCAG GGGAGATTTC 1760

mouse TGACTCGGAG CTTGAACAGA CAGATTCCTG TACAGACCCC CTCCCAGAGG GAAGGAAAAA GTCCAAGAAG TTAAAACGAA 1798
human CGACACTGAG CTTGAGCAGA CCGATTCCTG TGCAGAGCCC CTCTCAGAGG GAAGGAAAAA GGCCAAGAAA TTAAAAAGAA 1800

mouse TGAAGAAGGA GCTTTCCTTG GCAG▼GAAGTG TCTCGGA*** TAGCCCTGCC GTGCTCTTTG AAGTCCCTGA CACATGGTAG 1875
human TGAAGAAGGA GCTTTCTCCA GCAG▲GAAGCA TCTCGAAGAA CAGCCCTGCC ACACTCTTTG AAGTTCCTGA CACATGGTAA 1920

Figure 3.32. cDNA sequence of mouse PARN. The open reading frame of IMAGE clone 2101477 was sequenced and aligned with human PARN. The location of introns are indicated by arrowheads. ▼ shows the positions of predicted introns determined by the mouse genome BLAST of *Mus musdculus* WGS supercontig Mm16_WIFeb01_286, genomic accession number: NT_000107.1, ▼ indicates verified introns by sequencing either subclones or PCR products. ▲ the positions of predicted introns of *H. sapiens* chromosome 16 genomic contig , genomic accession number: NT_035359

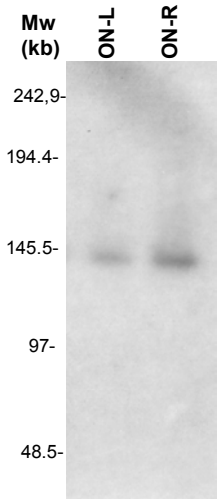

Figure 3.33. Size determination of pBeloBAC 25286. 1 µg pBAC25186 digested with 4U λ-terminase and hybridized to 250 fmol of the ^{32}P-labelled ON-L or ON-R oligonucleotides respectively. Separation of the digested DNA was carried out on a Bio-Rad CHEF-DR III puls-field gel electrophoresis apparatus for 20 hours at a field strength of 6V/cm in a 1% agarose gel in 0.5 x TBE at 14^{o}C with a linear pulse time ramping from 1-12 seconds. The gel was stained in EtBr to visualise the molecular weight marker (the sizes in kb are shown on the left side) and dried under vacuum before autoradiography.

puls-field gel electrophoresis. The size of the inserted DNA was estimated to 145 000 bp (Figure 3.33). Subclones were produced by digesting the BAC clone with *Eco RI*, *Hind III* or *Xba I* and shotgun cloned into pBluescripts II SK. The inserted DNA fragments ranged from 1 to 12 kb and clones were identified that hybridized to mouse PARN cDNA. Four introns were identified by sequencing subclones or PCR products and the locations were matching the predicted introns in the genomic However, attempts to generate PCR fragments with primers at the 3´ end of the cDNA ORF were unproductive, which might be explained by the presence of three large putative introns in this region (18 kb, 35 kb and 25 kb respectively).

4. DISCUSSION

Cap-dependent deadenylation has been investigated in HeLa cell extracts, by purified bovine PARN and by recombinant human PARN. Recombinant human PARN has been expressed and purified from *E. coli*, insect cells and human cells. Interaction of human PARN with translation initiation factors has been studied. Furthermore, a mouse PARN cDNA has been identified and partial analysis of the genomic organisation of this gene has been carried out.

4.1. Cap-dependent deadenylation in cell extracts

Polyadenylated RNA with a 7-methyl G-cap was deadenylated faster than uncapped RNA or RNA with a non-physiological ApppG-cap in HeLa cell extracts. Moreover, the m^7GpppG capped RNA was degraded with a previously described periodical decay pattern (*Körner and Wahle, 1997*) whereas the other two substrates were degraded without any visible decay intermediates. This degradation pattern was attributed to a partial protection of the poly(A) tail by PABPC (*Körner and Wahle, 1997*). The slow degradation rate of uncapped and ApppG-capped RNAs and the absence of degradation intermediates suggested that these substrates were degraded either by a different pathway or by a different reaction mechanism. As the RNA substrates used in these experiments were homogeneously labelled in the body of the RNA, it was not possible to determine a directionality of the degradation reaction. However, the ApppG-cap probably provided protection towards 5′ to 3′ exonucleases arguing that at least this RNA might be degraded by a 3′-5′ exonuclease. Instead, the difference could be caused by an increased affinity of PABPC for the RNA with a m^7GpppG-cap owing to the indirect interaction of the poly(A) tail with the 5′ cap via eIF4E and eIF4G. In this case one would expect the uncapped RNA to be less protected and to be deadenylated faster than the capped RNA. However, uncapped and ApppG-capped RNAs were more stable in HeLa cell extracts than RNAs with an authentic cap. A difference in protection of the poly(A) tail by PABPC is therefore unlikely to explain the difference in decay between these RNAs. That a connection between the deadenylating activity in HeLa cell extracts and the presence of a 7-methyl guanosine cap on the RNA is functionally significant has been confirmed by either blocking access to the cap through addition of the cap binding protein, eIF4E (*Gao et al., 2000*) or by competition with cap analogues (*Gao et al., 2000 and Figure 3.2*.).

Deadenylation in extracts derived from mature *Xenopus* oocytes also exhibited a preference for capped RNAs except that an RNA carrying the non-physiological ApppG-cap was deadenylated with a 20-fold less efficiency. Furthermore, cap-dependent deadenylation was observed *in vivo* when radiolabelled RNAs carrying a 5´-terminal ApppG-, GpppG- or a m^7GpppG-cap were injected into mature *Xenopus* oocytes again with the ApppG-capped substrate being the most stable RNA (results by Wormington published in *Dehlin et al., 2000*). It is clear that PARN is responsible for the observed deadenylating activity in *Xenopus* oocytes by several criteria. i) A poly(A)-specific ribonuclease has been purified from *Xenopus* oocytes and a cDNA with strong sequence homology to hPARN has been cloned (*Copeland and Wormington, 2001*). ii) Injection of antibodies directed against recombinant hPARN blocks deadenylation in mature *Xenopus* oocytes (*Körner et al., 1998*). iii) The nuclease responsible for default deadenylation activity is initially nuclear and activity cannot be detected before the germinal vesicle breakdown during maturation (*Varnum et al., 1992*). Western blot analysis with anti-PARN antibodies detected a polypeptide that was exclusively nuclear before maturation (*Körner et al., 1998*) and finally iv) if the oocytes are enucleated prior to maturation this activity is obstructed (*Varnum et al., 1992*). hPARN can restore default deadenylation upon progesterone treatment of enucleated oocytes (*Körner et al., 1998*). The observed cap-dependent deadenylating activity in *Xenopus* oocytes and HeLa cell extracts are therefore likely to be mediated by PARN.

S100 cytoplasmic HeLa cell extracts deprived of PARN by immunodepletion failed to deadenylate substrate RNAs but the activity could be restored by addition of recombinant hPARN. Whether the deadenylating activity in this extract was PARN or another deadenylase remains to be investigated as the antibodies that were used for the depletion were polyclonal and could share some epitopes with another ribonuclease (*Gao et al., 2000*). Such a candidate would be hPOP2/CALIF. Yeast Pop2p and human POP2/CALIF, like hPARN, belong to the RNase D family of nucleases. Pop2p has been shown to be a subunit of the Ccr4p/Pop2p/Notp mRNA deadenylase complex in *Saccharomyces cerevisiae* (*Daugeron et al., 2001*; *Tucker et al., 2002*). The ability of hPOP2/CALIF to associate with both hCCR4 and the hNOT proteins indicates that such a complex with deadenylating activity might also exist in mammalian cells (*Albert et al., 2000; Dupressoir et al., 2001*). Until today, a deadenylating activity of the human CCR4/POP2/NOT complex has not been demonstrated though human CCR4-FLAG expressed in yeast showed a weak enzymatic activity (*Chen et al., 2002*). Nevertheless, the deadenylating activities observed in HeLa cell extracts and in *Xenopus* oocytes function in a

cap-dependent manner and it is likely that PARN is the enzyme which is responsible for this activity.

4.2. Cap-dependent deadenylation by purified bovine PARN.

Assuming that PARN is the enzyme that is responsible for the observed activity in HeLa cell extracts, cap-dependent deadenylation catalyzed by purified PARN from calf thymus (*Körner and Wahle, 1997*) was examined. Indeed, RNA with a methylated cap was deadenylated at least four-fold faster than uncapped, ApppG-capped or GpppG-capped RNA. Also when RNA substrates carrying either a methylated or unmethylated cap were combined in the same reaction, the substrate with a methylated cap was deadenylated faster. Furthermore, when the calf thymus PARN preparation was assayed by the release of acid-soluble nucleotides from a radioactive labelled poly(A) tail, the m^7GpppG-capped RNA was deadenylated faster than a GpppG-capped RNA substrate. The difference in the initial deadenylation rate of RNAs with and without a methylated G-cap was comparable to the rates that were observed in the gel assays. The poly(A) tail-length of the substrate RNAs did not influence the deadenylation rate in these assays. Competition with free cap analogues showed that more than a 10-fold higher concentration of GpppG compared to m^7GpppG was needed to inhibit bPARN (*Körner, 1998b*) which in turn is equivalent to the observed differences in the HeLa cell extract and in the cytoplasmic S100 extract described by Gao et al. (*Gao et al., 2000*). All these results indicate that not only a cap but a methylated cap structure is crucial for mediating a stimulation of PARN. Other cellular reactions which depend on a bona fide cap are initiation of translation *(Shatkin, 1985*) and decapping in the cytoplasm (*LaGrandeur and Parker, 1998*), splicing (*Izaurralde et al., 1994; Lewis et al., 1996*), export from the nucleus (*Görlich et al., 1996; Visa et al., 1996; Shen et al., 2000*), and 3´ end formation (*Flaherty, et al., 1997*) in the nucleus. The different roles of the cap structure are usually mediated through cap-binding proteins, of which some are complexed with other factors. CBC, the nuclear cap-binding complex, is a heterodimer consisting of a cap-binding protein, CBP20 and CBP80 (*Ohono et al., 1990*). The cytoplasmic translation initiation complex eIF4F consists of the cap-binding subunit eIF4E in addition to eIF4G and eIF4A (see section 1.5). However, cap-dependent deadenylation does not appear to require any of the two known cap-binding proteins since neither eIF4E nor the CBP20/80 could be detected in the purified PARN fraction (*Körner, 1998b*). In fact, PARN itself is a cap-binding protein, which was

demonstrated by its ability to bind m^7GTP-Sepharose (Figure 3.6.). Even if an additional cap-binding protein were present in substoichiometric amounts to PARN in the purified enzyme fraction, one would expect a one to one ratio in the bound fraction. However, the only other protein showing specific binding to the m^7GTP resin was a proteolytic fragment of PARN. When a total *Xenopus* oocyte extract was incubated with m^7GTP-Sepharose, PARN was depleted from the extract and deadenylation in the depleted extract was inhibited, indicating that also *Xenopus* PARN is a cap binding protein (results by Wormington published in *Dehlin et al., 2000*). Furthermore, a similar inhibition of deadenylation was observed when S100 extracts were passed over a m^7GTP-Sepharose column (*Gao et al, 2000*). Both *Xenopus* PARN and human PARN in the HeLa cytoplasmic extract could be UV-crosslinked to a cap-labelled transcript verifying the intrinsic cap-binding activity of PARN (results by Wormington published in *Dehlin et al., 2000; Gao et al., 2000*). In conclusion, the ability of PARN to simultaneously interact with the 5´ cap and the 3´ poly(A) tail greatly enhances its activity.

A communication between the 5´cap structure and the 3´ poly(A) tail also results in an enhancement of translation. The cap and the poly(A) tail binding proteins eIF4E and PABPC are interacting with different parts of the translation initiation factor eIF4G to form the eIF4E/eIF4G/PABPC complex which circularizes mRNAs that are translated and presumably facilitates reinitiation (*Wells et al., 1998; Gallie, 1991; Iizuka et al., 1994*). As an authentic cap accelerates PARN mediated deadenylation but is not absolutely necessary for activity, one could speculate that the translation status of an mRNA could either allow or prevent PARN to have access to the cap. In this way it is possible to modulate the deadenylation rate and consequently mRNA stability.

4.3. Cap-dependent deadenylation by recombinant hPARN.

4.3.1. Purification of recombinant hPARN expressed in mammalian cells.

The expression of recombinant hPARN in human embryonic kidney (HEK293-EBNA) cells employed a large scale transient transfection procedure to avoid the cytotoxic effects of over-expressing PARN (*Wurm and Bernard, 1999; Meissner et al., 2000*). Maximal PARN production could be seen between 44 and 74 hours post-transfection (Figure 3.14), so the cells were harvested after 55 hours. At this time-point each cell contained approximately 0.2 fmol

PARN protein (estimated by Western blot). That 90% of the activity was lost during the purification may have been caused by a contribution of unspecific nuclease activity in the TCA-assays with crude extracts, since no competitor RNA was added, or by inactivation of the recombinant protein. Furthermore, some protein was probably retained in the Blue Sepharose column as the enzyme was eluted only in one step. This elution procedure was based on a previous purification of PARN in which the Blue Sepharose chromatography was performed at a later stage in the purification procedure (*Körner and Wahle, 1997*). Nevertheless, the recovered protein was more than 95% pure after a 50-fold purification (Figure 3.16 and Table 3.1), which indicated that the protein was well over-expressed in the transfected cells.

Like the purified bovine PARN, this enzyme preparation deadenylated RNAs with a methylated 5´ cap faster than RNAs with an unmethylated cap (Figures 3.17, 3.18 and 3.19). Furthermore, the nuclease could be bound to m7GTP-Sepharose and be UV-crosslinked to a cap-labelled RNA (data not shown), showing that the cap-binding activity of purified bPARN is a feature that is shared by recombinant hPARN.

The specific activity, under physiological salt conditions, of the *E. coli* expressed recombinant nuclease (*E. coli* PARN) was only about 10% of the nuclease that was purified from calf thymus (*Körner et al., 1998*). In contrast, hPARN expressed in HEK293-EBNA cells (HEK PARN) showed a four-fold higher specific activity than *E. coli* PARN under this reaction condition but was still not as active as the authentic PARN protein (Table 3.1. and *Körner et al.,1998*). As mentioned above, this difference may be explained by a larger fraction of inactive protein in the HEK PARN preparation although it cannot be excluded that the bovine PARN preparation still contained a possible activating factor.

4.3.2. Purification of recombinant hPARN from S2 cells.

Human PARN cDNA was placed under the control of an inducible metallothionein promoter in the pMT/V5-HisC vector and stable cell lines expressing hPARN with or without an N-terminal His_6-tag were generated.

The non-tagged enzyme was purified in parallel with hPARN expressed in HEK293 cells. As the loss of activity throughout this purification was very high it is possible, also in this case, that the activity measured in crude extract was too high due to unspecific nucleolytic activity. Furthemore, bovine PARN eluted at a higher concentration of $AmSO_4$ (~8-10%*) (T. Meyer, 1997*) from the final Phenyl-Superose column compared to the recombinant enzymes (Figures

3.10 and 3.16). Thus, in order to recover the entire activity from this column, the elution procedure should be optimized.

The activity of the His_6-PARN fusion protein was divided into two peaks after FPLC MonoQ fractionation and found to be associated with two polypeptides (74 kDa and 60 kDa) which reacted with anti-PARN antibodies (Figure 3.12). It is likely that the 60 kDa PARN fragment purified from S2 cells is a C-terminal truncation for two reasons. First, the His_6-tag is fused to the N-terminus of PARN, and the fragment was co-purified with the full-length protein on Ni^{2+}-NTA affinity chromatography. Second, as the fragment shows activity and the ExoI-III motifs, which are important for nucleolytic activity, are located in the N-terminal two thirds of the protein it is unlikely that the N-terminus is missing. In addition, a 54 kDa proteolytic fragment of PARN purified from calf thymus (*Martinez et al., 2000*) and a 62 kDa fragment of Xenopus PARN (*Copeland and Wormington, 2001; Körner et al., 1998*) exhibit nucleolytic activity and are likely to be C-terminal truncations. Whether the 60 kDa proteolytic hPARN fragment was generated *in vivo* in the S2 cells or during purification is not known.

4.3.3. Post-translational modification of recombinant PARN restores a stringent cap-dependency.

The non-tagged hPARN preparations from HEK293 cells and S2 cells were clearly stimulated by an authentic 5´ cap on the substrate RNA (Figures 3.11, 3.17, 3.18 and 3.19). The His_6-tagged PARN purified from S2 cells exhibited a similar preference for a m^7G-capped RNA (Figure 3.13). The difference in cap-dependence between the purified bovine PARN and recombinant hPARN expressed in *E. coli* is therefore most likely caused by some post-translational modification that does not take place in prokaryotes. Two such modifications that are known not to occur in *E. coli* are *N*-glycosylation and phosphorylation. Functions that have been attributed to glycosylation are e.g. maintenance of protein conformation and stability or protection against proteolytic activity (*Moens and Vanderleyden, 1997*). Neither of these functions are likely to contribute to cap-dependence as the recombinant enzyme is active and apparently not degraded. Interestingly, *E. coli* expressed PARN can be phosphorylated upon incubation in a translation active HeLa cell extract (data not shown) but failed to be phosphorylated in an *in vitro* phosphorylation assay by the mitogen-activated protein kinase-activated protein kinase 2, MAPKAP-kinase 2, (*A. Neininger, personal communication*). The

MAPKAP-kinase 2 signalling has been implicated in regulation of IL-6 mRNA stability through targeting its AU-rich elements (*Neininger et al., 2002*). The phosphorylation status of PARN still has to be investigated as phosphorylation often is involved in regulation of activity of proteins via signal transduction cascades for example. However, if phosphorylation contributes to the cap-dependence of PARN remains to be investigated.

As the shorter 60 kDa polypeptide that co-purified with His_6-PARN is likely to be a proteolytic fragment and showed nucleolytic activity, it was tested for cap-dependence. Although the fragment deadenylated an RNA substrate with a methylated cap faster than an RNA with an unmethylated cap, the overall deadenylation rate was slowed down (Figure 3.13). This behaviour is in analogy with results that were obtained with a C-terminal deletion mutant of hPARN, N-DAN (*Körner, 1998b*). A putative RNA recognition motif (aa 447-503), that may contribute to the poly(A)-binding activity of PARN (*Copeland and Wormington, 2001*), is missing in this mutant which might reduce binding of N-DAN to the poly(A) tail and slow down its activity. If the 60 kDa PARN fragment is a C-terminal truncation, this motif could still be intact but might not be correctly folded.

4.3.4. HEK PARN has a higher affinity to the m^7G-cap than *E coli* expressed PARN.

PARN is a cap-binding protein (Figure 3.6), and its activity is stimulated by a methylated 5′ cap on the RNA substrate (Figure 3.3). As the addition of cap-analogues inhibits this activity (Figure 3.2; *Körner, 1998b*), the concentration of free cap-analogue that reduces the activity by 50% would reflect the binding affinity of the enzyme for the cap. The activities were tested by the rate of released AMP in a TCA-precipitation assay and three observations were made: i) The affinity of *E. coli* PARN to a methylated cap was approximately ten-fold less than that of HEK PARN when the substrate was poly(A) (Figure 3.21). ii) The activity of *E. coli* PARN was stimulated by low concentrations of cap-analogue when the substrate was carrying an unmethylated cap but was significantly less stimulated when the substrate carried a methylated cap (Figure 3.20). iii) Inhibition of HEK PARN by free m^7GpppG did not change significantly whether the RNA carried a methylated cap or not (Figure 3.20).
The difference in affinity for the m^7GpppG-cap analogue between the *E. coli* and HEK PARN preparations with the poly(A) substrate is probably due to a post-translational modification of amino acids that are important for binding. Since the affinity for polyadenylated RNA is in the

nM range (*Martinez et al, 2001* and data not shown) and the affinity for the cap is in the µM range, binding to the cap probably takes place as an intramolecular event after binding the RNA. In the activity assays is the difference in cap-dependence between the two PARN preparations not so pronounced as in the competition assay, which may be explained if binding of the cap is an intramolecular event. Low concentrations of the trans-acting cap analogue might activate deadenylation of the *E. coli* PARN preparation by mimicking the role of a single methylated cap structure on the substrate RNA. As the affinity to m^7GpppG is higher for HEK PARN such an activation of this enzyme may occur at lower concentrations than was tested. A similar observation was made with the 54 kDa PARN fragment (*Martinez et al., 2001*).

4.3. 5. Binding of hPARN to the 5´cap induces a processive reaction mechanism.

Recombinant hPARN expressed in HEK293 cells and purified to near homogeneity cells showed a stringent cap-dependency and was therefore used for investigating the processivity of PARN. A definition of a processive enzyme is that it remains attached to its substrate and performs multiple rounds of catalysis before dissociating (*von Hippel et al., 1994*) whereas a distributive enzyme dissociates after one round of catalysis. Provided that the substrate concentration is higher than the enzyme concentration, a processive mode of deadenylation can be described as a reaction in which completely deadenylated products are produced while full-length RNA substrate still exist. In a distributive mode of deadenylation, the RNAs are deadenylated synchronously with an apparently slower rate. With this definition, HEK PARN exhibited a processive mode of deadenylation when the substrate RNAs were carrying a m^7G-cap whereas RNAs with an unmethylated cap were deadenylated in a distributive manner (Figure 3.17). The RNA substrates were radiolabelled in the cap in this experiment but the same result was obtained when the body of the RNA was labelled and the cap structures were added co-transcriptionally (Figure 3.18). A fraction of the body-labelled RNA with a methylated cap was deadenylated synchronously. This probably represent uncapped RNA since only about 60% of the transcripts recieve a cap when cap analogues are incorporated during transcription (*Pasquinelli, 1995*). Furthermore, 5 to 10-fold more enzyme was required to fully deadenylate RNA carrying an unmethylated cap relative to RNA with a methylated cap within the same reaction time (Figure 3.19). Also this assay was performed with cap-labelled RNA substrates, which due to the different capping efficiencies with or without S-

adenosyl methionine in the capping reaction, contained unequal fractions of uncapped RNA. As the purified bovine PARN most likely deadenylated uncapped and GpppG-capped RNAs in a distributive mode (Figure 3.3), the vast fraction of uncapped RNA in the GpppG-RNA substrate in this assay would most likely not contribute to any changes in the reaction mechanism. Moreover, the small fraction of fully deadenylated products seen before the bulk RNA was deadenylated is probably RNA with methylated cap-structures presumably generated by cap methyl transferase containing bound S-adenosyl methionine (see Figure 3.17 B).

4.4. PARN is a homodimer.

As the native molecular mass of purified bovine PARN was estimated as 257 kDa by gel filtration whereas the size in SDS-PAGE was 74 kDa, the enzyme might either be filamentous, a multimer, or exist as a part of protein complex (*T. Meyer, 1997*). To elucidate the structure of the nuclease, recombinant hPARN purified to near homogeneity was used to re-evaluate the native molecular mass. Sedimentation-equilibrium centrifugation allows an estimation of the molecular mass which is independent of the shape of the protein. By this method the native molecular mass was estimated to 150.4 kDa. Approximately 20% of the measured absorbance exhibited a higher molecular mass, which most likely were aggregates of the protein (Figure 3.31). This shows that hPARN, in its native form, is a homodimer. The high frictional ratio, (f/f_0), calculated from the estimated sedimentation coefficient (4.8×10^{-13}s) and the molecular mass (150.4 kDa), implied that the protein has an extended shape. Therefore, a dimeric structure and an extended shape of the protein may explain the high molecular mass that was estimated by gel filtration. In contrast, Martinez et al. showed that chemical cross-linking of PARN shifted the electrophoretic mobility to two slower migrating forms which suggested that hPARN consists of three subunits (*Martinez et al., 2000*). However, the cross-linkers used, *Bis*(Sulfosuccinimidyl) substrate and dimethyl pimelimidate, are relatively long and might lead to both intra- and inter-molecular cross-linking resulting in slower mobility in SDS-PAGE. Another explanation would be that aggregates of the protein have been cross-linked.

4. 5. PARN acts via both processive and distributive reaction modes.

Enzymes that are involved in synthesis, modification and degradation of nucleic acids or other polymers are often processive. When the substrate is a nucleic acid for example, electrostatic interactions can be repeated along the phosphate backbone (*Breyer and Matthews, 2001*). The active site of PARN has been found to reside within the three Exo domains and presumably carries out hydrolysis of phosphodiester bonds by using a two-metal ion mechanism for catalysis (*Ren et al., 2002;*). Taking into account that native PARN is a homodimer the enzyme might have two active sites.

Furthermore, a processive enzyme should have high affinity to its substrate. This can be achieved by having a large interaction surface, which can be generated by several different binding sites. Based on sequence homology, two putative RNA binding motifs have been identified in PARN: the R3H motif (aa 186-239) which is thought to be involved in binding single-stranded nucleic acids (*Grishin, 1998*) and a RRM motif (aa 447-503) proposed to be involved in binding the poly(A) tail (*Copeland and Wormington, 2001*). Processivity of exonucleases probably involves accessory RNA-binding domains, separate from the RNA-binding elements in the active site itself, as such elements also will be present in distributive Rnases (*Symmons et al., 2002*). PARN has the interesting feature that it can bind to the 5´ cap structure of mRNA. The observation that a m^7GpppG cap analogue acts as a non-competitive inhibitor of PARN activity suggests that the cap-binding site is separate from the active site (*Martinez et al., 2001*). Although binding to the cap structure is not necessary for activity, it may serve as a processivity inducer/enhancer in such a way that the interaction surface is increased, for example by inducing a conformational change of the protein.

The structures of processive enzymes can be divided into two classes, those that partially enclose their substrates and those that are capable of completely enclosing the substrate. An example of the latter is phage T7 DNA polymerase. The crystal structure shows an “open” configuration but it is thought that *E. coli* thioredoxin functions as a processivity factor by binding the polymerase to form a closed structure (*Breyer and Matthews, 2001*). Other enzymes encircle their substrate by forming symetric oligometric toroids. One might speculate that PARN is able to form such a structure due to its dimeric native form. However, PARN removes the poly(A) tails of RNAs without a cap structure in a distributive mode. It is therefore possible that the m^7G-cap might act as a processivity factor in the same manner as the *E. coli* thioredoxin.

PARN and most likely other exonucleases completely remove the substrate to which they are bound. Binding the cap structure may enable the enzyme to remain bound on the RNA until the poly(A) tail is fully removed. A second binding site on the substrate might also explain why the enzyme *in vitro* is capable of degrading further into the body of the RNA (Figures 3.3, 3.17 and 3.18). The results obtained in this thesis clearly shows that PARN acts in a distributive manner unless a methylated cap structure is present on the substrate RNA. I therefore propose a model in which PARN can act as both a distributive and processive exonuclease depending on the accessibility of a mehtylated cap structure at the 5´ end of an mRNA (Figure 4.1).

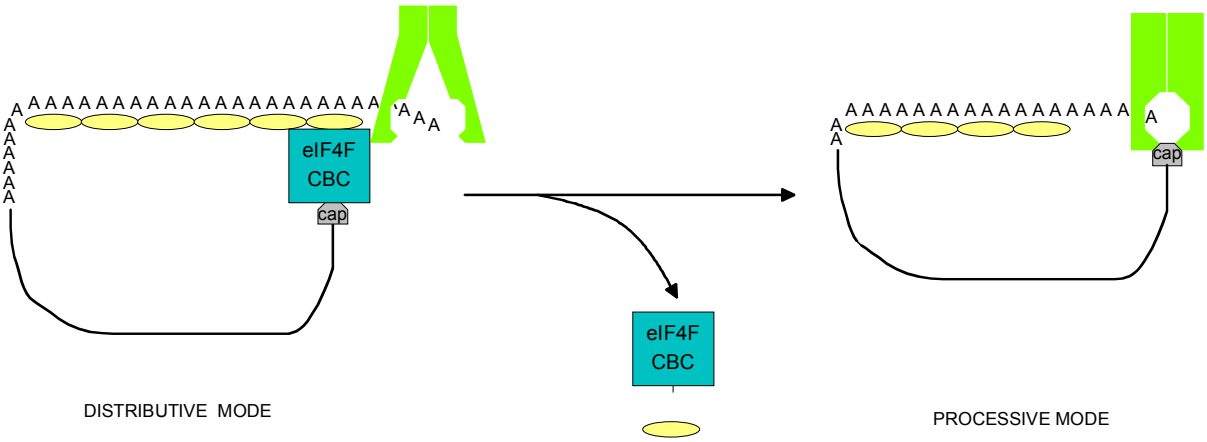

Figure 4.1. Transition from a distributive to a processive mode of deadenylation. When mRNAs are lacking a cap or when the cap is occupied by cap-binding proteins is PARN able to bind the poly(A) tail via RNA-binding domains positioned near the active centre. Binding can be achieved with one or both subunits but will not enclose the substrate completely. The enzyme can thus dissociate from the substrate after "nibbeling" off an adenosine residue and then bind to another RNA molecule (distributive mode). When the cap structure is free, for example when translation complex has been sequestered, can PARN bind the 5´ cap intra-molecularly. This will induce a conformational change which closes the protein structure so that PARN now encircles the substrate completely and deadenylation becomes processive.

Another model for PARN activity has been suggested by Martinez et al., where a 54 kDa fragment of PARN is described as a processive enzyme and that a methylated 5´ cap only enhances the processivity of the nuclease. This conclusion was based on two experiments: First, full-length RNA substrates with poly(A) tails of about 5 adenosine residues co-existed with completely deadenylated products whether the substrate was capped or not and second,

the PARN-RNA complex remained stable during the reaction cycles both in the presence and absence of a cap structure (*Martinez et al., 2001*). However, when the poly(A) tails were 30 nucleotides long, uncapped and GpppG-capped RNAs were clearly deadenylated synchronously which contradicts a processive deadenylation mode. It was further suggested that a methylated cap enhances the processivity of PARN by stabilizating its binding to the RNA in a sequence independent way. When the poly(A) tails are shorter than *in vivo* (5 to 30 nucleotides) this stabilization may lead to a reduction in the maximal rate, V_{max}, by which PARN removes adenosine residues (*Martinez et al., 2001*). It is possible that the kinetics of PARN mediated deadenylation functions in a biphasic manner with, for example, a decreased product release when the poly(A) tails become too short or that the stabilizing effect of cap-binding now becomes a sterical hindrance. Although the experiments in this thesis were performed with RNAs carrying poly(A) tails of 100 to 200 nucleotides in length, the obtained results show that PARN acts in a distributive manner unless a methylated cap structure is present on the RNA substrate. A co-crystalization of PARN with m^7GpppG-capped and uncapped RNA might help to understand how the m^7GpppG-cap contribute to the processivity of PARN.

4.6. Trimming or rapid deadenylation?

Considering that PARN can degrade poly(A) tails both in a processive and distributive mode one might hypothesize that the enzyme could be involved in mRNA decay as well as having a trimming function. The yeast poly(A) nuclease, PAN, has been proposed to play a role in the nucleus by trimming nascent poly(A) tails before export to the cytoplasm but may also be involved in cytoplasmic deadenylation (*Brown and Sachs,1998*). A function of PARN in the nucleus has, so far, not been demonstrated but is supported by transient transfection of GFP-PARN cDNA into mammalian cells, which showed that the fusion protein was distributed in both cell compartments (*Körner et al., 1998*). A trimming function or rapid deadenylation in the nucleus might be regulated by the binding status of the nuclear-cap binding complex, (CBC), while the translation initiation complex, eIF4F, would control PARN mediated deadenylation in the cytoplasm.

4.7. Inhibition of PARN by translation initiation factors is independent of the 5´ cap.

A "closed loop" configuration of the mRNA during translation enhances translation re-initiation and prevents exoribonucleases to have access to the RNA. In an attempt to evaluate if such a configuration would prevent PARN mediated deadenylation, eIF4E and eIF4GI were allowed to assemble on capped and polyadenylated RNA that was pre-incubated with PABPC before initiating deadenylation. As PABPC in saturating concentrations completely inhibits PARN mediated deadenylation (*Körner and Wahle, 1997; Wormington, 1996*) but is only partially inhibitory at lower concentrations, the experiment was made with a PABPC concentration that still allowed deadenylation. The partial inhibition of PARN, caused by PABPC, was further enhanced by assembly of the eIF4E/4G complex on the cap structure (Figure 3.22). Such a block of activity at equal concentrations of translation initiation factors and RNA is in accord with a circularization of the RNA which would prevent PARN from binding either to the poly(A) tail or the cap structure. If on the other hand, the poly(A) tail is accessible but the cap structure is blocked by binding to eIF4E/eIF4GI, one would expect that deadenylation could take place but in a distributive deadenylation mode (described in section 4.5). Inhibition could be seen but without a change in deadenylation mode when eIF4E/eIF4GI was allowed to assemble on the cap (Figure 3.23). Surprisingly eIF4GI alone inhibited deadenylation whereas the cap binding protein eIF4E by itself had no effect (Figure 3.23), presumably due to its low binding affinity to the cap (*Hsu et al., 2000*). The unexpected inhibition of PARN activity by eIF4GI was confirmed when the RNA substrate carried the non-physiological ApppG-cap (Figure 3.25). Thus, inhibition of PARN activity seemed to be caused by eIF4GI and not to a "closed loop" configuration of the RNA. A fragment of eIF4GI consisting of the middle domain (4GM), was the smallest portion of the protein which could inhibit PARN activity. 4GM inhibited PARN deadenylation of mRNA (data not shown) as well as poly(A) (Figure 3.26). Moreover, interference of PARN activity was examined in a TCA-precipitation assay by a titration of 4GM into the deadenylation reactions. In these assays PARN activity was reduced at high concentrations of 4GM but stimulated at low concentrations (data not shown). However, these results were difficult to interpret since the 4GM protein preparation itself contained a low exonucleolytic activity.

The middle domain is defined by cleavage sites for viral proteases which removes the eIF4E-dependent cap recognition function of eIF4G (*Ali et al., 2001*). In addition to binding sites for eIF4A and eIF3 (*Korneeva et al, 2*000), the 4GM fragment includes two putative RNA recognition motifs that are thought to be involved in stabilizing the binding of eIF4E to the

cap and to bind IRES in mediating cap-independent initiation of translation (*Goyer et al., 1993; Pestova et al., 1996, Gingras et al., 1999*). 4GM might therefore prevent PARN to have access to its substrate by binding to the RNA. A general RNA binding protein, PTB, prevents PARN to degrade into the RNA body by a non-specific binding of the RNA (Figure 3.27) but did not prevent eIF4GI inhibition of PARN activity (Figure 3.27). Binding of eIF4GI to the RNA body is probably not the reason for the obstruction of PARN activity although one can still not exclude that eIF4GI is able to bind to the poly(A) tail. However, the binding affinity of eIF4G to RNA is 1 μM (*Sha et al., 1995*) whereas PARN binds RNA with an affinity in the nM range (*Martinez et al., 2001*).

4.8. A physical interaction between PARN and eIF4G.

In order to analyse the inhibitory effect of eIF4G on PARN mediated deadenylation a possible protein-protein interaction was examined. A GST-PARN fusion protein efficiently pulled down eIF4G from a HeLa cytoplasmic extract (Figure 3.28). This extract was not treated with micrococcal nuclease, so endogenous RNA in the extract might mediate a possible interaction between eIF4G and GST-PARN. However, a PARN-eIF4G interaction was confirmed in a nuclease treated rabbit reticulocyte lysate (data not shown). Interactions between GST-PARN and the purified C-terminal domain (p100) of eIF4G as well as the middle domain (4GM), suggested that the middle domain might contain a binding site for PARN (Figure 3.29). A 60 kDa proteolytic fragment p100 was also efficiently pulled down. This fragment is probably a C-terminal truncation since the middle domain seemed to be the smallest fragment that binds to PARN. The resistance to micrococcal nuclease treatment suggested that the interactions are not mediated by RNA binding (Figure 3.29). Furthermore, the physical interaction between the eIF4G fragments and PARN was verified when the complexes were incubated with m^7GTP-Sepharose (Figure 3.30). A small amount of PABPC was recovered together with PARN in this assay as the anti-eIF4G antibodies that were used for detection of the eIF4G fragments in this assay also reacted with PABPC (Figure 3.30). However, an interaction between PARN and PABPC might occur but has to be further investigated. As the recombinant PARN preparation did not carry a GST tag in this experiment, binding of 4GM and p100 to the glutathione S-transferase tag can be excluded. Thus, 4GM which is the smallest segment of eIF4GI that is inhibiting PARN activity, is also sufficient for binding to PARN.

The middle domain of eIF4G (aa 642-1091) contains a conserved domain (MIF4G) is rich in alpha-helices and contains multiple alpha-helical HEAT repeats that might participate in protein-protein interactions (*Ponting, 2000; Marcotrigiano et al., 2001*). Further experiments have to be made in order to verify the interaction and to explain the effect on PARN activity. The eIF4G middle domain used in this study (4GM) is approximately 200 amino acids longer than the core MIF4G domain. To further investigate the interaction between PARN and the middle domain of eIF4G would include to generate deletions in 4GM be and to introduce mutations in both PARN and 4GM.

The middle domain of eIF4G contains significant sequence similarities to CBP80, a subunit of the nuclear cap-binding complex, CBC and yeast Upf2p/NMD2p. A multiple alignment of these sequences has revealed that homologues of the eIF4GI middle domain, MIF4G (*Ponting, 2000*) also named 4GM (this thesis) or 4GH (*Mendell et. al., 2000*), occur once in CBP80 and three times in Upf2p/NMD2p. The cytoplasmic translation initiation complex, the nuclear cap-binding complex and the NMD complex therefore all contain a MIF4G-domain-containing protein and all bind to proteins with repeated RRM domains (PABPC, CBP20 and Hrp1p respectively). Furthermore, the eIF4F and NMD complexes also contain helicases (eIF4A and Upf1p) (*Ponting, 2000*).

Upf2p homologues in *Schizosaccharomyces. pombe* and human (hUpf2/rent2) have been identified and found to contain MIF4G (4GH or 4GM) domains (*Mendell et al., 2000;*). Site-directed mutations within the 4GH domains of the *S. pombe* Upf2p were found to abolish NMD activity. Furthermore, the human Upf2/rent2 interacts with eIF4A and a subunit of eIF3 (Sui1) via its MIF4G/4GH domains. The authors suggested that Upf2p or rent2 competes with eIF4G for interactions via the 4GH (MIF4G) domain disrupting or preventing the formation of a “closed-loop” structure of mRNA. This would expose the cap structure to the decapping enzyme (*Mendell et al., 2000*). PARN could be inactivated by binding to another of the MIF4G/4GH domains thus preventing deadenylation to occur and promoting decapping by allowing its access to the 5´ cap. In another scenario one might speculate that hUpf2/rent2 is instrumental in recruiting PARN to mRNAs that are marked to be degraded. A two-hybrid system trying to find other binding partners to PARN might show if PARN also binds to proteins that are involved in NMD. Gene silencing either in a mouse knock-out or by RNAi may reveal if PARN plays a crucial role in NMD. Although NMD in *S. cerevisiae* is mediated through a deadenylation independent pathway and human orthologs to Dcp1p/Dcp2p and the 5´to 3´ exonuclease Xrn1p have been identified, it is still unclear what their roles are in

mammalian NMD. A recent report, using a transcription-pulsing approach to monitor deadenylation and decay, showed that a nonsense codon triggers accelerated deadenylation of mRNAs with a premature stop codon. The transcripts are stabilized when rapid deadenylation is impeded (*Chen and Shyu, 2003*).

A role of eIF4G in regulation of mRNA stability comes from *Saccharomyces cerevisiae* where mutations in eIF4G, eIF4A, eIF4E and Prt1 (eIF3 subunit) caused accelerated deadenylation and decay of mRNA (*Schwartz and Parker, 1999*).
Although recent results have shown that PARN is primarily localized in the nucleus (*M. Reuter, personal communication*), this may not necessarily rule out an interaction of PARN with proteins that are involved in translation as several of the translation factors are also found in the nucleus, (*Iborra et al., 2001; Wilkinson and Shyu, 2001; Lund and Dahlberg, 1998; Dostic et al., 2000a; Dostic et al., 2000b; Etchison and Etchison 1987; McKendrick et al., 2001*) including nuclear ribosomes (*Iborra et al., 2001; Mangiarotti, 1999*). The nuclear cap-binding complex, CBC, is supposed to bind nascent pre-mRNAs and promote splicing. But CBC-bound mRNAs can also be translated in which the CBC recruits eIF4G (*McKendrick et al., 2001*). The CBC may also recruit other initiation factors as the CBP80 subunit has a MIF4G domain that may bind eIF3 and eIF4A. Furthermore, the nuclear CBC has been implicated in mediating a “pioneer” round of translation that can detect nonsense codons (*Fortes et al., 2000; Ishigaki, et al., 2001*). Taken together, PARN may interact with MI4G-domains of both nuclear and cytoplasmic proteins but may only transiently shuttle into the cytoplasm. Future experiments will show in what cell compartment PARN exerts its major activity.

5. SUMMARY

Gene expression depends to a large extent on the concentration of mRNA in the cell, which in turn is determined by the ratio between transcription and degradation. A general mRNA-degradation pathway in both yeast and higher eukaryotes is usually initiated by a gradual shortening of the poly(A) tail, followed by a rapid cleavage of the 5´ cap structure and degradation of the mRNA body. One poly(A) specific ribonuclease, PARN has been purified and later cloned. The authentic and the recombinant enzymes are investigated with respect to their cap-dependencies

Polyadenylated RNA with an authentic m^7GpppG-cap was deadenylated faster than uncapped RNA or RNA with a non-physiological ApppG-cap in HeLa cell extracts. Furthermore the RNA with a 7-mehtyl G-cap was degraded with a previously described periodic decay pattern which has been attributed to a partial protection of the poly(A) tail by PABPC. Free m^7GpppG-cap analogue inhibited deadenylation at 20µM whereas roughly 300µM GpppG was needed to achieve the same effect. An unmethylated cap is thus recognized with much lower affinity.

The deadenylating nuclease purified from calf thymus, bPARN, degraded the poly(A) tail of a mRNA with a m^7GpppG-cap at a four-fold higher rate than uncapped, ApppG-capped or GpppG-capped RNA. Degradation beyond the poly(A) portion was also facilitated by the authentic cap structure. The higher deadenylation rate of m^7GpppG-capped RNA was confirmed when the initial rate of deadenylation was assayed by release of acid-soluble nucleotides. Hence, a bona fide cap structure on the RNA substrate stimulates the deadenylating activity both in a HeLa cell extract and of purified bovine PARN.

PARN itself is a cap-binding protein, which was demonstrated by its ability to bind m^7GTP-Sepharose. The ability of PARN to simultaneously interact with the 5´ cap and the 3´ poly(A) tail therefore enhances its activity.

Human recombinant PARN, expressed in *E. coli,* exhibited lower preference for m^7G-capped RNA substrate than the purified nuclease from calf thymus. However, when hPARN was expressed in human or insect cells the strict cap dependence was restored. This is probably due to a post-translational modification of the enzyme that does not occur in *E. coli*. A His_6-tag fused to the N-terminus of recombinant hPARN apparently did not influence the cap-dependence as both tagged and non-tagged enzyme, purified from *Drosophila* S2 cells, showed a strict cap-dependence.

The affinity for free m^7GpppG, as assessed by competition with free cap analogue in an TCA-precipitation assay, was 10-fold higher for recombinant hPARN expressed in mammalian

cells compared to hPARN that was expressed in *E. coli*. Thus is the difference in affinity for the m^7GpppG-cap analogue between the two PARN preparation probably due to a post-translational modification of amino acids that are important for binding.

A processive mode of deadenylation can be described as a reaction in which completely deadenylated products are generated while full-length RNA substrate still exists whereas in a distributive deadenylation mode, the poly(A) tails are degraded synchronously with an apparently slower rate. Recombinant hPARN, expressed in HEK293 cells and purified to near homogeneity, degraded the poly(A) tails of m^7GpppG-capped RNA in a processive mode poly(A) on RNA with an unmethylated cap in a distributive mode. The methyl group on the cap structure is important for binding as well as inducing a processive mode of deadenylation. Hence, binding to the cap structure is likely to induce a conformational change of the protein.

The native molecular mass was estimated to 257 kDa by gel filtration whereas the size in SDS-PAGE was 74 kDa. This discrepancy might indicate that the protein is either filamentous or exist as a multimer. The molecular mass was re-evaluated in a sedimentation-equilibration centrifugation as this allows an estimation of the molecular mass that is independent of the shape of the protein. By this method was molecular mass of the native form of PARN 150.4 kDa. Furthermore a high f/f_0 indicated that the protein has an extended shape. Native PARN most likely exists as a homodimer.

Different roles of the cap in care usually mediated by cap binding proteins complexed with other factors and might modulate PARN activity by allowing access of PARN to the cap or not. eIF4E, the cytoplasmic cap-binding protein did not inhibit PARN activity but did so when complexed with eIF4G and PABPC. These proteins are known to circularize mRNA that is translated and such a configuration will prevent PARN to bind either the poly(A) tail or the cap structure. However, GST-pulldown and m^7GTP-pulldown assays showed that the protein which is bridging the complex by binding to both RNA-binding proteins, was also binding to PARN and inhibits its activity. The smallest fragment that inhibited PARN activity was also sufficient for binding. Furthermore, a conserved domain within this fragment, MIF4G can be found in hCBP80 and hUpf2/rent2. Mutations in the MIF4G domain of the *S. pombe* Upf2 abolished nonsense-mediated decay (NMD) and recent data have shown that rapid deadenylation is triggered by a nonsense codon. This implicates that PARN might be involved in NMD by interacting with Upf2, however further experiments have to be made to confirm these interactions.

6. REFERENCES

Albert, T.K., Lemaire, M., van Berkum, N.L., Gentz, R., Collart, M.A., Timmers, H.Th.M. (2000) Isolation and characterization of human orthologs of yeast CCR4-NOT complex subunits. *Nucleic Acids Res*. 28:809-817

Ali IK, McKendrick L, Morley SJ, Jackson RJ. (2001) Truncated initiation factor eIF4G lacking an eIF4E binding site can support capped mRNA translation. *EMBO J.* 20:4233-42.

Allmang, C., Petfalski, E., Podtelejnikov, A., Mann, M., Tollervey, D., Mitchell, P. (1999a) The yeast exosome and human PM-Scl are related complexes of 3' --> 5' exonucleases. *Genes Dev.* 13:2148-2158

Allmang, C., Kufel, J., Chanfreau, G., Mitchell, P., Petfalski, E., Tollervey, D. (1999b) Functions of the exosome in rRNA, snoRNA and snRNA synthesis. *EMBO J*.18:5399-5410

Allmang, C., Mitchell, E., Petfalski, E., Tollervey, D. (2000) Degradation of ribosomal RNA precursors by the exosome. *Nucl. Acids Res*. 28:1684-1691

Åström, J., Åström, A., Virtanen, A. (1991) In vitro deadenylation of mammalian mRNA by a HeLa cell 3' exonuclease. *EMBO J.* 10:3067-71.

Åström, J., Åström, A., Virtanen, A. (1992) Properties of a HeLa cell 3' exonuclease specific for degrading poly(A) tails of mammalian mRNA. *J. Biol Chem.*267:18154-9.

Atasoy, U., Watson, J., Patel, D., Keene, J.D. (1998) ELAV protein HuA (HuR) can redistribute between the nucleus and cytoplasm and is upregulated during serum stimulation and T cell activation. *J. Cell. Sci.* 111:3145-3156

Audic, Y., Omili, F., Osborne, H.B. (1997) Postfertilization deadenylation of mRNAs in *Xenopus laevis* embryos is sufficient to cause their degradation at the blastula stage. *Mol. Cell. Biol.* 17:209-218

Ausubel, F.M., Brent, R., Kingston, R.E., Moore, D.D., Seidman, J.G., Smith, J.A., Struhl, K. (1994) Current Protocols in Molecular Biology. New York: *Greene Publishing Associates and Wiley-Interscience*

Baggs, J.E., Green, C.B. (2003) Nocturnin, a deadenylase in *Xenopus laevis* retina: a mechanism for posttranscriptional control of circadian-related mRNA. *Current Biol.* 13:189-198

Bai, Y., Salvadore, C., Chiang, Y.C., Collart, M.A., Liu, H.Y., Denis, C.L. (1999) The CCR4 and the CAF1 proteins of the CCR4-NOT complex are physically and functionally separated from NOT2, NOT4 and NOT5. *Mol. Cell. Biol.* 19:6642-6651

Beelman, C.A., Stevens, A., Caponigro, G., LaGrandeur, T.E., Hatfield, L., Parker, P. (1996) An essential component of the decapping enzyme required for normal rates of mRNA turnover. *Nature* 382:642-646

Bienroth, S., Wahle, E., Suter-Crazzolara, C., Keller, W. (1991) Purification of the cleavage and polyadenylation factor involved in the 3´-processing of messenger RNA precursors. *J. Biol. Chem*. 266:19768-19776

Birnboim, H.C., Doly, J. (1979) A rapid alkaline extraction procedure for screening recombinant plasmid DNA. *Nucleic Acids Res*. 7:1513-1523

Boeck, R., Tarun, S., Rieger, M., Deardorff, J., Müller-Auer, S., Sachs, A.B. (1996) The yeast Pan2 protein is required for poly(A)-binding protein stimulated poly(A)-nuclease activity. *J. Biol. Chem.* 271:432-438

Bogdan, J.A., Adams-Burton, C., Pedicord, D.L., Sukovich, D.A., Benfield, P.A., Corjay, M.H., Stoltenborg, J.K., Dicker, I.B. (1998) Human carbon catabolite repressor protein (CCR4)-associative factor 1: cloning , expression and characterization of its interaction with the B-cell translocation protein BTG1. *Biochem J.* 336:471-481

Bouveret, E., Rigaut, A., Shevchenko, M., Wilm, B., Seraphin, A. (2000) Sm-like protein complex that participates in mRNA degradation. *EMBO J.* 19:1661-1671

Bouvet, P., Omili, F., Yannick, A.-B., Legagneux, V., Roghi, C., Bassez, T., Osborne, H.B. (1994) The deadenylation conferred by the 3´ untranslated region of a developmentally controlled mRNA in *Xenopus* embryos is switched to polyadenylation by deletion of a short sequence element. *Mol. Cell. Biol*. 14:1893-1900

Brewer, G. (1991) An A+U-rich element RNA-binding factor regualates *c-myc* mRNA stability *in vitro*. *Mol. Cell. Biol*. 11:2460-2466

Brewer, G., Ross, J. (1988) Poly(A) shortening and degradation of the 3´A+U-rich sequences of human c-myc mRNA in a cell free system. *Mol. Cell. Biol.*, 8, 1697-1708

Breyer, W.A., Matthews, B.W. (2001) A structural basis for processivity. *Protein Science* 10:1699-1711

Briggs, M.W., Burkard, K.T., Butler, J.S. (1998) Rrp6p, the yeast homologue of the human PM-Scl 100-kDa autoantigen, is essential for efficient 5.8 S rRNA 3' end formation. *J. Biol. Chem*. 273:13255-63

Brouwer, R., Allmang, C., Raijmaker, R., van Aarssen, Y., Egberts, W.V., Petfalski, E., van Venrooij, W.J., Tollervey, D., Pruijn, G.J. (2001) Three novel components of the human exosome. *J. Biol. Chem.* 276:6177-6184

Brown, C.E., Tarun, S., Boeck, R., Sachs, A.B. (1996) PAN3 encodes a subunit of the Pab1p-dependent poly(A) nuclease in *Saccharomyces cerevisiae*. *Mol. Cell. Biol.* 16:6744-5753

Brown, C.E., Sachs, A.B. (1998) Poly(A) tail length control in *Saccharomyces cerevisiae* occurs by message-specific deadenylation. *Mol. Cell. Biol.* 18:6548-6559

Bunch, T.A., Grinblat, Y., Goldstein, L.S. (1988) Characterization and use of the Drosohphila metallothionein promoter in cultured Drosophila melanogaster cells. *Nucleic Acids Res.* 16:1043-1061

Buzby, J.S., Brewer, G., Nugent, D.J. (1999) Developmental regulation of RNA transcript destabilization by A+U-rich elements is AUF1-dependent. *J. Biol. Chem*. 274:33973-33978

Campos, A.R., Grossman, D., White, K. (1985) Mutant alleles at the locus elav in *Drosophila melanogaster* lead to nervous system defects: A developmental-genetic analysis. *J. Neurogenet.* 2:197-218

Caponigro, G., Parker, R. (1996) mRNA turnover in yeast promoted by the MATalpha1 instability element. *Nucleic Acids Res*. 24:4304-4312

Carballo, E., Lai, W.S., Blackshear, P.J. (1998) Feedback inhibition of macrophage tumor necrosis factor-alpha production by tristetraprolin. *Science* 281:1001-1005

Carballo, E., Lai, W.S., Blackshear, P.J. (2000) Evidence that tristetraprolin is a physiological regulator of granulocyte-macrophage colony-stimulating factor messenger RNA deadenylation and stability. *Blood* 95:1891-1899

Chen, C.Y., Gherzi, R., Ong, S.E., Chan, E.L., Raijmakers, R., Pruijn, G.J., Stroecklin, G., Moroni, C., Mann, M., Karin, M. (2001) AU binding proteins recruit the exosome to degrade ARE-containing mRNAs. *Cell* 107:451-464

Chen, C.Y., Shyu, A.B. (2003) Rapid deadenylation triggered by a nonsense codon precedes decay of the RNA body in mammalian cytoplasmic nonsense-mediated decay pathway. *Mol. Cell. Biol*. 23:4805-4913

Chen, J., Chiang, Y.C., Denis, C.L. (2002) CCR4, a 3′-5′ poly(A) RNA and ssDNA exo-nuclease, is the catalytic component of the cytoplasmic deadenylase. *EMBO J.* 21:1414-1426

Copeland, P.R., Wormington, M. (2001) The mechanism and regulation of deadeylation: identidication and characterisation of Xenopus PARN. *RNA* 7:875-886

Cosson, B., Couturier, A., Chabelskaya, S., Kiktev, D., Inge-Vechtomov, S., Philippe, M., Zhouravleva, G. (2002) Poly(A)-binding protein acts in translation termination via eukaryotic release factor 3 interaction and does not influence [PSI^+] propagation. *Mol. Cell. Biol.* 22:3301-3315

Cui, Y., Hagan, K.W., Zhang, S., Peltz, S.W. (1995) Identification and characterization of genes that are required for the accelerated degradation of mRNAs containing a premature translational termination codon. *Genes Dev*. 9:423-436

Czaplinski, K., Wenig, Y., Hagan, K.H., Peltz, S.W. (1995) Purification and characterization of the Upf1p protein: A factor involved in translation and mRNA degradation. *RNA* 1:610-623

Czaplinski, K., Ruiz-Echevarria, M.J., Paushkin, S.V., Han, X., Wenig, Y., Perlick, H.A., Dietz, H.C., Ter-Avanesyan, M.D., Peltz, S.W. (1998) The surveillance complex interacts with the translation release factors to enhance termination and degrade aberrant mRNAs. *Genes Dev.* 12:1665-1677

Daugeron, M.-C., Mauxion, F., Séraphin, B. (2001) The yeast POP2 gene encodes a nuclease involved in mRNA deadenylation. *Nucl. Acids Res.* 29:2448-2455

Decker, C.J., Parker, R. (1993) A turnover pathway for both stable and unstable mRNAs in yeast: evidence for a requirement for deadenylation. *Genes. Dev.* 1632-1643

Diskic, M. (2000) Functionally unrelated signalling proteins contains a fold similar to Mg^+-dependent endonucleases. *Trends Biochem. Sci.* 25:272-273

Dignam, J.D. (1990) Preparation of extracts from higher eukaryotes. in *Methods in Enzymology*, vol. 182 pp 194-203

van Dijk, E, Cougot, N., Meyer, S., Babajko, S., Wahle, E., Seraphin, B. (2002) Human Dcp2: a catalytically active mRNA decapping enzyme located in specific cytoplasmic structures. *EMBO J.* 21(24):6915-24.

Dlakic, M. (2000) Functionally unrelated signalling proteins contain a fold similar to Mg^{2+}-dependent endonucleases. *Trends Biochem. Sci.* 25:272-273

Dostie, J., Lejkowicz, F., Sonenberg, N. (2000a) Nuclear eukaryotic initiation factor 4E (eIF4E) colocalizes with splicing factors in speckles. *J Cell Biol*. 148:239-47.

Dostie J, Ferraiuolo M, Pause A, Adam SA, Sonenberg N. (2000b) A novel shuttling protein, 4E-T, mediates the nuclear import of the mRNA 5' cap-binding protein, eIF4E. *EMBO J.* 19:3142-56.

Dreyfuss, G., Kim, V.N., Kataoka, N. (2002) Messenger-RNA-binding proteins and the messages they carry. *Nat. Res. Mol. Cell. Biol.* 3:195-205

Dunckley, T., Tucker, M., Parker, R. (2001) Two related proteins, Edc1p and Edc2p, stimulate mRNA decapping in *Saccharomyces cerevisiae*. *Genetics* 157:27-37

Dupressoir, A., Morel, A.P., Barbot, W., Loireau, M.P., Corbo, L., Heidmann, T. (2001) Identification of four families of yCCR4- and Mg2+-dependent endonuclease-related proteins in higher eukaryotes, and characterization of orthologs of yCCR4 with a conserved leucine-rich repeat essential for hCAF1/hPOP2 binding. *BMC Genomics*. 2:9.

Elbashir, S.M., Harborth, J., Lendeckel, W., Yalcin, A., Tuschl, T. (2001) Duplexes of 21-nucleotide RNAs mediate RNA interference in cultured mammalian cells. *Nature* 411:494-498.

Etchison, D., Etchison, J.R. (1987) Monoclonal antibody-aided characterization of cellular p220 in uninfected and poliovirus-infected HeLa cells: subcellular distribution and identification of conformers. *J Virol*. 61:2702-10.

Evdokimova, V., Ruzanov, P., Imataka, H., Raught, B., Svitkin, Y., Ovchinnikov, L.P., Sonenberg, N. (2001) The major mRNA-associated protein YB-1 is a potent 5´ cap-dependent mRNA stabilizer. *EMBO J*. 20:5491-5502

Fan, X.C., Steitz, J.A. (1998a) Overexpression of HuR, a nuclear-cytoplasmic shuttling protein, increases the *in vivo* stability of ARE-containing mRNAs. *EMBO J.* 17:3448-3460

Fan, X.C., Steitz, J.A. (1998b) HNS, a nuclear-cytoplasmic shuttling sequence in HuR. *Proc. Natl. Acad. Sci.* 95:15293-15298

Fan, K., Yang, X., Wang, W., Wood III, W.H., Becker, K.G., Gorospe, M. (2002) Global analysis of stress-regulated mRNA turnover by using cDNA arrays. *Proc. Natl. Acad. Sci.* 99:10611-10616

Flaherty, S.M., Fortes, P., Izaurralde, E., Mattaj, I.W., Gilmartin, G.M. (1997) Participation of the nuclear cap binding complex in pre-mRNA 3´ processing. *Proc. Natl. Acad. Sci*. 94:11893-11898

Fortes, P., Inada, T., Preiss, T., Hentze, M.W., Mattaj, I.W., Sachs. A.B. (2000) The yeast nuclear cap binding complex can interact with translation factor eIF4G and mediate translation initiation. *Mol. Cell* 6:191-196

Fortes, P., Inada, T., Preiss, T., Hentze, M.W., Mattaj, I.W., Sachs, A.B. (2000) The yeast nuclear cap binding complex can interact with translation factor eIF4G and mediate translation initiation. *Mol Cell*. 6:191-6.

Fox, C.A., Wickens, M. (1990) Poly(A) removal during oocyte maturation: a default reaction selectively prevented by specific sequences in the 3´ UTR of certain maternal mRNAs. *Genes Dev.* 4:2287-2298

Frischmeyer, P.A., van Hoof, A., O´Donnell, K., Guerrerio, A.L., Parker, R., Dietz, H.C. (2002) An mRNA surveillance mechanism that eliminates transcripts lacking termination codons. *Science* 295:2258-2261

Frolova, L., Le Goff, X., Zhouravleva, G., Davydova, E., Philippe, M., Kisselev, L. (1996) Eukaryotic polypeptide chain release factor eRF3 is an eRF1- and ribosome-dependent guanosine triphosphatase. *RNA* 4:334-341

Gao, M., Fritz, D.T., Ford, L.P. and Wilusz, J. (2000) Interaction between a poly(A)-specific ribonuclease and the 5' cap influences mRNA deadenylation rates in vitro. *Mol. Cell* 5:479-488

Gallie, D.R. (1991) The cap and poly(A) tail function synergistically to regulate mRNA translational efficiency. *Genes Dev.* 5:2108-2116

Gingras, A.C., Raught, B., Sonenberg, N. (1999) eIF4 initiation factors: effectors of mRNA recruitment to ribosomes and regulators of translation. *Annu. Rev. Biochem.* 68:913-963

Gradi, A., Imataka, H., Svitkin, Y.V., Rom, E., Raught, B., Morino, S., Sonenberg, N. (1998) A novel functional human eukaryotic translation initiation factor eIF4G. *Mol. Cell. Biol.* 18:334-342

Green, C.B., Besharse, J.C. (1996) Use of a high stringency differential display screen for identification of retinal mRNAs that are regulated by a circadian clock. *Brain Res. Mol. Brain Res.* 37:157165

Green, C.B. (2003) Molecular control of Xenopus retinal circadian rhythms. *J. Neuroendocrinol.* in press

Grosset, C., C.-Y. A. Chen, Xu, N., Sonenberg, N., Jacquemin-Sablon, H., Shyu, A.B. (2000) A mechanism for translationally coupled mRNA turnover: Interaction between the poly(A) tail and a *c-fos* coding determinant via a protein complex. *Cell* 103:29-40

Görlich, D., Kraft, R., Kostka, S., Vogel, F., Hartmann, E., Laskey, R.A., Mattaj, I.W., Izaurralde, E., (1996) Importin provides a link between nuclear protein import and U snRNA export. *Cell* 87:21-32

Hagan, K.W., Ruiz-Echevarria, M.J., Quan, Y., Peltz, S.W. (1995) Characterisation of cis-sequences and decay intermediates involved in nonsense-mediated mRNA turnover. *Mol. Cell. Biol.* 15:809-823

Haghighat, A., Sonenberg, N. (1997) eIF4G dramatically enhances the binding of eIF4E to the mRNA 5´-cap structure. *J. Biol. Chem*. 272:21677-21680

Harlow, E., Lane, D. (1988) Antibodies:A Laboratory Manual. pp. 488-489*, Cold Spring Harbor Laboratory Press*

Hatfield, L., Beelman, C.A., Stevens, A., Parker, R. (1996) Mutations in *trans*-acting factors affecting mRNA decapping in *Saccharomyces cerevisiae. Mol. Cell. Biol.* 16:5830-5838

He, F., Jacobson, A. (1995) Identification of a novel component of the nonsense-mediated mRNA decay pathway using an interacting protein screen. *Genes Dev.* 9::437-454

Hershey, J.W.B. (1991) Translational control in mammalian cells. *Annu. Rev. Biochem*. 60:717-755

Hilleren, P., Parker, R. (1999) Mechanisms of mRNA surveillance in eukaryotes. *Annu. Rev. Genet.* 33:229-260

von Hippel, P.H., Fairfield, F.R., Dolejsi, M.K. (1994) On the processivity of polymerases. *Ann. NY Acad. Sci.* 726:118-131

Holcik, M., Liebhaber, S.A. (1997) Four highly stable eukaryotic mRNAs assemble 3´ untranslated region RNA-protein complexes sharing *cis* and *trans* components. *Proc. Natl. Acad. Sci.* 94:2410-2414

van Hoof, A., Parker, R. (2002) Messenger RNA degradation: Beginnig at the end. *Current Biol.* 12:R285-R287

van Hoof, A., Frischmeyer, P.A., Dietz, H.C., Parker, R. (2002) Exosome-mediated recognition and degradation of mRNAs lacking a termination codon. *Science* 295:2262-2264

van Hoof, A., Parker, R. (1999) The exosome: A proteasome for RNA? *Cell* 99:347-350

van Hoof, A., Lennertz, P., Parker, R. (2000) Yeast exosome mutants accumulate 3´-extended polyadenyalated forms of U4 small nuclear RNA and small nucleolar RNAs. *Mol. Cell. Biol*. 20:441-452

Hoshino, S., Miyazawa, H., Enomoto, T., Hanaoka, F., Kikuchi, A., Ui, M. (1989) A human homologue of the yeast GST1 gene codes for a GTP-binding protein and is expressed in a proliferation-dependent manner in mammalian cells.
EMBO J. 8(12):3807-14.

Hoshino, S., Imai, M., Mitzutani, M., Kikuchi, Y., Hanaoka, F., Ui, M., Katada, T. (1998) Molecular cloning of a novel member of the eukaryotic polypeptide chain-releasing factors (eRF). Its identification as eRF3 interacting with eRF1.
J. Biol. Chem. 273:22254-9.

Hoshino, S., Imai, M., Kobayashi, T., Uchida, N., Katada, T. (1999) The eukaryotic polypeptide chain releasing factor (eRF3/GSPT) carrying the translation termination to the 3´-poly(A) tail of mRNA. *J. Biol. Chem.* 274:16677-16680

Hunt, L., Jordan, M., De Jesus, M., Wurm, F.M. (1999) GFP-expressing mammalian cells for fast, sensitive, noninvasive cell growth assessment in a kinetic mode. *Biotechnol. Bioeng*. 65:201-205

Hsu, C.L., Stevens, A. (1993) Yeast cells lacking 5´ to 3´ exoribonuclease I contain mRNA species that are poly(A) deficient and partially lack the 5´ cap structure. *Mol. Cell. Biol*. 13:4826-4835

Hsu, P.-C., Hodel, M.R., Thomas, J.W., Taylor, L.J., Hagedorn, C.H., Hodel, A.E. (2000) Structrural requirements for the specific recognition of an m^7G mRNA cap. *Biochemistry* 39:13730-13736

Huang, Y., Carmichael, G.C. (1996) Role of polyadenylation in nucleocytoplasmic transport of mRNA. *Mol Cell Biol.* 16:1534-42.

Iborra, F.J., Jackson, D.A., Cook, P.R. (2001) Coupled transcription and translation within nuclei of mammalian cells. *Science*. 293:1139-42

Iizuka, N., Najita, L., Franzusoff, A., Sarnow, P. (1994) Cap-dependent and cap-independent translation by internal initiation of mRNAs in cell extracts prepared from *Saccharomyces cerevisiae*. *Mol. Cell. Biol*. 14:7322-7330

Imataka, H., Sonenberg, N. (1997) Human eukaryotic translation initiation factor 4G (eIF4G) possesses two separate and independent binding sites for eIF4A. *Mol. Cell. Biol.* 17:6940-6947

Ishigaki, Y., Li, X., Serin, G., Maquat, L.E. (2001) Evidence for a pioneer round of mRNA translation: mRNAs subject to nonsense-mediated decay in mammalian cells are bound by CBP80 and CBP20. *Cell* 106: 607-617

Ito, J., Jacobs-Lorena, M. (2001) Functional mapping of destabilizing elements in the protein-coding region of the *Drosophila fushi tarazu* mRNA. *J. Biol. Chem*. 276:23525-23530

Izaurralde, E., Lewis, J., McGuigan, C., Janowska, M., Darzynkiewicz, E., Mattaj, I.W. (1994) A nuclear cap binding protein complex involved in pre-mRNA splicing. *Cell* 78:657-668

Jacobs Anderson, J.S., Parker, R. (1998) The 3´ to 5´ degradation of yeast mRNAs is a general mechanism for mRNA turnover that requires the SKI2 DEVH box protein and 3´ to 5´ exonucleases of the exosome complex. *EMBO J.* 17:1497-1506

Jacobson, A., Peltz, S.W. (1996) Interrelationships of the pathways of mRNA decay and translation in eukaryotic cells. *Annu. Rev. Biochem.* 65:693-739

Jain, R.G., Andrews, L.G., McGowan, K.M., Pekala, P.H. Keene, J.D. (1997) Ectopic exression of Hel-N1, an mRNA-binding protein, increases glucose transporter (GLUT1) expression in 3T3-L1 adipocytes. *Mol. Cell. Biol.* 17:954-962

Kajita, Y., Nakayama, J., Aizawa, M., Ishikawa, F. (1995) The UUAG-specific RNA binding protein, heterogenous nuclear ribonucleoprotein D0. Common molecular structure and binding properties of the 2xRBD-Gly family. *J. Biol. Chem*. 270:22167-22175

Korneeva, N.L., Lamphear, B.J., Hennigan, F.L.C., Rhoads, R.E. (2000) Mutually cooperative binding of eukaryotic translation initiation factor (eIF) 3 and eIF4A to human eIF4G-1. *J. Biol. Chem.* 275:41369-41376

Kozak, M. (1989) The scanning model for translation: an update. *J. Cell. Biol.* 108:229-241

Kruys, V., Marinx, o., Shaw, G., Deschamps, J., Huez, G. (1989) Translational blockade imposed by cytokine-derived UA-rich sequences. *Science* 245:852-855

Kühn, U. (2003) The RNA-binding domains of nuclear poly(A)-binding protein. *J. Biol. Chem.* in press

Körner, C.G., Wahle, E. (1997) Poly(A) tail shortening by a mammalian poly(A)-specific 3´-exonuclease. *J. Biol. Chem.* 272:10448-10456

Körner, C.G., Wormington, M., Muckenthaler, M., Schneider, S., Dehlin, E., Wahle, E. (1998) The deadenylating nuclease (DAN) is involved in poly(A) tail removal during the meiotic maturation of Xenopus oocytes. *EMBO J.* 17:5427-5437

Körner, C.G. (1998b) Eukaryontischer mRNA-Abbau: Reinigung, cDNA-Klonierung und Charakterisierung einer Poly(A)-spezifischen 3´-Exoribonuklease (DAN) aus Säugerzellen. Inaguraldissertation., Giessen, April 1998

Lai, W.S., Carballo, E., Strum, J.R., Kennington, E.A., Philips, R.S., Blackshear, P.J. (1999) Evidence that tristetraprolin binds to AU-rich elements and promotes the deadenylation and destabilization of tumor necrosis factor alpha mRNA. *Mol. Cell. Biol*. 19:4311-4323

Laird-Offringa, I., de Wit, C., Elfferich, P., van der Eb, A. (1990) Poly(A) tail shortening is the translation-dependent step in *c-myc* mRNA degradation. *Mol. Cell. Biol*. 19:6132-6140.

LaGrandeur, T., Parker, R. (1999) The context of the translation start codon, in combination with other mRNA features, contributes to mRNA decay rates in *Saccharomyces cerevisiae*. *RNA* 5:420-433

LaGrandeur, T., Parker, R. (1998) Isolation and characterization of Dcp1p, the yeast mRNA decapping enzyme. EMBO J. 17:1487-96.

LaGrandeur, T., Parker, R. (1996) mRNA decapping activities and their biological roles. *Biochimie* 78:1049-1055

Laroia, G., Cuesta, R., Brewer, G., Schneider, R.J. (1999) Control of mRNA decay by heat shock-ubiquitin-proteasome pathway. *Science* 284:499-502

Le Hir, H., Moore, M.J., Maquat, L.E. (2000) Pre-mRNA splicing alters mRNP composition: evidence for a stable association of proteins at exon-exon junctions. *Genes Dev.* 14:1098-1108

Lewis, J.D., Görlach, D., Mattaj, I.W. (1996) A yeast cap binding protein complex (yCBC) acts at an early step in pre-mRNA splicing. *Nucleic Acids Res*. 24:3332-3336

Lingner, J., Radtke, I., Wahle, E., Keller, W. (1991) Purification and characterization of poly(A) polymerase from Saccharomyces cerevisiae. *J. Biol. Chem*. 266:8741-8746

Liu, H., Rodgers, N.D., Jiao, X., Kiledjian, M. (2002) The scavenger mRNA decapping enzyme DcpS is a member of the HIT family of pyrophosphatases. *EMBO J.* 21:4699-4708

Liu, H.Y., Badarinarayana, V., Audino, D.C., Rappsilber, J., Mann, M., Denis, C.L. (1998) The NOT proteins are part of the CCR4 transcriptional ccomplex and affect gene expression both positively and negatively. *EMBO J.* 171096-1106

Loflin, P., Chen, C.Y., Shuy, A.B. (1999) Unraveling a cytoplasmic role for hnRNP D in the in vivo mRNA destabilization directed by the AU-rich element. *Genes Dev*. 13:1884-1897

Lomakin, I.B., Hellen, C.U.T., Pestova, T.V. (2000) Physical association of eukaryotic initiation factor 4G (eIF4G) with eIF44A strongly enhances binding of eIF4G to the internal ribosome entry site of encephalomyocarditis virus and is required for internal initiation of translation. *Mol. Cell. Biol.* 20:6019-6029

Lund, E., Dahlberg, J.E. (1998) Proofreading and aminoacylation of tRNAs before export from the nucleus. *Science*. 282:2082-5.

Lykke-Andersen, J., Shu, M.-D., Steitz, J.A. (2000) Human Upf proteins target an mRNA for nonsense-mediated decay when bound downstream of a termination codon. *Cell* 103:1121-1131

Ma, W.-J., Chung, S., Furneaux, H. (1997) The Elav-like proteins bind to AU-rich elements and the poly(A) tail of mRNA. *Nucleic Acids Res*. 25:3564-3569

Marcotrigiano J, Lomakin IB, Sonenberg N, Pestova TV, Hellen CU, Burley SK. (2001) A conserved HEAT domain within eIF4G directs assembly of the translation initiation machinery. *Molec. Cell* 7:193-203

Martinez, J., Ren, Y.G., Thuresson, A.C., Hellman, U., Åström, J., Virtanen, A. (2000) A 54-kDa fragment of the Poly(A)-specific ribonuclease is an oligomeric, processive, and cap-interacting Poly(A)-specific 3' exonuclease. *J. Biol Chem.* 275:24222-30.

Mangiarotti, G. (1998) Coupling of transcription and translation in Dictyostelium discoideum nuclei. *Biochemistry.* 38:3996-4000.

Martinez, J., Ren, Y.-G., Thuresson, A.-C., Hellman, U., Åström, J., Virtanen, A. (2001) A 54-kDa fragment of the poly(A)-specific ribonuclease is an oligometric, processive, and cap-interacting poly(A)-specific 3′ exonuclease. *J. Biol. Chem*. 275:24222-24230

McKendrick, L., Thomson, E., Ferreira, J., Morley, S.J., Lewis, J.P. (2001) Interaction of eukaryotic translation initiation factor 4G with the nuclear cap-binding complex provides a link between nuclear and cytoplasmic functions of the m(7)guanosine cap. *Mol. Cell. Biol.* 21:3632-3641

Meissner, P., Pick, H., Kulangara, A., Chatellard, P., Friedrich, K., Wurm, F.M. (2000) Transient gene expression: recombinant protein production with suspension-adapted HEK293-EBNA cells. *Biotechnol. Bioeng*. 75:197-203

Mendell, J.T., Medghalchi, S.M., Lake, R.G., Noensie, E.N., Dietz, H.C. (2000) Novel Upf2p orthologues suggest a functional link between translation initiation and nonsense surveillance complexes. *Mol. Cell. Biol*. 20:8944-8957

Mitchell, P., Petfalski, E., Schevchenko, M., Mann, D., Tollervey, D. (1997) The exosome: a conserved eukaryotic RNA processing complex containing multiple 3´ to 5´ exoribonucleases. *Cell* 91:457-466

Mitchell, P., Tollervey, D. (2000) Musing on the structural organization of the exosome complex. *Nature Struct. Biol*. 7:843-846

Moens, S., Vanderleyden, J. (1997) Glycoproteins in prokaryotes. *Arch. Microbiol.* 168:169-175

Morino, S., Imataka, H., Svitkin, Y.V., Pestova, T.V., Sonenberg, N. (2000) Eukaryotic translation initiation factor 4E (eIF4E) binding site and the middle one-third of eIF4GI constitute the core domain for cap-dependent translation, and the C-terminal one-third functions as a modulatory region. *Mol. Cell. Biol.* 20:468-477

Moser, M.J., Holley, W.R., Chatterjee, A., Mian, J.S. (1997) The proofreading domain of *Escherichia coli* DNA polymerase 1 and other DNA and/or RNA exonuclease domains. *Nucl. Acids Res.* 25:5110-5118

Muckenthaler, M., Gunkel, N., Stripecke, R., Hentze, M.W. (1997) Regulated poly(A) tail shortening in somatic cells mediated by cap-proximal translation repressor proteins and ribosome association. *RNA* 3:983-995

Muhlrad, D., Parker, R. (1994) Premature translational termination triggers mRNA decapping. *Nature* 340:578-581

Muhlrad, D., Decker, C.J., Parker, R. (1994) Deadenylation of the unstable mRNA encoded by the yeast MFA2 gene leads to decapping followed by 5´ to 3´ digestion of the transcript. *Genes Dev.* 8, 855-866

Muhlrad, D., Decker, C.J., Parker, R. (1995) Turnover mechanisms of the stable yeast PGK1 mRNA. *Mol. Cell. Biol.* 15, 2145-2156

Mukherjee, D., Gao, M., O´Connor, J.P., Raijmakers, R., Pruijn, G., Lutz, C.S., Wilusz, J. (2002) The mammalian exosome mediates the efficient degradation of mRNAs that contain AU-rich elements. *EMBO J.* 21:165-174

Neininger, A., Kontoyiannis, D., Kotlyarov, A., Winzen, R., Eckert, R., Volk, H.-D., Holtmann, H., Kollias, G., Gaestel, M. (2002) MK2 targets AU-rich elements and regulates biosynthesis of tumor necrosis factor and interleukin-6 independently at different post-trascriptional levels. *J. Biol. Chem.* 277:3065-3068

Niedzwiecka, A., Marcotrigiano, J., Stepinski, J., Jankowska-Anyszka, M., Wyslouch-Cieszynska, A., Dadlez, M., Gingras, A.C., Mak, P., Darzynkiewicz, E., Sonenberg, N., Burley, S.K., Stolarski, R. (2002) Biophysical studies of eIF4E cap-binding protein: recognition of mRNA 5´ cap structure and synthetic fragments of eIF4G and 4E-BP1 proteins. *J. Mol. Biol*. 319:615-635

Ohno M, Kataoka N, Shimura Y. (1990) A nuclear cap binding protein from HeLa cells. *Nucleic Acids Res*. 18:6989-95

Olivas, W., Parker, R. (2000) The Puf3 protein is a transcript-specific regulator of mRNA degradation in yeast. *EMBO J*. 19:6602-6611

Paillard, L., Omilli, F., Legagneux, V., Bassez, T., Maniey, D., Osborne, H.B. (1998) EDEN and EDEN-BP, a *cis* element and an associated factor that mediate sequence-specific mRNA deadenylation in *Xenopus* embryos. *EMBO J.* 17:278-287

Paillard, L., Legagneux, V., Maniey, D., Osborne, H.B. (2002) c-jun ARE targets mRNA deadenylation by an EDEN-BP (Embryo Deadenylation Element-binding Protein)-dependent pathway. *J. Biol. Chem*. 277:3232-3235

Parker, R., Jacobson, A. (1990) Translation and a 42-nucleotide segment within the coding region of the mRNA encoded by the MAT alpha 1 gene are involved in promoting rapid mRNA decay in yeast. *Proc. Natl. Acad. Sci*. 87:2780-2784

Pasquinelli, A.E., Dahlberg, J.E., Lund, E. (1995) Reverse 5´ caps in mRNAs made in vitro by phage RNA polymerases. *RNA* 1:957-967

Pende, A., Tremmel, K.D., DeMaria, C.T., Blaxall, B.C., Minobe, W.A., Sherman, J.A., Bisognano, J.D., Bristow, M.R., Brewer, G., Port, J. R (1996) Regulation of the mRNA binding protein AUF1 by activation of the beta-adrenergic receptor signal transduction pathway. *J. Biol. Chem*. 271:8493-8501

Peng, S.S., Chen, C.Y., Xu, N., Shuy, A.B. (1998) RNA stabilization by the AU-rich element binding protein, HuR, and ELAV protein. *EMBO J.* 17:3461-3470

Pestova, T.V., Hellen, C.U.T. (2001) Functions of eukaryotic factors in initiation of translation. in Cold Spring Harbor Symposia on Quantitative Biology: The Ribosome. Volume LXVI, Cold Spring Harbor Lab. Press pp. 389-396

Pestova, T.V., Shatsky, I.N., Hellen, C.U. (1996) Functional dissection of eukaryotic initiation factor 4F: the 4A subunit and the central domain of the 4G subunit are sufficient to mediate internal entry of 43S preinitiation complexes. *Mol. Cell. Biol*.16:6870-8.

Pick, H.M., Meissner, P., Preuss, A.K., Tromba, P., Vogel, H., Wurm, F.M. (2002) Balancing GFP reporter plasmid quantity in large-scale transient transfections for recombinant anti-human rhesus-D IgG1 synthesis. *Biotechnol. Bioeng*. 79:595-601

Ponting, C.P. (2000) Novel eIF4G domain homologues linking mRNA translation with nonsense-mediated mRNA decay. *Trends Biochem, Sci.* 2000 25:423-6.

Putland, R.A., Sassinis, T.A., Harvey, J.S., Diamond, P., Coles, L.S., Brown, C.Y., Goodall, G.J. (2002) RNA destabilization by the granulocyte colony-stimulating factor stem-loop destabilizing element involves a single stem-loop that promotes deadenylation. *Mol. Cell. Biol.* 22:1664-1673

Reichlin, M., Maddison, P.J., Targoff, I., Bunch, T., Arnett, F., Sharp, G., Treadwell, E., Tan, E.M. (1984) Antibodies to a nuclear/nucleolar antigen in patients with polymyositis overlap syndromes. *J Clin Immunol*. 4:40-4

Ren, Y.-G., Martinez, J., Virtanen, A. (2002) Identification of the active site of poly(A)-specific ribonuclease by site-directed mutagenesis and Fe^{2+}-mediated cleavage. *J. Biol. Chem.* 277:5982-5987

Richardson, C.D., ed. (1995) Baculovirus expression protocols. *Methods in Molecular Biology*, Vol.39 (J.M. Walker, ed.) Humana Press, Totowa, NJ

Richter, J.D. (1999) Cytoplasmic polyadenylation in development and beyond. *Microbiol. Mol. Biol. Rev*. 63:446-456

Robbie, E.P. Peterson, M., Amaya, E., Musci, J. (1995) Temporal regulation of then Xenopus FGF receptor in development: a translation inhibitory element in the 3´ untranslated region. *Development* 121:1775-1785

Sachs, A.B. , Deardorff, J.A. (1992) Translation initiation requires the PAB-dependent poly(A) ribonuclease in yeast. *Cell* 70:961-973

Sambrook, J., Fritsch, E.F., Maniatis, T. (1989) Molecular Cloning: A Laboratory Manual, Second Edition, *Cold Spring Harbor Laboratory Press*

Sanger, F., Nicklen, S., Coulson, A.R. (1977) DNA sequencing with chain-terminating inhibitors. *Proc. Natl. Acad. Sci*. 74:5463-5467

Schiavi, S., Wellington, C., Shyu, A.B., Chen, C., Greenberg, M., Belasco, J. (1994) Multiple elements in the *c-fos* protein-coding region facilitate mRNA deadenylation and decay by a mechanism coupled to translation. *J. Biol. Chem*. 269:3441-3448

Schneider, I. (1972) Cell lines derived from late embryonic stages of Drosophila melanogaster. *J. Embryol. Exp. Morph*. 27:363-365

Schwartz, D., Decker, C.J., Parker, R. (2003) The ennhancer of decapping proteins, Edc1p and Edc2p, bind RNA and stimulate the activity of the decapping enzyme. *RNA* 9:239-251

Schwartz, D., Parker, R. (1999) Mutations in translation initiation factors lead to increased rates of deadenylation and decapping of mRNAs in *Saccharomyces cerevisiae. Mol. Cell. Biol*. 19:5247-5256

Shatkin, A.J. (1985) mRNA cap binding proteins: Essential factors for initiating translation. *Cell* 40:223-224

Sheets, M.D., Fox, C.A., Hunt, T., Woude, G.V., Wickens, M. (1994) The 3´-untranslated regions of c-mos and cyclin mRNAs stimulate translation by regulating cytoplasmic polyadenylation. *Genes Dev*. 8:926-938

Shen, E.C., Stage-Zimmermann, T., Chui, P., Silver, P.A. (2000) The yeast mRNA binding protein Npl3p interacts with the cap-binding complex. *J. Biol. Chem*. 275:23718-23724

Shim, J., Karin, M. (2002) The control of mRNA stability in response to extracellular stimuli. *Mol. Cells* 14:323-331

Shirley, R.L., Lelivelt, M.J. Schenkman, L.-R., Dahlseid, J.N., Culbertson, M.R. (1998) A factor required for nonsense-mediated mRNA decay in yeast is exported from the nucleus to the cytoplasm by a nuclear export signal sequence. *J. Cell Sci.* 111:3129-3143

Shyu, A.-B., Belasco, J.G., Greenberg, M.E. (1991) Two distinct destabilizing elements in the *c-fos* message trigger deadenylation as a first step in rapid mRNA decay. *Genes Dev.* 5, 221-234

Si, K., Maitra, U. (1999) The *Saccharomyces cerevisiae* homologue of mammalian translation initiation factor 6 does not function as a translation initiation factor. *Mol. Cell. Biol.* 19:1416-1426

Smith, M.H. (1970) Handbook of Biochemistry and Molecular Biology (2nd ed.), p. C-10, Sober, H.A. (Ed.) *CRC Press*

Sonenberg, N., Hershey, J.W.B., Mathews, M.B. eds. (2001) Translational control of gene expression. Cold Spring Harbor, NY: Cold Spring Harbor Lab. Press pp. 33-88

Song, H., Mugnier, P., Das, A.K., Webb, H.M., Evans, D.R., Tuite, M.F., Hemmings, B.A., Barford, D. (2000) The crystal structure of human eukaryotic release factor eRF1 – Mechanism of stop codon recognition and peptidyl-tRNA hydrolysis. *Cell* 100:311-321

Sonoda, J., Wharton, R. (1999) Recruitment of Nanos to *hunchback* mRNA by Pumilo. *Genes Dev*. 13:2704-2712

Standart, N., Jackson, R. (1990) Do the poly(A) tail and 3´ untranslated region control mRNA translation? *Cell* 62:15-24

Steiger, M., Carr-Schmid, A., Schwartz, D., Kiledjian, M., Parker, R. (2003) Analysis of recombinant yeast decapping enzyme. *RNA* 9:231-238

Stoecklin, G., Colombi, M., Raineri, I., Leuenberger, S., Mallaun, M., Schmidlin, M., Gross, B., Lu, M., Kitamura, T.,, Moroni, C. (2002) Functional cloning of BRF1, a regulator of ARE-dependent mRNA turnover. *EMBO J.* 21:4709-4718

Svitkin, Y.V., Ovchinnikov, L.P., Dreyfuss, G., Sonenberg, N. (1996) General RNA binding proteins render translation cap dependent. *EMBO J.* 15:7147-7155

Symmons,M.F., Williams, M.G., Luisi, B.F., Jones, G.H., Carpousis, A.J. (2002) Running rings around RNA: a superfamily of phosphate-dependent RNases. *Trends Biochem. Sci*. 27:11-18

Szabo, A., Dalmau, J., Manley, G., Rosenfeld, M., Wong, E., Henson, J., Possner, J.B., Furneaux, H.M. (1991) HuD, a paraneoplastic encephalomyelitis atigen, contains RNA-binding domains and is homologous to Elav and Sex-lethal. *Cell* 67:325-333

Tarun, S.Z.J., Sachs, A.B. (1996) Association of the yeast poly(A) tail binding protein with translation initiation factor eIF-4G. *EMBO J.* 15:7168-7177

Tarun,S.Z.J., Wells,S.E., Deardorff,J.A., Sachs, A.B. (1997). Translation initiation factor eIF4G mediates in vitro poly(A) tail-dependent translation. *Proc. Natl. Acad. Sci. USA* 94:9046-9051

Tarun, S., Parker, R. (2001) Targeting an mRNA for decapping: displacement of translation factors and association of the Lsm1p-7p complex on deadenylated yeast mRNAs. *Mol.Cell.*8(5):1075-83.

Thompson, S.R., Goodwin, E.B., Wickens, M. (2000) Rapid deadenylation and poly(A)-dependent translational repression mediated by *Caenorhabditis elegans tra-2* 3´ untranslated region in *Xenopus* embryos. *Mol. Cell. Biol*. 20:2129-2137

Tucker, M., Valencia-Sanchez, M.A., Staples, R.R., Chen, J., Denis, C.L., Parker, R. (2001) The transcription factor associated Ccr4 and Caf1 proteins are components of the major cytoplasmic mRNA deadenylase in *Saccharomyces cerevisiae*. *Cell* 104:377-386

Tucker, M., Staples, R.R., Valencia-Sanchez, M.A., Muhlrad, D., Parker, R. (2002) Ccr4p is the catalytic subunit of a Ccr4p/Pop2p/Notp mRNA deadenylase complex in *Saccharomyces cerevisiae*. *EMBO J.* 21:1427-1436

Ueno, S., Sagata, N. (2002) Requirement for both EDEN and AUUUA motifs in translational arrest of *mos* mRNA upon fertilization of *Xenopus eggs*. *Dev. Biol*. 250:156-167

Uschida, N., Hoshino, S., Imataka, H., Sonenberg, N., Katada, T. (2002) A novel role for the mammalian GSPT/eRF3 associating with poly(A)-binding protein in cap/poly(A)-dependent translation. *J. Mol. Biol.* 277:50286-50292

Varnum, S.M., Wormington, M. (1990) Deadenylation of maternal mRNAs during *Xenopus* oocyte maturation does not require specific *cis*-sequences: a default mechanism for translational control. *Genes Dev.* 4:2278-2286

Varnum, S.M. Hurney, C.A., Wormington, W.M. (1992) Maturation-specific deadenylation in *Xenopus* oocytes requires nuclear and cytoplasmic factors. *Dev. Biol.* 153:283-290

Vasudevan, S., Peltz, S.W. (2001) Regulated ARE-mediated mRNA decay in *Saccharomyces cerevisiae*. *Mol. Cell* 7:1191-1200

Vieltz, G.K., Ongkasuwan, J., Standart, N., Steitz, J.A. (2001) A novel embryonic poly(A) binding protein, ePAB, regulates mRNA deadenylation in Xenopus egg extracts. Genes Dev. 15:774-788

Visa, N., Izaurralde, E., Ferreira, J., Daneholt, B., Mattaj, I.W. (1996) A nuclear cap-binding complex binds Balbiani ring pre-mRNA cotranscriptionally and accompanies the ribonucleoprotein particle during nuclear export. *J. Cell Biol*. 133:5-14

Voeltz, G.K., Steitz, J.A. (1998) AUUUA sequences direct mRNA deadenylation uncoupled from decay during Xenopus early development. *Mol. Cell. Biol*. 18:7537-7545

Wahle, E. (1991) A novel poly(A)-binding protein acts as a specificity factor in the second phase of messenger RNA polyadenylation. *Cell* 66:759-768

Wang, Z., Kiledjian, M. (2001) Functional link between the mammalian exosome and mRNA decapping. *Cell* 107:751-762

Wang, Z., Jiao, X., Carr-Schmid, A., Kiledjian, M. (2002) The hDcp2 protein is a mammalian mRNA decapping enzyme. *Proc Natl Acad Sci U S A.* 99(20):12663-8

Wellington, C.L., Greenberg, M.E., Belasco, J.G. (1993) The destabilizing elements in the coding region of *c-fos* mRNA are recognized as RNA. *Mol. Cell. Biol*. 13:5034-5042

Wells, S., Hillner, P.E., Vale, R.D., Sachs, A.B. (1998). Circularization of mRNA by eukaryotic translation initiation factors. *Molecular Cell* 2, 135-140

Weng, Y., Czaplinski, K., Peltz, S.W. (1996a) Genetic and biochemical characterization of mutations in the ATPase and the helicase regions of the Upf1 protein. *Mol. Cell. Biol.* 16:5477-5490

Weng, Y., Czaplinski, K., Peltz, S.W. (1996b) Identification and characterization of mutations in the UPF1 gene that affect the Upf protein complex, nonsense suppression but not mRNA turnover. *Mol. Cell. Biol*. 16:5491-5506

Weng, Y., Czaplinski, K., Peltz, S.W. (1998) ATP is a cofactor of the Upf1protein that modulates its translation termination and RNA binding activities. *RNA* 4:205-214

Wharton, R., Sonoda, J., Lee, T., Patterson, M., Murata, Y. (1998) The Pumilo RRNA-binding domain is also a translational regulator. *Mol. Cell* 1:863-872

Whisstock, J.C., Romero, S., Gurung, R., Nandurkar, H.,Ooms, L.M., Bottomley, S.P., Mitchell, C.A. (2000) The inositol polyphosphate 5-phosphatases and the apurinic/apyrimidnic base excision repair endonucleases share a common mechanism for catalysis. *J. Biol. Chem.* 275:37055-37061

Wickens, M., Goodwin, E.B., Kimble, J., Strickland, S., Hentze, M. (2000) Translational control of developmental decisions. *In Translational Control of Gene Expression* (eds. N. Sonenberg, J.W.B. Hershey, and M.B. Mathews) pp. 295-370. Cold Spring Harbor Laboratory Press, Cold Spring Harbor, NY

Wilkinson, M.F., Shyu, A.-B. (2001) Multifunctional regulatory proteins that control gene expression in both the nucleus and the cytoplasm. *Bioessays*. 23:775-87.

Wisdom, R., Lee, W. (1991) The protein-coding region of *c-myc* mRNA contains a sequence that specifies rapid mRNA turnover and induction by protein synthesis inhibitors. *Genes Dev*. 5:232-243

Wurm, F., Bernard, A. (1999) Large-scale transient expression in mammalian cells for recombinant protein production. *Curr. Opin. Biotechnol*. 10:156-159

Xu, N., Chen, C.-Y. A., Shyu, A.-B. (1997) Modulation of the fate of cytoplasmic mRNA by AU-rich elements: key sequence features controlling mRNA deadenylation and decay. *Mol. Cell. Biol.*, 17(8):4611-4621

Xu, N., Chen, C.Y., Shuy, A.B. (2001) Versatile role for hnRNP D isoforms in the differential regulation of cytoplasmic mRNA turnover. *Mol. Cell. Biol.* 21:6960-6971

Zamore, P.D., Williamson, J.R., Lehman, R. (1997) The pumilo protein binds RNA through a conserved domain that defines a new class of RNA-binding proteins. *RNA* 3:1421-1233

Zhang, B., Gallegos, M., Puoti, A., Durkin, E., Fields, S., Kimble, J., Wickens, M.P. (1997) A conserved RNA-binding protein that regulates sexual fates in the *C.elegans* hermaphrodite germ line. *Nature* 390:477-484

Zhang, J., Wagner, B.J., Ehrenman, K., Schaefer, A.W., DeMaria, C.T., Crater, D., DeHaven, K., Long, L., Brewer, G. (1993) Purification, characterization, and cDNA cloning of an AU-rich element RNA-binding protein, AUF1. *Mol. Cell. Biol*. 13:7652-7665

Zhang, J., Sun, X., Qian, Y., Maquat, L.E. (1998) Intron function in the nonsense-mediated decay of β-globin mRNA: indications that pre-mRNA in the nucleus can influence mRNA translation in the cytoplasm. *RNA* 4:801-815

VECTOR FOR EXPRESSING PARN IN HEK293-EBNA CELLS

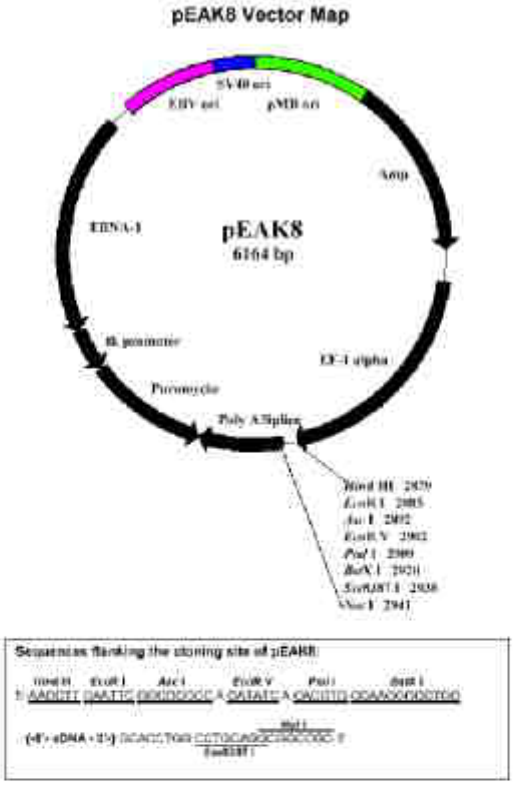

VECTOR FOR EXPRESSING PARN IN SCHNEIDER 2 CELLS

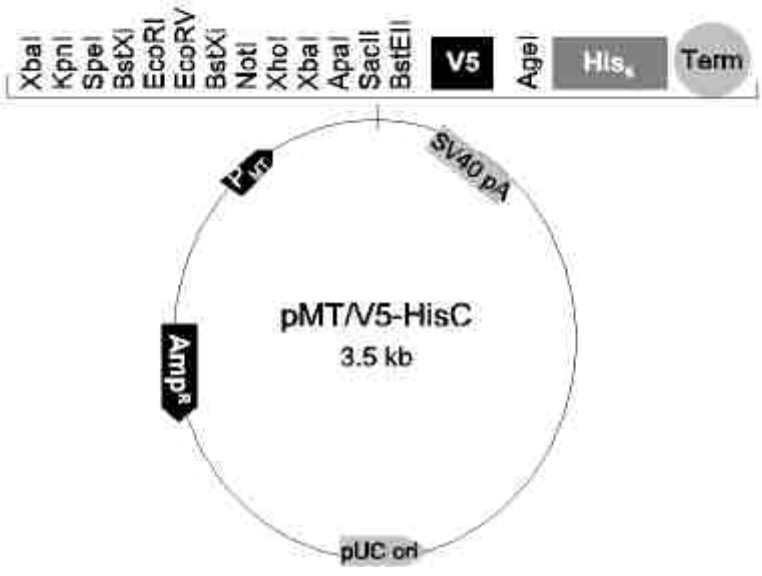

ABBREVIATIONS

A	adenosine
aa	amino acids
$AmS0_4$	ammonium sulphate
AUF	AU-binding factor, an hnRNP D protein
AUG	translation start codon
AUUUA	core sequence of mRNA instability element (ARE)
ARE	AU-rich element
BRF	butyrate response factor
CBC	nuclear cap binding complex
CBP	nuclear cap binding protein
cDNA	copy DNA; DNA synthesized with mRNA as template
CPE	cytoplasmic polyadenylation element
CRD	coding region instability determinant
CLPD	crosslink / pulldown
C-terminus	carboxy terminal end of a protein
DSE	downstream element
EBNA	Eppstein-Barr nuclear antigen
eEF	eukaryotic translation elongation factor
eIF	eukaryotic translation initiation factor
eRF	eukaryotic translation release factor
EDEN	embryo deadenylation element
ELAV	embryonic lethal abnormal vision
ePAB	embryonic poly(A)-binding protein
FPLC	fast protein liquid charomatography
G	guanosine
GFP	green fluorescence protein
GST	glutathione S-transferase
HEK	Human embryonic kidney cells
His_6	Met-Ala-His-His-His-His-His-His
IRES	internal ribosome entry site
KAc	potassium acetate

kDa	kilo Dalton
KSRP	K-type RNA binding protein
M	molar; moles per litre
m^7G-cap	m^7G(5´)ppp(5´) G cap structrure
MIF4G	middle domain of eIF4G (aa 642-1091)
mRNA	messinger ribonucleic acid
N-DAN	C-terminal deletion of hPARN
NMD	nonsense-mediated mRNA degradation
NSD	nonstop-mediated mRNA degradation
N-terminus	amino terminal end of a protein
ORF	open reading frame
PABPC	cytoplasmic poly(A)-binding protein
PAGE	polyacrylamide gel electrophoresis
PARN	poly(A)-specific ribonuclease (previously DAN)
bPARN	bovine PARN
hPARN	human PARN
xPARN	*Xenopus laevis* PARN
poly(A)	polyadenylic acid
R3H	RNA binding motif; (arginine-$(x)_3$ histidine)
RNase	ribonuclease
RRM	RNA recognition motif
S2	Schneider 2 cells derived from *Drosophila melanogaster*
SDS	sodiumdodecylsulphate
TIE	translational inhibitory element
TIF	translation initiation factor
TGE	tra-2 and GLI element
TTP	tristetraprolin
UTR	untranslated region

Curriculum vitae

Name: Eva Dehlin
Date of birth: March 23, 1954
Place of birth: Umeå, Sweden
Nationality: Swedish

Education

1970-1973:	Gymnasium, Rodenskolan, Norrtälje, Sweden
1976-1983	Umeå University, Umeå, Sweden Chemistry, Physics and Microbiology studies
1983	Högskole examen, (BS)
1977-1978	Västerbottens Vårdskola, Umeå, Sweden, (Laboratory technician)
1981	Stockholm University, Stockholm, Sweden, Biochemistry studies
1993-1996	Karolinska Institutet, Stockholm, Sweden, Postgraduate studies at the Microbiology and Tumorbiology Center (MTC), Department of Bacteriology.
Jan. 1996	Licenciate in medical sciences. (Master degree)
1998-2003	Martin-Luther University, Halle, Germany, Postgraduate studies at the Department of Biochemistry.

Positions

1973-1976	Nursing aid at the University Hospital in Umeå, Sweden
1978-1982	Laboratory technician at the Department of Pathology, Umeå University, Sweden
1982-1983	Laboratory engineer at the Department of Zoophysiology, Umeå University, Sweden
1983-1986	Research assistant at the Department of Appl. Cell and Mol. Biol., Umeå Universtity, Sweden
1986-1993	Research assistant at the Department of Bacteriology, MTC, Karolinska Institutet, Sweden.
1993-1995	Graduate student at the Institute for Microbiology and Genetics, Vienna Biocenter, Vienna, Austria.
1996-1997	Research assistant, EVAX Technologies (now Apovia Inc.), Vienna, Austria.
1998-2003	Graduate student at the Department of Biochemistry, Martin-Luther University, Halle, Germany.

Scientific papers

Dehlin, E., Marcusson,J., Fowler, C.J. and Winblad, B. (1982) The binding of ^{3}H-5-hydroxytryptamine to homogenates of human brain. *J. Neural Transmission*, 54: 91-103

Melin, L. and Dehlin, E. (1987) Differential expression of late and early promoters from the coliphage T5 in *Bacillus subtilis*. *FEMS letters*, 41: 141-146

Melin, L., Friden, H., Dehlin, E., Ruthberg, L. and von Gabain, A. (1990) The importance of the 5´-region in regulating the stability of *sdh* mRNA in *B. subtilis*. *Mol. Microbiol*. 4(11): 1881-1889

Dehlin, E., von Gabain, A., Alm, G., Dingelmayer, R. and Resnekov, O. (1996) Repression of β-IFN gene expression in virus infected cells is correlated with a poly(A) tail elongation. *Mol. Cell. Bio*. 16(2): 468-474

Szostak, M.P., Mader, H., Truppe, M., Kamal, M., Eko, F.O., Huter, V., Marchart, J., Jechlinger, W., Haidinger, W., Brand, E., Denner, E., Resch, S,. Dehlin, E., Katinger, A., Kuen, B., Haslberger, A., Hensel, A., and Lubitz, W. (1997) Bacterial ghosts as multifunctional vaccine particles. *Behring. Inst. Mitt*. 98: 191-196

Körner, C.G., Wormington, M., Muckenthaler, M., Schneider, S., Dehlin, E., and Wahle, E. (1998) The deadenylating nuclease (DAN) is involved in poly(A) tail removal during the meiotic maturation of *Xenopus* oocytes. *EMBO J*. 17(18): 5427-5437

Dehlin, E., Wormington, M., Körner, C.G., and Wahle, E. (2000) Cap-dependent deadenylation of mRNA. *EMBO J*. 19(5): 1079-1086

ACKNOWLEDGEMENTS

At first I would like to thank my supervisor **Professor Elmar Wahle** for allowing me to work in his group. It was reassuring to discover that honesty in science can also be productive. I am also grateful for the sharp, always at the point, comments and discussions throughout this work.

Dr. Christof Körner who introduced me to the topic and whose project I took over.
Dr. Mike Wormington for sharing his data and making good suggestions how to proceed in the project.
Claudia Temme and **Michael Reuter** my fellow Ph.D. students on the mRNA degradation project and **Dr. Ulla Niesbach-Klösgen** who joined the degradation group later. Claudia who has followed me the entire time, who was a friend and support in the very beginning in Halle but also later. Michael, who is the only one left working with PARN, I wish you all the best.
Dr. Uwe Kühn, for fruitful discussions and helping me out (patiently) with the computers and the computer programs.
Dr. Sylke Meyer for introducing me to the FPLC and for generously opening up her home to me.
Dr. Kai Tittman for helping me with a protein purification and for being a very good friend within as well as outside the institute.
Dr. Jason Smith for sharing the first months in Halle with me and cardboard boxes from the floor to the ceiling, in a lab at 37^{o}C.
Dr. Yvonne Kerwitz, Barbe Schulz, Anne Knoth, Henning Friedrich and Anke Grzam, for a nice time in the lab as well as outside. **Corneila Herrmann**, for helping me with the German bureaucracy.
Marina Schulze for making the glassware clean and **Gudrun Scholz** for being helpful in general.
Dr. Simon Morley for sending us eIF4E and eIF 4G preparations over and over again. And when it became to embarrassing for us, sending the plasmids and the virus stock.
Dr. Lucia Baldi for performing the transient transfections in HEK293 cells.
Dr. Hauke Lilie for performing the sedimentation-equilibration centrifugation.
Dr. Antje Ostareck-Lederer and **Dr. Dirk Ostareck** for reading through the thesis
Gert Bange for interesting discussions about everything and Gert, thank you for the music.
Ramona Bange for showing me that there is a world outside the lab and for being a friend.
Michael Spinka for giving me shelter when I was homeless and, of course, for interesting talks in the evenings and the weekends.
The entire working group of Prof. G. Hübner for being good neighbours.
Professor Milton Stubbs for interesting discussions, both in English and Swedish.
Professor Bengt Winblad for always being supportive.
To my mother, **Hildegard Dehlin**, who always stood by my side.

Erklärung

Hiermit versichere ich, daβ ich die voliegende Arbeit selbständig verfaβt und keine anderen Hilfsmittel als die angegebenden benutzt habe. Jene Stellen, die ich anderen Untersuchungen und Arbeiten dem Wortlaut oder Sinn entsprechend entnommen habe, sind durch Quellenangaben gekennzeichnet.

Halle, den 28. Juli 2003